E.U. GRADUATE SCHOOL OF NATURAL AND APPLIED SCIENCES

EGE UNIVERSITY

DOCTORATE THESIS

POLYMERIZATION OF FUNCTIONAL CYCLIC MONOMERS AND INVESTIGATION OF INITIATOR EFFICIENCY BY COMPUTATIONAL CHEMISTRY

Sıla GÜMÜŞTAŞ

Supervisor: Prof. Dr. Armağan KINAL

Department of Chemistry

Presentation Date: 30/11/2018

Bornova-İZMİR

2018

EGE UNIVERSITY GRADUATE SCHOOL OF NATURAL AND APPLIED SCIENCES

(DOCTORATE THESIS)

POLYMERIZATION OF FUNCTIONAL CYCLIC MONOMERS AND INVESTIGATION OF INITIATOR EFFICIENCY BY COMPUTATIONAL CHEMISTRY

Sıla GÜMÜŞTAŞ

Supervisor: Prof. Dr. Armağan KINAL

Department of Chemistry

Date of Presentation: 30/11/2018

Bornova-İZMİR

2018

Sıla GÜMÜŞTAŞ tarafından **doktora tezi** olarak sunulan **"Polymerization of functional cyclic monomers and investigation of initiator efficiency by computational chemistry"** başlıklı bu çalışma E.Ü. Lisansüstü Eğitim ve Öğretim Yönetmeliği ile E.Ü. Fen Bilimleri Enstitüsü Eğitim ve Öğretim Yönergesi'nin ilgili hükümleri uyarınca tarafımızdan değerlendirilerek savunmaya değer bulunmuş ve 30/11/2018 tarihinde yapılan tez savunma sınavında aday oybirliği/~~oyçokluğu~~ ile başarılı bulunmuştur.

Jüri Üyeleri:		**İmza**
Jüri Başkanı	: Prof. Dr. Armağan KINAL	.....
Raportör Üye	: Prof.Dr. Erdener KARADAĞ	.....
Üye	: Doç.Dr. Hakan AKAT	.....
Üye	: Doç.Dr. Nursel ACAR SELÇUKİ	.....
Üye	: Doç.Dr. Kamil ŞİRİN	.....

EGE ÜNİVERSİTESİ FEN BİLİMLERİ ENSTİTÜSÜ

ETİK KURALLARA UYGUNLUK BEYANI

EÜ Lisansüstü Eğitim ve Öğretim Yönetmeliğinin ilgili hükümleri uyarınca Doktora Tezi olarak sunduğum "**Polymerization of functional cyclic monomers and investigation of initiator efficiency by computational chemistry**" başlıklı bu tezin kendi çalışmam olduğunu, sunduğum tüm sonuç, doküman, bilgi ve belgeleri bizzat ve bu tez çalışması kapsamında elde ettiğimi, bu tez çalışmasıyla elde edilmeyen bütün bilgi ve yorumlara atıf yaptığımı ve bunları kaynaklar listesinde usulüne uygun olarak verdiğimi, tez çalışması ve yazımı sırasında patent ve telif haklarını ihlal edici bir davranışımın olmadığını, bu tezin herhangi bir bölümünü bu üniversite veya diğer bir üniversitede başka bir tez çalışması içinde sunmadığımı, bu tezin planlanmasından yazımına kadar bütün safhalarda bilimsel etik kurallarına uygun olarak davrandığımı ve aksinin ortaya çıkması durumunda her türlü yasal sonucu kabul edeceğimi beyan ederim.

30/11/2018

Sıla GÜMÜŞTAŞ

ÖZET

FONKSİYONEL HALKALI MONOMERLERİN POLİMERLEŞTİRİLMESİ VE BAŞLATICI ETKİNLİĞİNİN HESAPSAL YÖNTEMLERLE ARAŞTIRILMASI

Sıla GÜMÜŞTAŞ

Doktora Tezi, Kimya Anabilim Dalı

Tez Danışmanı: **Prof. Dr. Armağan KINAL**

Kasım 2018, 130 sayfa

Bu çalışmada biyobozunur ve biyouyumlu fonksiyonel laktonların halka açılma polimerizasyon reaksiyonu deneysel ve hesapsal olarak incelenerek, başlatıcı etkinliği araştırıldı. Amaç, polimerizasyon sürecini hesapsal kimya ile aydınlatmak, en etkin başlatıcıyı öngörebilmek ve deneysel olarak doğrulamaktır.

Poly(α-angelica lactone), PAL, $SnAcet_2$ ve $ZnAcet_2$ varlığında halka açılma polimerizasyonu ile sentezlendi, ancak düşük molekül ağırlıklı ürün elde edildi (1000-1500 g/mol). Halka açılma polimerleşme mekanizmasının başlama ve büyüme basamakları yarı deneysel ve DFT yöntemleri ile çalışıldı. Bağ kırılma adımında ortaya çıkan tepkime bariyeri, $SnAcet_2$ ve $ZnAcet_2$ için ωB97X-D metodu ile sırasıyla 30.2 kcal/mol ve 23.4 kcal/mol olarak bulundu. Tepkimenin polimerizasyon entalpisi hesaplanarak, sürecin termodinamiği tartışıldı. Ayrıca, α-angelica lactone'nun iyonik polimerizasyon tepkime bariyeri ise ωB97X-D metodu ile 24.6 kcal/mol olarak bulundu. Buna göre, teorik olarak da yüksek moleküler ağırlıklı PAL sentezlenemeyeceği ilk kez ortaya konuldu.

Poly(δ-valerolactone), PVL, $SnAcet_2$, $PbAcet_2.3H_2O$, $CdAcet_2.2H_2O$, $NiAcet_2.4H_2O$ ve $CuAcet_2.H_2O$ başlatıcıları kullanılarak ilk kez halka açılma polimerizasyonu yöntemi ile sentezlendi ve en yüksek molekül ağırlığı (45438 g/mol, %91 verim) $CdAcet_2.2H_2O$ başlatıcısı ile elde edildi. Sn, Cd ve Pb içeren asetat kompleksleriyle sentezlenen PVL'ler için toksisite testleri yapıldı. Başlatıcı etkinliği DFT metotları kullanılarak elde edilen NBO ve LUMO analizi ile araştırıldı. $SnAcet_2$ varlığında reaksiyon mekanizması ωB97X-D metodu ile çalışıldı ve tepkime bariyeri 28.9 kcal/mol olarak hesaplandı. Elde edilen verilere göre en etkin başlatıcının $CdAcet_2.2H_2O$ olduğu görüldü.

δ-valerolactone ve glycidol kopolimeri ilk kez $SnAcet_2$ varlığında sentezlendi. Ayrıca glycidol yapısındaki –OH grubu, tosyl-klorür ile korunarak, poly(δ-valerolactone-co-glycidol) kopolimeri de ilk kez sentezlendi. Fakat koruma grubunun sterik etkisinden dolayı düşük molekül ağırlıklı kopolimer elde edildi (~1500 g/mol). Glycidolün, $SnAcet_2$ ile polimerleşme tepkime bariyeri ωB97X-D metodu ile 40.3 kcal/mol olarak bulunmasına karşın, oluşan ürünün Gibbs serbest enerji değişimi ise -10 kcal/mol olarak bulundu. Teorik verilere göre bu tepkimenin termodinamik açıdan istemli olduğu sonucuna varıldı.

Anahtar sözcükler: Poly(α-angelica lactone), Poly(δ-valerolactone), glycidol, halka açılma polimerizasyonu, DFT, tepkime mekanizması

ABSTRACT

POLYMERIZATION OF FUNCTIONAL CYCLIC MONOMERS AND INVESTIGATION OF INITIATOR EFFICIENCY BY COMPUTATIONAL CHEMISTRY

GÜMÜŞTAŞ, Sıla

PhD thesis in Chemistry

Supervisor: **Prof. Dr. Armağan KINAL**

November 2018, 130 pages

In this study, the ring opening polymerization (ROP) of biodegradable and biocompatible functional lactones and also initiator efficiency was investigated experimentally and computationally. The aim is to illuminate the polymerization process with computational chemistry, to predict the most effective initiator and to confirm it experimentally.

Poly(α-angelica lactone), PAL, was synthesized by ring opening polymerization in the presence of $SnAcet_2$ and $ZnAcet_2$, but a low molecular weight product (1000-1500 g/mol) was obtained. However, initiation and propagation stages of the ROP mechanism were studied by semi empirical and DFT methods. The reaction barriers arising in the bond breaking steps was found to be 30.2 kcal/mol and 23.4 kcal/mol by means of the ωB97X-D method for $SnAcet_2$ and $ZnAcet_2$, respectively. The thermodynamics of the process was discussed by calculating the enthalpy of polymerization of the reaction. In addition, the ionic polymerization reaction barrier of α-angelica lactone was also found to be 24.6 kcal/mol with the ωB97X-D method. Accordingly, it was theoretically revealed for the first time that the high molecular weight polymer could not be synthesized.

Poly(δ-valerolactone), PVL, was synthesized by ring opening polymerization using $SnAcet_2$, $PbAcet_2.3H_2O$, $CdAcet_2.2H_2O$, $NiAcet_2.4H_2O$ and $CuAcet_2.H_2O$ initiators and the highest molecular weight (45438 g/mol, 91% yield) is obtained with the initiator $CdAcet_2.2H_2O$. Toxicity tests were performed for PVLs synthesized with acetate complexes containing Sn, Cd and Pb. The initiator activity was investigated by NBO and LUMO analyses using several DFT methods. In the presence of $SnAcet_2$, the reaction mechanism was studied with the ωB97X-D method and the reaction barrier was calculated as 28.9 kcal/mol. According to the computational data, it was determined that the most effective initiator was $CdAcet_2.2H_2O$.

The δ-valerolactone and glycidol copolymer were first synthesized in the presence of $SnAcet_2$. In addition, the -OH group in the glycidol structure was protected with tosyl-chloride and the poly (δ-valerolactone-co-glycidol) copolymer was also synthesized for the first time. However, due to the steric effect of the protecting group, low molecular weight copolymer was obtained (~1500 g/mol). Glycidol was found to be 40.3 kcal/mol by polymerization reaction with $SnAcet_2$, whereas Gibbs free energy exchange was found to be -10 kcal/mol. According to the theoretical data, this reaction is thermodynamically spontaneous.

Keywords: Biodegradable and biocompatible polymers, α-angelica lactone, ROP, Poly(δ-valerolactone), DFT, copolymerization, reaction path, NBO analysis

ACKNOWLEDGMENT

In the first place, I would like to give my best thanks to my supervisor Prof. Dr. Armağan KINAL, for his deep knowledge, valuable suggestions, his endless patience, precious helps and for giving importance to my ideas, during this long study. In chemistry field, I am grateful to for the new information I have gained. I'm very lucky and happy to work with him. I would also like to special thank to Prof. Dr. Mehmet BALCAN for his precious suggestions, support, valuable contribution, his deep knowledge, experiences and everything he teaches.

I would like to thank to Prof. Dr. Erdener KARADAĞ and Assoc. Prof. Dr. Hakan AKAT, members of Ph. D. thesis committee, for their valuable advices and comments during my study.

I would like to special thank to my dear friend Assoc. Prof. Dr. Esra Evrim YALÇINKAYA for her valuable advices, lasting friendship and moral support.

I would like to sincere thanks to M.Sc. Merve GÜREŞCİ for her precious helps and supports about everything.

I would like to thank to my friend Dr. Fehmi SALTAN for his help and moral support.

I want to thank to Research Grand Office of Ege University for supporting the 2016 Fen 041 numbered project and TUBITAK ULAKBIM, High Performance and Grid Computing Center (TRUBA resources) for numerical calculations.

Finally, I am greatful to my husband Barış GÜMÜŞTAŞ, whole BALCAN and GÜMÜŞTAŞ families for their precious helps and moral support. I owe them a great deal. And also I would like to my greatest thanks to my son Çınar, who gave me powerful with his presence.

İzmir / November 2018 **Sıla GÜMÜŞTAŞ**

CONTENTS

Page

CONTENTS (Continued)

Page

CONTENTS (Continued)

Page

CONTENTS (Continued)

Page

LIST OF FIGURES

Figure **Page**

LIST OF FIGURES (Continued)

Figure **Page**

LIST OF FIGURES (Continued)

Figure **Page**

LIST OF FIGURES (Continued)

Figure **Page**

LIST OF FIGURES (Continued)

Figure **Page**

LIST OF FIGURES (Continued)

Figure **Page**

LIST OF FIGURES (Continued)

Figure **Page**

LIST OF TABLES

Table **Page**

LIST OF TABLES (Continued)

Table **Page**

ABBREVIATIONS

Å	Angstrom
AL	α-angelica lactone
DFT	Density Functional Theory
DSC	Differential Scanning Calorimetry
DTG	Differential Thermal Analysis
ECP	Effective Core Potential
FTIR	Fourier Transform Infrared Spectroscopy
GPC	Gel Permeation Chromatography
GL	Glycidol
^{1}H NMR	Proton Nuclear Magnetic Resonance Spectroscopy
HOMO	Highest Occupied Molecular Orbital Energy
IRC	Intrinsic reaction coordinate
LUMO	Lowest Unoccupied Molecular Orbital
NBO	Natural Bond Orbital
Mn	Number-average Molecular Weight
Mw	Weight- average Molecular Weight
PAL	Poly(α-angelica lactone)
PCM	Polarized Continuum Model
PDI	Polydispersity Index
PES	Potential Energy Surface
PGL	Polyglycidol
PVL	Poly(δ-valerolactone)
ROP	Ring Opening Polymerization
TG	Thermogravimetry
TS	Transition state structure
δVL	δ-valerolactone

1. INTRODUCTION

The stability as a plastic material of the polymeric materials prepared from petroleum-derived monomers by means of pathway has led to numerous applications (Vainionpää et al., 1989). Packaging, structure, medical products and other fields of use have brought about the problem of waste of such polymeric materials. As a result, the interest in polymers that have been prepared by way of renewable and sustainable sources has increased with each passing day (Gunatillake et al., 2006). These polymers undergo microbial degradation and do not accumulate in the environment as other petroleum-derived polymers. Biodegradation occurs with enzyme activity and/or continues as chemical degradation with living organisms. The polymer is first broken down into smaller chains and in the second step, with the abiotic reaction, e.g. oxidation, photodegradation, hydrolysis or biotic reactions are completed by microorganisms (Jakubowicz, 2003). Biodegradation is directly dependent on the chemical structure of the polymer, the source of the polymer and the degradation conditions as well as the physical structure of the polymer (Chandra and Rustgi, 1998). Synthetic polymers containing hydrolyzable groups in the main chain are hydrolyzed under certain conditions. Such polymers are polyester, polyamide, polyurethane, polyurea, poly (amide-enamine), polyanhydrides (Nair and Laurencin, 2007). Aliphatic polyesters are the most studied polymers because of their diversity in terms of synthetic. They are also biodegradable since ester bonds can be hydrolyzed. The polymers synthesized by polycondensation reaction of two functional monomers have low molecular weight, so ring opening polymerization (ROP) is preferred to achieve high molecular weights (Okada, 2002). It is very difficult to determine the ROP mechanism by kinetic studies or analysis of the end groups and reaction products.

In the literature, three major ring opening polymerization mechanisms are recommended depending on the initiator. These are anionic, cationic and coordination insertion polymerization mecahanisms (Albertson and Varma, 2003). In addition, the polyesters with high molecular weight and having controllable stereochemistry can be achieved by coordination-insertion mechanism (Sattayanon et al., 2015). Kricheldorf and Serra (1985) showed that when metal octoates, carboxylates, oxides or alkoxides was used as an initiator, ROP mechanism proceeds via the coordination insertion. In this mechanism, the covalent metal alkoxides or carboxylates with vacant d orbitals form an active

complex via interact with a compound which has a hydroxide group. And then the resulting new actual initiator reacts with the monomer.

Many theoretical study using DFT on the ROP of lactones such as lactide (LA) (Schenck et al., 2002; Cheshmedzhieva et al., 2012; Lawan et al., 2013), ε-caprolactone (Jones et al., 2015; Liu et al., 2009; Ling et al., 2009) and 1,5-dioxepan-2-one (DXO) (Ryner et al., 2001), have been reported so far. The reaction mechanism through which the reaction proceeded, activation barriers, initiators activity have been investigated in these studies.

Different kinds of alkoxide (Williams et al., 2003; Kricheldorf et al., 1988), alkyl (Chakraborty and Chen, 2003) carboxylates (Kricheldorf and Damrau, 1997) and oxides (Kricheldorf and Serra, 1985) complexes containing several metals such as Sn, Al, Fe, Zn, Ca, Sm, Ti, Y and Mg have been used for the ROP of lactones (Kricheldorf et al., 1988; Meelua et al., 2012, Sattayanon et al., 2014). Among them tin complexes; particularly tin(II) 2-ethyl hexanoate, ($SnOct_2$), are highly effective in ROP due to their high catalytic and low racemization effects (Kricheldorf el al., 1995). It is used prevalently in the industry and academy. However, from the industry point of view, the long duration of induction, toxicity and the uncontrollable molecular weight are disadvantages of this initiator. Therefore, studies on alternative initiators are important. The new initiators including zinc (Vivas and Contreras, 2003), magnesium (Sarazin et al., 2004), calcium (Dobrzyński et al., 1999) and iron (Stolt et al., 2005) metals have been proposed for the synthesis of polymers intended for use in biomedical applications. Also Kricheldorf et al. (1985) have investigated the initiator activity of various metal halides and metal salts, showed that the iron halide and zinc acetate/zinc halide are active in the ROP. So, the theoretical and experimental investigation of the activity of various metal acetates as initiators is one of the purposes of our study.

The polymerizability depends on the ring dimension and the number, size, and position of the substituent. The presence of substituent for all sized-rings decreases thermodynamic stability of the ring and make it feasible for polymerization. The five-membered γ-butyrolactone is generally poorly polymerized, only low molecular weight oligomers are obtained. Since the three-member lactones are very reactive, they are difficult to isolate and there are not much data about them (Odian, 2004). Among the usual cyclic esters (lactones); four-, six-, and seven- membered rings can be easily polymerized by ROP. To

date, β-butyrolactone (Guillaume et al., 2009; Xu et al., 2012), lactide (Balcan et al., 2013; Schwach et al., 1997), glycolide (Frazza and Schmitt, 1971), ε-caprolactone (Kaoukabi, 2015) have been widely studied. However, five-membered lactones (e.g., γ-butyrolactone and γ- valerolactone) are poorly reactive under normal conditions and are impracticable for ROP since they are thermodynamically stable. This is normally attributed to the low strain energy of the ring and to the positive Gibbs free energy related to the polymerization (Gagliardi, 2015). The structures of some lactone are depicted in Figure1.1.

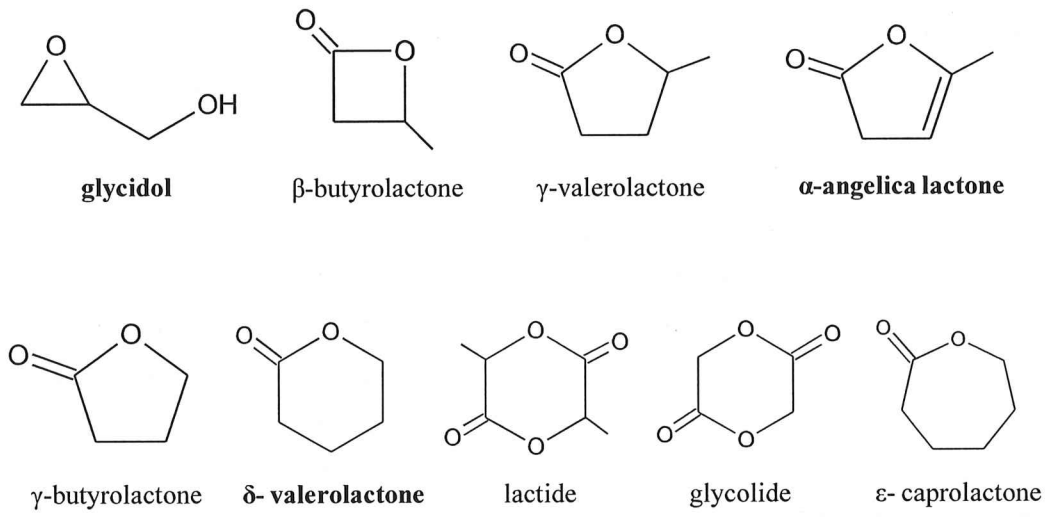

Figure 1.1 Molecular structures of some lactones.

Biodegradable, five-membered, unsaturated, α-angelica lactone (AL), (5-methyl-2(3H)-furan-1-one), can be obtained by dehydration of levulinic acid, a renewable natural raw material, is of interest recently (Tarabanko et al., 2008; Chen et al., 2011). It has been investigated whether AL can be a chemoprotective agent due to its ability to prevent tumor formation (Rodríguez et al, 2007). The structure of AL contains two different functional groups (carbonyl and carbon-carbon double bonds) so its polymerization can proceed through two possible pathways. One of them is ionic polymerization with opening of double bonds (polyfuran formation), and the other is ring opening polymerization (polyester formation). Poly(α-angelica lactone), PAL, synthesized by ROP, has carbon-carbon double bonds (C=C) in its repeating units making it possible to form many polymers by chemical modification. However, there are not many studies in the literature on the ROP of AL. Some of them are mentioned as follows. Chen et al. (2011) have reported ROP of AL with tin(II) 2-ethylhexanoate, ($SnOct_2$), and they obtained fairly high molecular weight (29357 g/mol) and reasonably good yield

up to now. They also investigated the reaction kinetics for ring opening polymerization of AL and the degradability of the obtained polymer. Tarabanko et al. (2008) have synthesized polyesters of AL by using alkali based catalyst with low molecular weight (2000 g/mol). In another study, copolymer of AL with styrene was synthesized and its biodegradation by microorganisms were investigated (Tarabanko et al., 2010). However, homopolymer of AL and its copolymer with ε-caprolactone using $SnOct_2$ were synthesized by Xi et al. (2013). The molecular weight of obtained PAL is 5237 g/mol. Moreover, Danko and Mosnázek (2017) have reported that the reactivity of AL is low and the high molecular weight polymer is difficult to obtain. In this sense, theoretical investigation of the reaction mechanism and thermodynamics sounded us interesting.

Poly(δ-valerolactone) (PVL), obtained by ring opening polymerization of six-membered δ-valerolactone is an important aliphatic polyester since it has good biodegradability, bio-compatibility and permeability properties. Besides, Fay et al. (2006) showed that the copolymerization of ε-caprolactone with δ-valerolactone caused to degradation more rapidly than PCL homopolymer. Therefore, homopolymerization or copolymerization of δ-valerolactone can be suitable for biological applications, e.g. drug delivery and tissue engineering. In the study of Nair et al. (2011), the PVL copolymer was used as a hydrophobic block which is suitable for forming micelle carrier systems of hydrophobic antitumor drugs. Nakayama et al. (1997) studied about enzymatic and nonenzymatic hydrolyse for investigating of biodegradability of poly(valerolactone-co-L-lactide). Until today; PVL was synthesized with N-heterocyclic carbene complexes, metal salts, tin carboxylates and phosphido-diphosphine Group 3 complexes. The enzymatic ring opening polymerization was investigated, too. In a study by Gowda and Chakraborty (2010), it has been found that, in the ROP mechanism of cyclic esters, the ligand groups on the metal catalyst do not have a significant effect in facilitating polymerization. Besides, they reported that the important thing is that determinate the initiator which provides the bond cleavage in the monomer. However, there are not too much studies about PVL in the literature.

In the ROP the electrophilicity of the metal center have an important role. In the polyester synthesized with the initiator having the lowest unoccupied molecular orbital (LUMO), the tendency towards formation of the metal-oxygen bond is high (Schenck et al., 2002). This leads to an increase in the polarization of the active carbonyls. Thus, a product having a higher molecular weight and a

higher polymerization yield is obtained. Another determining factor is atomic charges. It is known that there is a good correlation between the charge of nucleophilic center and reactivity (Sattayanon et al., 2015). Therefore, when it is desired to compare the activity of initiators containing different metals with similar ligand group or when it is desired to make an initiator proposal without conducting an experiment, the LUMO and natural orbital analysis (NBO) of the complexes should be investigated.

Glycidol is an attractive monomer because polyglycidol obtained by ring opening polymerization have a hydroxyl-functional structure. The polyglycidol, a biomaterial with biological inertness and hyperbranched structure, has been the focus of many applications and several studies (Royappa et al., 2012). However, theoretical study on the mechanism of polymerization is not included in the literature. Petchsuk et al. (2009) synthesized random copolymerization of glycidol and lactide and analyzed hydrolyzability, thermal behavior and biodegradability. They found that thermal stability and structural properties changed according to the rate of glycidol in copolymer. Pitet et al. (2007) studied the ROP of lactide in the presence of $SnOct_2$ and glycidol. They found that the opening of the glycidol ring at the low temperature was prevented and located at the polymer chain end. On the other hand, at high temperatures, they showed the ring opening of glycidol cause to form hyperbranched polyesters with lactide. Gottschalk et al. (2007) used polyglycidol as multifunctional initiator for lactide polymerization and synthesized star block copolymers. Some studies have suggested that the protection of the OH group provides a higher molecular weight polymer (Dimitrov et al., 2002). Any study about copolymerization of glycidol and other lactones are absent from the literature. Therefore, we investigated copolymerization synthesis of δ-valerolactone and glycidol. Furthermore, copolymer synthesis was carried out by protecting the -OH function in the glycidol monomer and the process was investigated.

In this study, biodegradable and biocompatible, functional poly(α-angelica lactone) and poly(δ-valerolactone) were synthesized by ring opening polymerization in the presence of metal acetate complexes as alternatives to previously studied initiators. Besides, synthesis of poly(δ-valerolactone-co-glycidol), not included in the literature, was carried out with $SnAcet_2$. The obtained polymers were characterized by FTIR, ^{1}H-NMR, GPC, and TG. Initiation and propagation stage for coordination insertion reaction mechanisms of monomers were studied by semiemprical and DFT methods. The thermodynamics

of the system were also discussed. In addition, initiators ($SnAcet_2$, $PbAcet_2.3H_2O$, $CdAcet_2.2H_2O$, $NiAcet_2.4H_2O$ and $CuAcet_2.H_2O$) efficiency was analyzed by natural bond orbital (NBO) and LUMO analysis using several DFT methods and compared with experimental data. Toxicity tests for PVLs synthesized with acetate complexes containing Sn, Cd and Pb were also carried out. Our motivation in this study is to explain the ring opening polymerization process of lactones, to give direction to the process and to predict initiator efficiency before conducting experiment by means of computational chemistry methods.

2. POLYMER SYNTHESIS METHODS

Polymer synthesis reactions are generally divided into two groups as addition polymerization and step polymerization. In the addition polymerization, the chain grows by repeatedly and rapidly addition of monomer molecules to the active center. Propagation reactions always occur between monomer molecules with active chains. At the beginning of polymerization high molecular mass polymer is formed while only high molecular weight polymer and monomer are present in the media throughout the reaction. Step polymerization progresses stepwise between molecules having functional groups. First, two monomers enter the reaction to form a dimer, which interacts with another monomer or dimer to form a trimer or tetramer. Then, with similar reactions, the chains continue to grow. Different sized molecules in the medium react with each other, and the molecular weight of the polymer gradually increases with time (Odian, 2004).

2.1 Step Polymerization

Many chemical reactions can be used for synthesis of polymers by stepwise polymerization. Examples of such reactions include esterification, amidation, formation of urethanes, aromatic substitution and others. Polymerization usually results in reactions between two different groups such as hydroxyl and carboxyl groups or isocyanate and hydroxyl groups. There is a difference between the polycondensation (a) and the polyadditions (b) depending on the separation of the small molecule at the initiation step of the polymerization reaction (Odian, 2004).

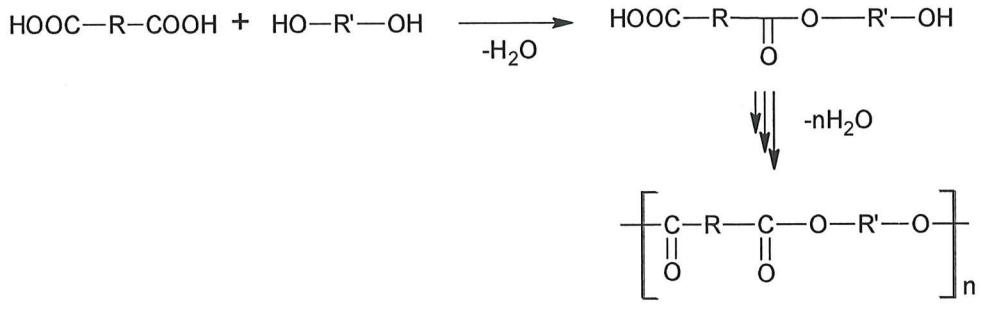

(a)

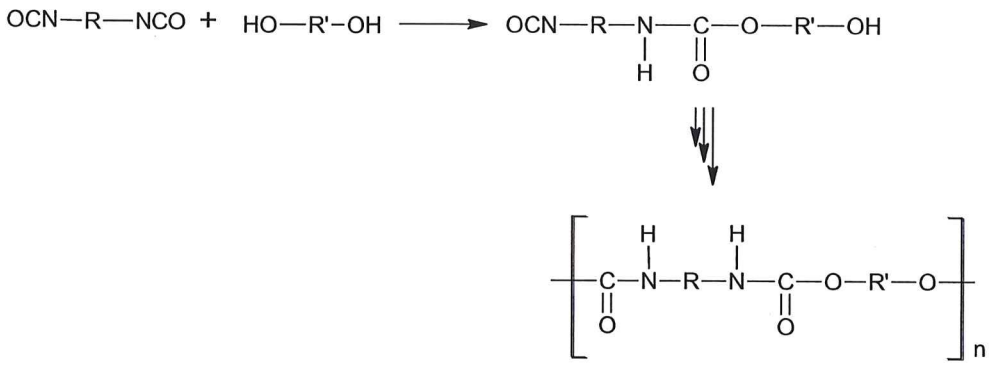

(b)

It can be said that polymer chain cannot form from monofunctional molecules through step growth polymerization. In fact, as in each monomer molecule, there should be two functional groups in all intermediates. If there are more than one functional group in a monomer, branched or crosslinked polymers are obtained. Furthermore, step growth polymerizations are classified according to how the functional groups are assigned to the monomers. If each monomer has two identical functional units, the resulting reaction is called AABB-type polycondensation/ polyaddition. Mixtures of at least two monomers having complementary functional groups are required here (eqs a and b). If two different functional groups are present on each monomer, this process is called AB type polycondensation/polyaddition (eqs. c and d).

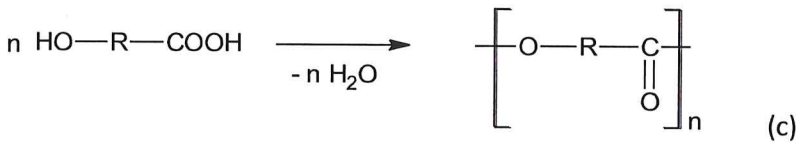

(c)

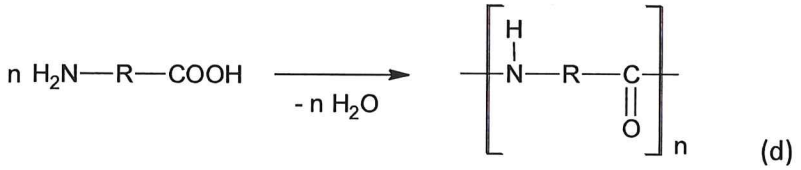

(d)

Chain formation in stepwise polymerization occurs via a series of random and free reaction events due to the absence of specific active centers. The reaction proceeds from the dimers to short and long oligomers in the formation of condensation polymers or additional polymers. In addition, the 1: 1 equivalence of complementary functional groups is important to obtain high molar masses and large conversion ratio. (Braun et al., 2005) Characteristic features of chain and step polymerization mechanism was given at Table 2.1.

Table 2.1 Characteristic features of chain and step polymerization mechanism (Billmeyer, 1984).

Chain Polymerization	**Step Polymerzation**
In the growth step, monomers are added one by one in the chain.	Any two monomers present in the medium may interact with each other.
As the reaction progresses, the monomer concentration decreases continuously.	In the first stages of the reaction the monomer concentration decreases rapidly.
While the high molecular weight polymer occurs at the beginning of the reaction, it does not change much during the reaction.	The molecule weight of polymer consistently increases during the reaction.
Longer reaction times lead to higher yields, but a slight influence on molecular weight.	Long reaction times to obtain high molecular weights are required.
Reaction mixture comprises only monomer, high polymer, and about 10-8 part of growing chains.	All molecular species are present in the computable distribution at each step.

2.2 Condensation Polymerization

The condensation reaction is the most suitable organic reaction to synthesize stepped polymer. This reaction takes place among the molecules including functional groups such as -OH, -NH_2, -COOH. The monomers entering the

reaction combine via leaving a small molecule such as water or methanol. For the polymerization reaction there must be at least two functional group on the monomer that can enter the condensation. As the condensation reactions progress from one point to the next, polymer chains form. Examples of condensation reactions suitable for polymer formation are given below.

a) The polyesters can be synthesized from condensation reactions between diol and dicarboxylic acid.

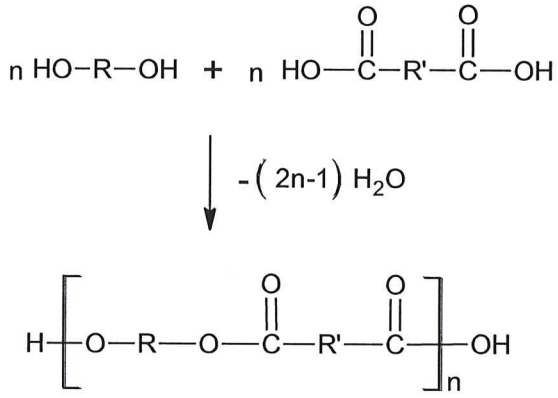

polyester

If the components have two functional groups, the condensation product is linear, but if at least one of the reactants is tri or tetra functional, then the resulting polymer is cross-linked.

The polyamides can be synthesized from the condensation reactions between the diamine and the carboxylic acids. For example, Nylon is a very common condensation polyamide.

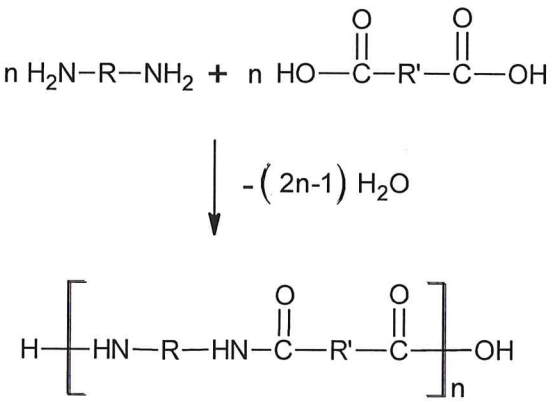

polyamide

b) The bifunctional molecules carrying -OH and -COOH or $-NH_2$ and -COOH groups may enter the condensation reaction to give the polyester and polyamide, respectively.

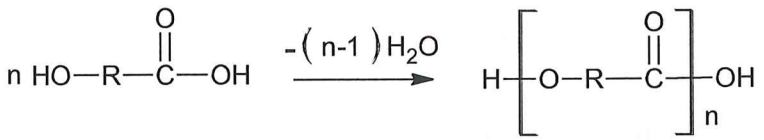

polyester

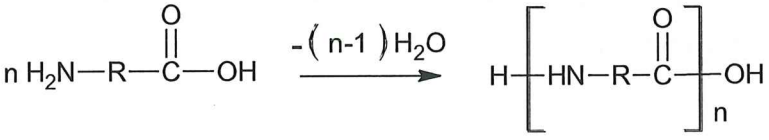

polyamide

c) The reactions between the dicarboxylic acid esters and the diols proceed through the condensation, while the small molecule separated in the reaction is the alcohol.

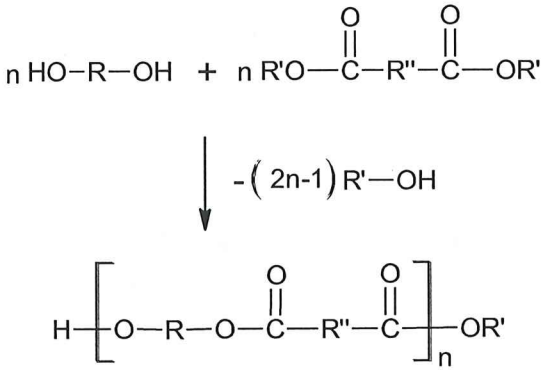

d) Polyamide synthesis by leaving of HCl between dicarboxylic acid chlorides with diamides is another example.

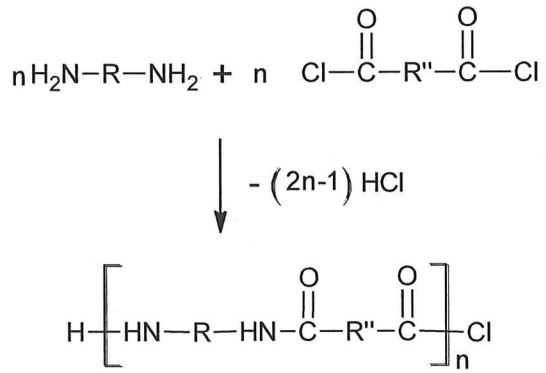

polyamide

2.3 Radical Chain (Addition) Polymerization

Polymerization reactions of monomers containing unsaturated groups in the structure involve a chain reaction. The polymer may be synthesized through a radical or ionic mechanism.

Radical addition polymerization is a well-known polymerization method. In 1920, Staudinger gave the first information on addition polymerization. In 1937 Flory described that, similar to the chain reactions of low molecular weight substances, radical polymerization proceeds through the steps of initiation, propagation and termination.

Polymerization starts over radicals and chain growth proceeds over radicals. In the propagation step, the single electron at the end of the active chain reacts with one of the π-electrons in the double bond of the monomer to form a new monomeric chain. The other π-electron is transmitted to the chain end.

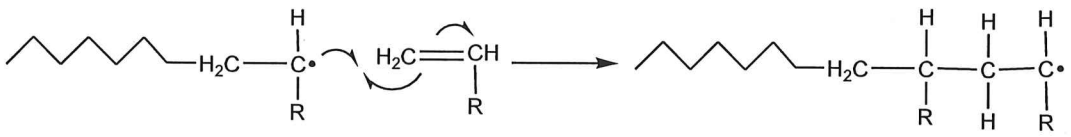

Carbon-carbon double bond, due to its relatively low stability, is particularly susceptible to attack by a free radical. The monomers containing double bond such as CH_2=CHX and CH_2=CXY called vinyl monomers (Billmeyer, 1984).

2.3.1 Initiation of Radical Addition Polymerization

Polymerization of a suitable monomer for radical addition polymerization is initiated by formation of free radicals in the medium. These free radicals are produced by using chemical substances or using some physical factors. The chemical substances listed in Table 2 are compounds that can form radicals by decomposing spontaneously or under the influence of heat under normal conditions. When physical factors such as heat, light, beam with high energy are used, the first radicals are composed of monomer, solvent or other substance present in the polymerization medium. In addition, electrochemical method is another way to produce radical.

Table 2.2 Chemical substances and physical factors used in the initiation of radicalic polymerization.

Chemicals	**Physical factors**
organic peroxide or hydroperoxides	heat
azo compounds	light and UV-rays
redox initiators	high energy beams
organometallic compounds	electrochemical method

2.3.2 Ionic and Coordination Chain (Addition) Polymerization

Chain reaction polymerization takes place with many mechanisms other than those involving free radicals. The most remarkable of these are the so-called *anionic and cationic polymerizations*, in which the chain carriers are carbanion or carbenium ions. And also; polymerization can take place with mechanisms involving coordination compounds (formed between catalyst, monomer and growing chain, *coordination or insertion polymerization).* Another chain polymerization is the *ring-opening polymerization* reaction.

2.4 Ring Opening Polymerization (ROP)

The ring opening polymerization is used to mean the polymerization of ring structures, to produce linear macromolecules. Cyclic ethers, cyclic esters (lactones), cyclic amides (lactams) and cyclic amines are polymerizable monomers with ring opening polymerization (Table 2.3).

Table 2.3 Examples of polymers synthesized by ring opening polymerization.

Polymer Type	Monomer structure	Polymer repeating group	Monomer type
Polyalkene	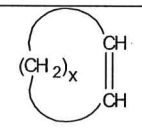	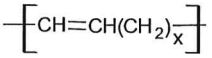	Cyclic alkane
Polyether	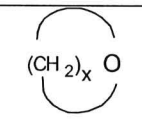	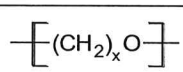	Cyclic ether
Polyester	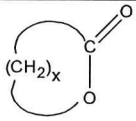	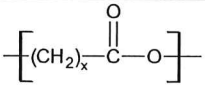	Lactone
Polyamide	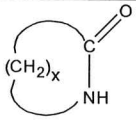	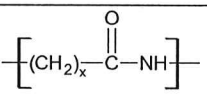	Lactam
Polysiloxane	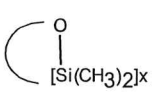	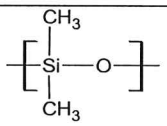	Cyclic siloxane
Polyphosphazene	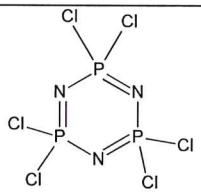	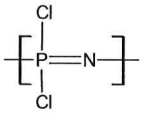	Hexachloro-cyclotriphosphazene
Polyamine		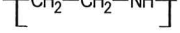	Aziridene

In ROP, the monomers are added one by one to the chains and the polymerization reaction is only observed between the active chains and monomer molecules, furthermore two molecules larger than the monomer, such as dimer or trimer, cannot enter the reaction as in addition polymerization. Because of these similar properties, ring-opening polymerization is similar to addition polymerization. However, they differ from each other at some points. Addition polymerizations require the presence of double bonds in the monomer structure and high molecular weight polymers are achieved in the initial stages of polymerization. However, in the ring-opening polymerization there is no requirement for double bond in the monomer structure and polymerization with high molecular mass polymers is achieved in the last stages.

2.4.1 General Mechanisms in Ring-Opening Polymerization

The polymerization reaction mechanism is classified depending on the type of initiator. There are three major mechanisms; cationic, anionic and coordination-insertion. Besides, high molecular weight polyester synthesis is usually obtained by anionic and coordination-insertion ring opening polymerization. In addition, there are a variety of very unpopular mechanisms in which radicalic, zwitterionic or active hydrogen initiators are used (Jerome and Teyssie, 1989).

2.4.1.1 Anionic Ring Opening Polymerization

Many ionic and covalent anionic initiators have been used for the polymerization of lactones (Penczek and Duda, 1993; Jedlinski, 2002). Examples of the most effective anionic initiators are alkali metals, alkali metal oxides, alkali metal naphthalenide complexes with crown ethers, etc. Depending on the nature of the initiator and the monomer and on the reaction conditions, the polymerization process can proceed through the living or a nonliving mechanism (Duda and Penczek, 2001). When the nucleophilic anion of the initiator attacks the carbonyl group of the lactone, resulting in cleavage of the carbonyl carbon and endocyclic oxygen bond, the polymerization reaction is initiated. This oxygen then becomes the new anion that allows the reaction to proceed. However, the initiators which are highly nucleophilic at elevated temperature are sufficiently basic to deprotonate the monomer; leading to racemization, back biting reaction and other side reactions which inhibit chain propagation. For this reason, it is difficult to attain high molecular weight polymer by this polymerization method. However, high molecular weight polymers were obtained by anionic polymerization carried out in polar solvent (Jedlinski et al., 1985).

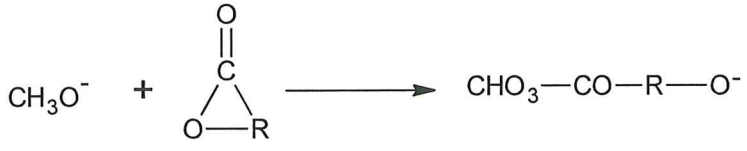

with propagation as

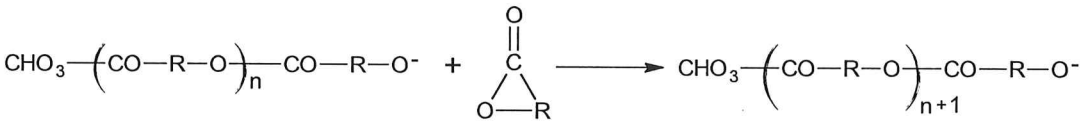

Figure 2.1 Anionic ring opening polymerization.

2.4.1.2 Cationic Ring Opening Polymerization

The catalyst for the cationic ring opening polymerization can be several strong acids such as triethyloxonium, tetrafluoroborate, borontrifluoride, trifluoroacetic acid and carbenium ion donors. Also using this method, 4-, 6- and 7-membered cyclic lactones can be polymerizable. In the initiation stage of cationic polymerization, it is suggested that the ring is not opened and a coordination intermediate which interacts with the monomer (usually an oxonium ion) is initially formed and the catalyst then acts as an initiator. A nucleophilic attack by a second monomer acting as an initiator breaks the ring to form another electrophilic carbenium ion. The propagation step of this polymerization is repeated as a nucleophilic attack by the other monomers, and the polymerization continues until it is terminated with a monofunctional nucleophile such as water. High temperature in the cationic polymerization caused racemization, due to the attack of the second monomer to chiral center in propagation chain and cationic polymerization is difficult to control. Indeed, the racemization temperature is very slow at > 50 °C, but at this temperature the reaction rate is very slow and does not give a high molecular weight polymer.

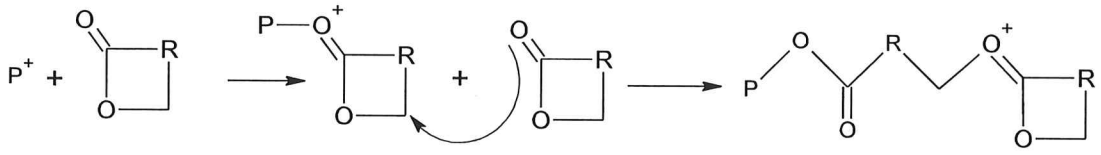

Figure 2.2 Cationic ring opening polymerization.

2.4.1.3 Coordination Insertion Ring Opening Polymerization

In this method, metal alkoxides and carboxylates with free p-d orbital are the most widely used initiators (Mg, Sn, Ti, Zr, Zn, Al alkoxides). These initiators, which have a covalent bond between the metal and the oxygen atom, react in the polymerization as coordination initiators not anionic. Because it is thought that the growth step proceeds by the coordination of the monomer with the active species and the addition of the monomer to the metal-oxygen bond via rearrangement of the electrons. Carboxylates, which are weaker nucleophiles compared to alkoxides, are thought to act as catalyst instead of initiator. For this reason, better results are obtained if the metal carboxylates are used together with an active hydrogen compound (e.g., alcohols) as co-initiator. This reaction mechanism begins with the interaction between the exocyclic oxygen atom of the cyclic monomer and the metal atom of the initiator. The coordination of the exocyclic oxygen with the metal atom causes polarization, which makes the carbonyl of the monomer more responsive for nucleophilic attack. The reaction proceeds by breaking the acyl-oxygen bond present in the monomer and adding the new monomers into the bond between the metal atom and its adjacent oxygen atom, while the other end becomes an alkoxylating dead chain of the initiator. By varying, the polymerization variables enable a wide range of molecular weights to can be controlled. High molecular weight is obtained when this method is employed (Gupta and Kumar, 2007).

Both inter- as well as intramolecular transesterification reactions is leaded by ring-opening polymerization of lactones with these organometallic initiators at high temperatures or long reaction times. Both types of transesterification reactions cause an increase in polydispersity of the polyesters.

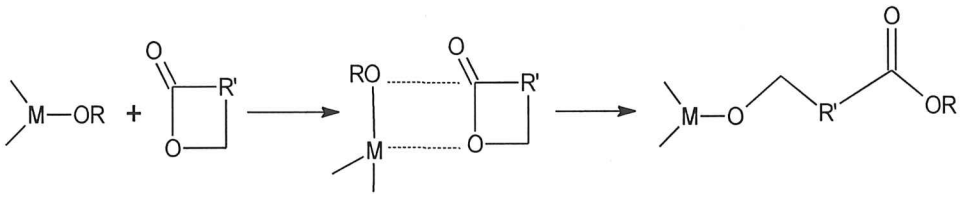

Figure 2.3 Coordination ring opening polymerization.

2.4.2 Initiators for ROP

Synthesis of new initiators; the ring opening polymerization of existing or new monomers and macromers substituted with functional groups provides a very interesting and promising strategy for producing structurally improved macromolecules. Catalysts used for efficient polymer synthesis are metal powders, organometallic compounds, metal carboxylates, metal alkoxides, lewis acids, lewis bases and different salts of metals (Lundberg and Cox, 1969). Many polymerization reactions catalyzed by metal complexes are specific. In addition, a desired polymer structure can be produced by reactions formed by careful selection of metal and ligands (Gupta and Kumar, 2007). The covalent metal alkoxides with free p or d orbitals react as coordination initiators and not as anionic or cationic initiators (Kricheldorf et al., 1988).

Table 2.4 Metal-containing initiators used in ring-opening polymerization.

Zn, **Pb**, Sb, Bi, salts	*J Macromol Sci Pure Appl Chem 1993;A30(6/7):441–8*
Iron	*Macromolecules 1999;32(20):6412–7*
Zn salts and Zn(II) L-lactate	*Makromol Chem Phys 1997;198(6):1753–66*
Aluminum/Schiff base	*J Polym Sci Part A PolymChem 2004;42(23):5974–82.*
Gold(I)	*Eur J Inorg Chem 2006;2006(18):3724–30*
Yttrium(III)	*Macromolecules 2000;33:3970–7*
Zn lactate	*Polym Bull 1996;37(6):771–6*
Zinc(II) complexes	*Eur J Inorg Chem 2002;2002(8):1948–51*
Tin(II) complexes	Eur J Inorg Chem 2002;2002(8):1948–51
Zinc metal and zinc lactate	Polym Int 1998;46(3):177–82
Organomagnesium complexes	Organometallics 2005;24:580–6.
Zn and Al	Makromol Chem 1993;194(3):907–12.
Yttrium octoate	USPatent No. 5208297; 1993
Germanium	J Polym Sci Part A Polym Chem 2003;41(19):3074–82.

2.4.3 Polymerizability of Cyclic Monomers

Thermodynamics and kinetic factors have a decisive influence on the polymerization of cyclic structure. The only significant factor determining whether a cyclic monomer can be converted into linear polymer is the thermodynamic factor, i.e., the relative stability of the cyclic monomer and linear polymer structure. The thermodynamic stability of the monomers is related to the strain in the ring structure. The strain in the cyclic structure is very high for 3 and 4 member rings, sharply reduced for 5-, 6- and 7-member rings, increased for 8-13

member rings and then reduced again for larger rings. The strain in the ring structures consists of two types, angle and conformational strain. Thermodynamically, structures other than 6-membered ring monomers are suitable for polymerization. Generally, polymerizations of 6 membered rings are not observed. The bond angle strain in 3-4 membered rings, the conformational strain existing in 5 membered ring, and transannular strain in 7-8 membered rings when compared; the thermodynamic stability can be given by 3, 4 << 5, 7-13 < 6, 14 and larger. The semi- experimental enthalpy, entropy and free energy changes for the conversion of the cyclic monomers into linear polymers are shown in table 2. ΔH is a very significant agent in ΔG determination in 3 and 4 member rings, while ΔS is important in 5 and 6 member rings. In larger cyclic structure enthalpy and entropy factors contribute equally. The presence of substituents in the ring acts on reducing the thermodynamic suitability for polymerization of ring structures. The interaction between the substituents in the linear polymer is more intense than that of the cyclic monomer, with the result that entropy is less negative than enthalpy.

Table 2.5 Thermodynamics parameters of polymerization of different membered rings at 25 ^{0}C (Odian, 2004).

$(CH_2)_n$ (n)	ΔH (kJ mol^{-1})	ΔS (J mol^{-1} K^{-1})	ΔG (kJ mol^{-1})
3	-113.0	-69.1	-92.5
4	-105.1	-55.3	-90.0
5	-21.2	-42.7	-9.2
6	+2.9	-10.5	+5.9
7	-21.8	-15.9	-16.3
8	-34.8	-3.3	-34.3

While all ring structures except 6-membered cycloalkanes were expected to thermodynamically polymerize, mostly cyclopropane derivatives have been studied and only oligomers are obtained. As a result, it can be said that the thermodynamic suitability does not guarantee the polymerization of a cyclic monomer. Polymerization requires the presence of a kinetic pathway for the opening of the ring and for reaction. While cyclic monomers such as lactones, lactams, cyclic ethers can undergo polymerization, cycloalkanes cannot be polymerized easily because they do not contain a heteroatom that provides a site

for electrophilic and nucleophilic attack. Thus, such monomers are suitable for both kinetic and thermodynamically for polymerization.

2.5 Thermodynamics of Polymerization

It is known that whether a chemical reaction occurs spontaneously depends on Gibbs free energy (spontaneous if $\Delta G < 0$, non-spontaneous if $\Delta G > 0$). Likewise, the ability of a monomer to polymerize depends on the free enthalpy of polymerization, i.e. Gibbs free energy.

$$\Delta G_p = \Delta H_p - T\Delta S_p \tag{2.1}$$

The magnitude of ΔG related with the lowest energy state, not how fast the reaction will take place. Employment of different catalysts can affect the transition state of reaction in various ways but does not change the basic features of the system. The Gibbs free energy of the polymerization reaction determines the polymerization equilibrium behavior of different membered lactones according to ring size and substituent degree (Figure 2.4).

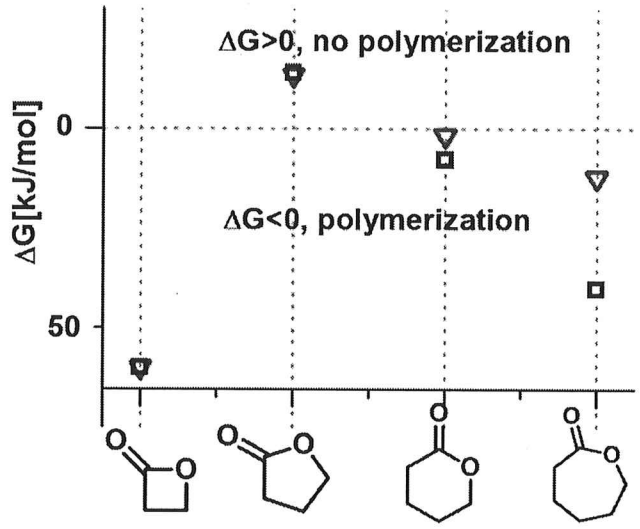

Figure 2.4 Difference in ΔG as a function of ring-size at normal pressure and at 25 °C; blue squares and red triangles represent different extracted values from the literature (Olsén et al., 2016).

Ring strains (angular, conformational, and translational strains) are usually the driving force in ring opening polymerization of most cyclic monomers. At the same time, the polymerization enthalpy is a measure of the ring strain when there is no interaction of the solvent with monomer and polymer.

Entropy is reduced during the polymerization process of the monomers, usually due to a decrease in the translational degrees of freedom. Hence, effect of the positive entropic contribution ($-T\Delta S_p$) that influence ΔG_p will decrease when exothermicity of enthalpy is large. (|when $\Delta H_p < 0$ and $\Delta S_p < 0$, $|\Delta H_p| > -T\Delta S_p$ is required). For this reason, the higher the ring tension, the higher the concentration of polymer at equilibrium. Angle and bond deformations, which are apparent for three and four member rings, cause a high ring strain and good polymerization. Some of the five- and six-membered ring cyclic alkanes cannot polymerize due to low ring strain. However, if a sulfur atom or a carbonyl group is introduced into some of five-membered rings under normal conditions, they can be polymerized but resulting composition provide low molecular weight polymer formation (Duda and Kowalski, 2009). Besides, the presence of the ester or siloxane groups in the six-membered ring structure increases the ring tension and monomer is polymerized easily.

2.6 Copolymerization

Polymer synthesis in its chains with multiple monomer units having different chemical structure is called copolymerization. The resulting structure is called the copolymer. If there are three or four different monomers in the copolymer chains, it is called as terpolymers and quaterpolymers, respectively. Although copolymers can be synthesized by step polymerization or addition polymerization methods, the addition polymerization is more suitable for copolymer synthesis and most commercial copolymers are produced by this method.

The polymerization method employed and the mechanism of polymerization may affect the array of monomer molecules along the chain in a copolymer synthesized from two monomers of type A and B. Units A and B may be take part in the main chain as random, sequential or blocks.

i) random copolymer: In such copolymers, there is no particular order in which the A and B monomer units are arranged along the chain. The radical copolymerization of olefins generally yields a random copolymer. The

properties of random copolymers are often different from the properties of the homopolymers that form it.

$$-A-B-B-A-A-A-B-A-B-B-B-B-A-$$

ii) alternating copolymers: In the sequential copolymer, the A and B monomer units are arranged in the polymer chain to be A and B. The properties of such copolymers differ from those of their homopolymers.

$$-A-B-A-B-A-B-A-B-A-B-A-$$

iii) block copolymer: Block copolymers are formed by linking two homopolymers, which have different chemical structure, from the chain ends. In the two-block copolymer formed by the monomers A and B, a part of the chain contains the A monomer block and the other part of chain contains the B monomer block. If the chain is followed by the block consisting of the A monomer again, three block copolymer is occurred. The number of blocks can be increased by similar operations. The physical property of most of the block copolymers, unlike other copolymer types, is among the physical properties of the homopolymers that forms itself.

$$-A-A-A-A-A-A-A-A-B-B-B-B-B-B-B-$$

two-block monomer

$$-A-A-A-A-A-A-B-B-B-B-B-B-A-A-A-A-$$

three-block monomer

iv) graft copolymer : In graft copolymers, two polymer chains with different chemical structures are bonded together at a location other their chain ends. The number of bonding points (graft points) may be more or less. The properties of the graft copolymers generally fall between the properties of their homopolymers.

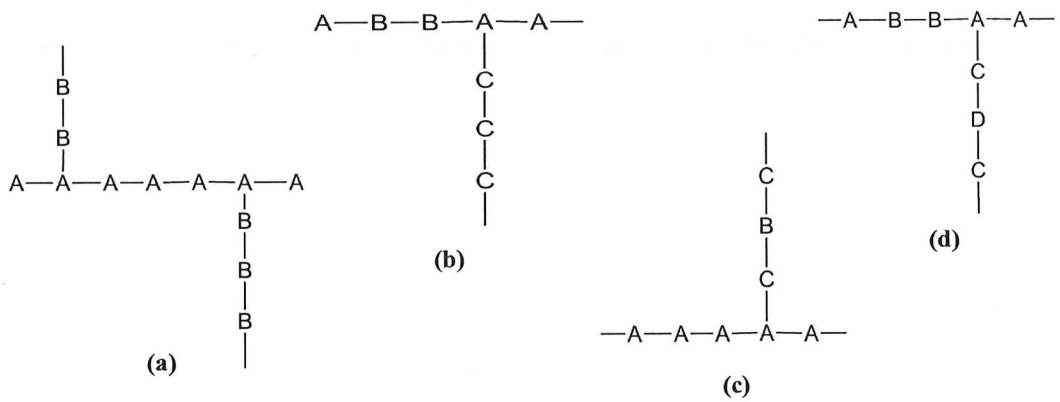

Figure 2.5 a) main chain and graft chains are homopolymer, b) main chain is copolymer and grafted chains are homopolymer, c) main chain is homopolymer and graft chains are homopolymer, d) main chain and the grafted chains are copolymers.

3. THEORETICAL CALCULATION METHODS

'Scientific discovery and scientific knowledge have been achieved only by those who have gone in pursuit of them without any practical purpose whatsoever in view'
Max Planck

Chemistry is the science dealing with construction, transformation and properties of molecules (Jensen, 2007). Computational chemistry is a subfield of chemistry that aims to explain chemical processes and problems using computers with the help of basic laws of physics or quantum mechanical methods. Energy, optimum geometry, orbital energy levels (HOMO, LUMO, others), electron density, vibrational frequencies (IR spectra), electronic excitation energy (UV-VIS spectra), reaction rate, reaction path and barrier height can be calculated. Computational chemistry, which has become very popular nowadays, can be used more effectively for the development of complex chemical and biological processes by the developments in computer hardware and software (Ramachandran et al., 2008).

Molecular mechanics or electronic construction methods (quantum mechanics) are used to calculate the properties of molecules. Molecular mechanics calculations are based on classical mechanical methods. The electronic structure methods are much more complex and take much longer computational time than the molecular mechanics methods do. The basis of modern electronic structure methods is based on the equation proposed by Schrödinger in 1926.

Despite the Schrödinger equation can be fully solved for single electron systems, it is impossible to solve mathematically for systems with more than one electron number. In this case, the equation is solved by making some approaches. (Lee and Yang, 1959; Macke, 1955)

3.1 Molecular Mechanics

In generally; the molecular mechanics method used to model very large and unsymmetrical chemical systems, such as proteins or polymers, establish a simple algebraic expression for the energy of a compound, without calculating a wave function or the total electron density of the system. Energy expression of the system to describe energy associated with intermolecular forces such as tension, bending, rotation, van der Waals interactions and hydrogen bonding; it consists of

simple classical equations such as the harmonic oscillator equation. The constants in this equation are obtained either from spectroscopic data or from ab initio calculations (Young, 2001).

In molecular mechanics, a set of related constants and equations is called the force field. Transferability of parameters (if two atoms are in similar environment their parameters will be very similar to each other) is the main supposition of this theory. The data base of the compounds used in the parameterization of the method is very important since they determine the success of the molecular mechanical method. In addition, a molecular mechanics method can be parameterized against a specific class of molecules such as proteins, organic molecules, organometallics, etc. On the contrary, molecular mechanics calculations cannot solve problems such as breaking or formation of bond since molecular mechanics methods use harmonic oscillator potentials.

3.2 Molecular Dynamics

Molecular dynamics (MD) is a simulation of time-dependent behavior of a molecular system such as vibrational or Brownian motion. Generally, in an MD simulation, molecular mechanics methods that calculate the forces on the atoms for any given geometry is used to compute the energy of the system (Young, 2001). The MD methods are used to determine the physical properties (conformational changes, dynamics and thermodynamics of systems) of multi particulate systems at a specified time interval, exploiting classical physics rules.

3.3 Electronic Structure Methods (ESM)

Electronic construction methods use quantum mechanical laws instead of classical physics laws. The energy of a stable geometry of a molecule is calculated from solution of the time-independent Schrödinger equation (Lowe and Peterson, 2006). The time-independent and non-relativistic form of the Schrödinger wave equation is given below (equation 3.1).

$$\hat{H}\Psi = E\Psi \qquad (3.1)$$

Here, H is the Hamilton operator that expresses the total energy in atomic units, E is the energy of the level, and ψ is the wave function. The wave function is the

function of the Cartesian coordinates and spin coordinates of all the nuclei and electrons in the molecule (equation 3.2).

$$\hat{H} = \underbrace{-\sum_{i=1}^{N}\frac{1}{2}\nabla_i^2}_{T_e} \underbrace{-\sum_{a=1}^{M}\frac{1}{2M_a}\nabla_a^2}_{T_N} \underbrace{-\sum_{i}^{N}\sum_{a}^{M}\frac{Z_a}{r_{ia}}}_{V_{En}} + \underbrace{\sum_{i}^{N}\sum_{j>i}^{N}\frac{1}{r_{ij}}}_{V_{ee}} + \underbrace{\sum_{a}^{M}\sum_{b>a}^{M}\frac{Z_a Z_b}{R_{ab}}}_{V_{NN}}$$

$$\hat{H} = T_e + T_n + V_{ne} + V_{ee} + V_{nn} \tag{3.2}$$

Here, i and j are indices of electrons whereas a and b are indices of atomic nuclei. ∇^2 stands for the Laplace operator; M_a is the mass of a^{th} nucleus; Z_a and Z_b are atomic numbers of nuclei a and b, respectively; r_{ia} is the distance between the electron i and the nucleus a; r_{ij} is the distance between i and j electrons; R_{ab} is the distance between a and b nuclei. Also, the symbol T and V refer to kinetic and potential energy terms, respectively.

As the number of electrons and nuclei increases, solution of this partial differential equation becomes harder and harder.

3.3.1 The Born-Oppenheimer Approximation

The Born Oppenheimer approximation (Born and Oppenheimer, 1927) is an approach based on the assumption that nucleus is stationary because the difference between the masses of electrons and nuclei is very large. This approach divides wave function into nuclear and electronic parts. Kinetic energy term for nucleus, T_N, can be neglected and potential energy term becomes constant V_{NN}, due to fixed nucleus, the number of variables is reduced by a considerable amount in the solution of the electronic part.

$$\hat{H}_{el} = -\sum_{i=1}^{N}\frac{1}{2}\nabla_i^2 - \sum_{i}^{N}\sum_{a}^{M}\frac{Z_a}{r_{ia}} + \sum_{i}^{N}\sum_{j>i}^{N}\frac{1}{r_{ij}} \tag{3.3}$$

3.3.2 Ab Initio Methods

The meaning of "*ab initio*" in Latin is "from the beginning" or "from first principles". This name is given to the calculations which are derived from quantum chemistry (i.e. the Schrödinger equation) without any usage of

experimental data other than physical constants. Moreover, ab initio methods try to solve the Schrödinger equation via several approaches. These are usually mathematical approaches such as using a simpler functional form for a function or invention an approximate solution for a differential equation (Young, 2001). Ab initio electronic structure methods are Hartree–Fock, Post-Hartree–Fock and Multi-reference methods.

3.3.3 The Hartree-Fock (HF) Approximation

Even though the Born-Oppenheimer approach significantly reduces the complexity of the Schrödinger equation, the electronic Schrödinger equation due to electron-electron interactions is still extremely complex. The most common kind of *ab initio* calculation is named Hartree-Fock calculation (abbreviated HF), in which the fundamental approximation is called the mean field approximation. This means that the method does not explicitly involve Coulombic electron-electron repulsion in the calculation, but its average effect is attached to the calculation. In this theory, each electron moves independently and experiences all the others as an average potential, and with this approach, the multi-electron wave function can be expressed as the product of the eigenfunctions (ψ_i) of single electron Hamiltonian operators (Hartree, 1928; Fock, 1930) (equation 3.4).

$$\psi(r_1 r_2 \dots \dots r_N) = \psi_1(r_1)\psi_2(r_2) \dots \dots \psi_N(r_N) \tag{3.4}$$

Since the Hartree multiplication of equations does not provide the Pauli excursion principle, indicating that all quantum numbers of the two fermions cannot be the same, the wave function, is antisymmetrized via establishing in the form of Slater determinant.

$$\psi_{SD} = \frac{1}{\sqrt{N!}} \begin{vmatrix} x_1(1) & x_2(1) & \dots & x_N(1) \\ x_1(2) & x_2(2) & \dots & x_N(2) \\ \vdots & \vdots & \ddots & \vdots \\ x_1(N) & x_2(N) & \dots & x_N(N) \end{vmatrix} \tag{3.5}$$

The row components of the Slater determinant (equation 3.5) indicate the availability of an electron in different spin orbitals, and when two line or columns are replaced, the determinant changes sign and Pauli principle is provided. If there are two identical rows (or columns) in the determinant, the value of the determinant is zero.

The fact that the time-independent Schrödinger equation is not a definitive analytical solution for systems containing an excess of electrons is the reason for the emergence of the second approach of the HF theory. In this method, the wave function is formed by the linear combination of atomic orbitals (Linear Combination of Atomic Orbitals, LCAO) obtained by solving the Schrödinger equation for single electron atoms.

$$\psi_i = \sum_i^N a_i \phi_i \tag{3.6}$$

ϕ_i refers to atomic orbital and a_i refers to the orbital coefficients in equation 3.6.

3.4 Semi empirical Methods

Semi empirical methods are based on Hartree-Fock theory. However, they contain lots of approximations and also they have some parameters obtained from experimental data. In these methods, some pieces of data, such as two electron integrals, are approximated or completely excluded. Generally, a minimal basis set is used and core electrons are not included in the calculation. The semi empirical methods are parameterized to correct errors coming from the omitted part of the calculation. These parameters are obtained by fitting the results that best agree with experimental data or ab initio results.

Semi empirical methods including lot of approximations require much less computation time than the ab initio methods, but the results obtained by semi empirical methods are most probably less reliable. For example, when the molecule to be calculated is similar to the molecules in the database used to parameterize the method, the results may be very good. If it is significantly different from any molecules in the parameterization set, the results may be too weak. The success of semi-empirical methods depends on how well the parameters are. In addition, the good parameters are related to the larger molecular database (Jensen, 2007).

Semi-empirical methods are very successful in the definition typical organic and biological systems but they may not to be true for situations involving hydrogen bonding, chemical transitions, or nitrated compounds.

Some of the most common semi-empirical methods can be classified according to their handling of electron-electron interactions. Hückel theory is the oldest and

fundamental one. The Hückel theory only models the pi valence electrons, while all the valence electrons are modeled in the extended Hückel theory. Being applicable to all elements in the periodic table has made the Extended Hückel theory attractive. It is preferred in inorganic modeling and band structure calculations because of having low calculation time. However, it is known that it is rather weak for predicting molecular geometries.

The NDO methods ignore some of the electron-electron interactions and they model valence orbitals. Almost all types of electron-electron interactions are ignored in the complete neglect of differential overlap (CNDO) method which is the simplest NDO method. This method therefore cannot differentiate between states with the same electronic configuration but with different values of electron spins. Semi-neglected method of corrected differential overlap (MINDO) is a reformulation version of the INDO improved to predict enthalpies and appropriate molecular geometries for chemical systems, particularly sulfur-containing compounds, carbocations and polynitro organic compounds. The ZINDO method is a version of the INDO method developed for use in molecular systems involving transition metals (Young, 2001).

Another method in this group is the Neglect of Differential Diatomic Overlap (NDDO) methods. Whereas INDO added all one-centre two electron integrals to the CNDO/2 formalism, NDDO adds all two centre integrals for repulsion between a charge distribution on one centre and a charge distribution on another centre (Cramer, 2002). Otherwise the zero-differential overlap approximation is used. The most often used methods (MNDO, AM1, PM3) are all based on the NDDO integral approximation. MNDO, AM1 and PM3 methods are parameterized via expressing the calculated energies as heats of formations instead of total energies.

3.5 Density Functional Theory

The Density Functional Theory (DFT), which has become quite popular in recent years, offers an alternative approach to electron correlation (Kohn and Sham, 1965). Hohenberg and Kohn proposed a practical basis for the use of electron density instead of the wave function, by proving the one-to-one relationship between external potential (v) and electron density (ρ) (Hohenberg and Kohn, 1964). The first Hohenberg-Kohn (HK) theory shows that the ground state observable properties of a molecule are determined by the electron density. The

second theory of HK reveals that the true gorund state electron density minimizes the defined energy functional (Kohn et al., 1996).

$$E[\rho] = E_T[\rho] + E_V[\rho] + E_{XC}[\rho] \tag{3.7}$$

In Equation 3.7, in the total energy expression, the exact forms of the terms other than potential energy is unknown. In the Kohn-Sham approach; instead of the kinetic energy of the real system, kinetic energy expression, which is exact for a fictitious system where the electron density is assumed to be the same and the electrons do not interact, is used. The difference between the statements that belong to real and fictitious system is grouped in the term of E_{xc}, which represents the energy of exchange and correlation, with other unknowns (Cohen et al., 2011). In this regard, the problem of finding the universal form of the total energy function has turn into produce an approximate expression for the E_{xc} term, which prevents the expression from being definite.

DFT calculations are divided into three general categories: *local density approximations (LDA)*, *generalized gradient approximations (GGA)*, and *"hybrid" combinations of Hartree-Fock terms with DFT*. The LDA exchange and correlation functional only include terms related to electron density. The *GGA* functional include terms that are both dependent on electron density and density gradients. Hybrid functions parametrize the full energy expression of these approaches together with HF energy. In the literature, there is varieties of the hybrid functions (most popular is B3LYP), that give changes and correlations of energy contributions in different ways. Therefore, while systems such as metal complexes, organic compounds and metallic surfaces are modeled, careful selection of the function to be used by taking into account the prominent parameters such as the amount of change or dispersion energy is one of the important issues in DFT analysis.

3.6 Basis Sets

A basis set is a mathematical definition of orbitals of a system. In other words, basis set is a schedule of numbers that mathematically calculates places where electrons can be found.

A molecular orbital; it can be written as the linear combination of atomic orbitals because the molecules are made up of atoms and the same kind of atoms show

similar properties in different kinds of molecules. The relation between molecular orbital (ψ) and atomic orbitals (ϕ_k) is shown below (equation 3.8).

$$\psi = a_1\phi_1 + a_2\phi_2 + \cdots\cdots\cdots + a_k\phi_k \tag{3.8}$$

Here a_1, a_2, ...a_k are the molecular orbital expansion coefficient, k is the size of the basis set and the ϕ_k are the atomic orbitals which are called *basis functions/basis sets.*

Slater Type Orbitals (STO) and Gaussian Type Orbitals (GTO) are two common types of basis functions commonly used in electronic structure calculations.

3.6.1 Slater Type Orbital (STO)

First, John C. Slater tried to calculate orbital by using basis sets known as Slater Type Orbitals (STO). The slater-type orbitals used to describe the orbitals of hydrogen atoms and other electron ions are discontinuous in the nucleus and the radial part of the function is proportional to $e^{-\xi r}$, which correctly defines the distance-dependent exponential decrease. STO have the functional form depend on spherical coordinates, shown in equation 3.9 (Slater, 1930).

$$\phi_{\xi,n,l,m}(r,\theta,\varphi) = NY_{l,m}(\theta,\varphi)r^{n-1}e^{-\xi r} \tag{3.9}$$

Here the r, θ and φ are spherical coordinates, N is a normalization constant, $Y_{l,m}$ is the angular momentum part and the n, l, and m are quantum numbers.

The exponential dependence on the distance between the nucleus and the electron reflects the exact orbitals of the hydrogen atom. However, exponential dependence provides a quite fast convergence with increasing numbers of functions, and consequently the calculation of two and three-electron integrals with three and four centers cannot be performed analytically.

3.6.2 Gaussian Type Orbitals

In the 1950s, Frank Boys proposed a modification to the wavefunction by presenting Gaussian functions involving exponential e^{-ar^2} rather than $e^{-\xi r}$ of the STOs. Thus, the analytical solution of Gaussian-type orbitals molecular

integrals is proportional to the feasible e^{-ar^2}, and STOs can be adequately expressed with only a few linear combinations of GTOs.

$$\phi_{a,n,l,m}(r,\theta,\varphi) = NY_{l,m}(\theta,\varphi)r^{n-1}e^{-ar^2} \tag{3.10}$$

In equation 3.10; α is an exponent controlling the width of the GTO and l, m and n are the parameters controlling the spatial properties of orbitals. The behavior of electron density both in ionic molecules and excited by chemical bonds can be improved by adding functions such as polarization or diffuse to the GTO basis set.

The minimal basis sets contain the least number of atomic orbital basis functions needed to describe each atom. Although the minimal basis sets are not recommended for consistent and accurate estimates of molecular energies, their simplicity is a good tool to demonstrate the qualitative appearance of chemical binding. STO-3G, which uses three Gaussian type orbital (3G) per basis function to approximate Slater type atomic orbitals, is an example of the minimal basis set.

In the late 1970s, ***the split-valence basis sets*** were presented by John Pople and his group. This is to make the total function more accurate and reliable by extending the basis sets. The split-valence basis sets are characterized by number of functions which is separated to valence orbitals. The split valence basis sets are represented by the number of Gaussian functions, used to identify inner and outer shell electrons. Thus, "6-21G" defines a contracted Gaussian inner shell atomic orbital consisting of six primitive Gaussian, a two-primitive contracted Gaussian inner valence root, and a primitive outer valence root. Other split-valance basis sets include 3-21G, 4-31G and 6-311G sets.

The polarized basis sets, which allow the molecular orbitals to be more asymmetric around the nucleus, provide flexibility within the basis set. This is important for the correct definition of the bonding between atoms, because the existence of the other atom disrupts the electrons' boundary and distributes the spherical symmetry. Polarization functions are the basic functions of type p or d added to define the distortion of s or p orbitals, respectively. Polarization functions take the name 'd' for carbon atoms, 'p' for hydrogen atoms, and 'f' for transition metals. The polarization functions are significant for chemical bond propagation and should be included in all calculations where electron correlation is important. Examples include 6-31G (d) and 6-31G (d, p) basis functions.

Species with significant electron density away from the nucleus centers (for example, anions, unpaired electron pairs and excited states) require ***diffusion functions*** that add weakly connected electrons to the farthest from the center. Diffusion basis sets are suggested for electron affinity, proton affinity, inversion barriers, and calculations of bond angle of anions. For non-hydrogen atoms, the addition of s and p-type Gaussian functions is indicated by a plus sign, e.g. "3-21+G". Addition of diffusion functions to both hydrogen and large atoms is indicated by a double plus.

3.6.3 Pople Style Basis Sets

For the split valence type basis sets, designed by John Pople, the demonstration type is k-nlm ++ G^{**} or k-nlm ++ G (idf, jpd). Here, k symbolizes the number of primitive GTOs for core electrons, n and l show primitive GTOs for inner valence orbitals, m indicates primitive GTOs for outer valence orbitals. In addition, them + and * means that, diffuse functions or polarization functions added to heavy atoms, respectively.

In systems involving elements with a large number of core electrons, it is necessary to use a number of basis functions to expand the orbitals concerned. Otherwise, valence orbitals will not be properly identified. This problem can be solved by modeling the core electrons with an appropriate function and adding only the valence electrons to the account. *The Effective Core Potential (ECP)* approach allows the inner shell electrons, which do not generally affect chemical bonds, to be represented by an average potential. Some common core potential basis sets are LanL2DZ, Hay±Wadt VDZ, CREN, SBKJC VDZ etc. (Young, 2001).

3.7 Potential Energy Surfaces

The Potential Energy Surface (PES) describes the relationship between the energy and geometry of a system, and also provides information about the dynamics of a chemical reaction and the stable conformation of a molecule. In other words, PES is the full definition of all conformers, isomers and energetically reachable movements of a system. Minima on this surface correspond to optimized geometries. The global minimum is the lowest energy minimum. High-energy conformers or isomers can be examples for many local minima. On the PES the intermediate products and transition states in chemical reactions are associated

with stationary points that are a point on the potential energy surface where the forces are zero. While the energy minimums from the nuclear coordinates, where the gradient vector is zero, represent the equilibrium geometries of a chemical system, the first degree saddle points characterize the transition states. The first derivative of energy known as gradient is zero at both the minimum and the saddle points. To characterize a stationary point, it is required to calculate frequency on the optimized geometry. The obtained frequency calculation will include a variety of results such as frequencies, intensities, the associated normal modes, and the zero-point energy of the structure and various thermochemical properties (Ramachandran, 2008).

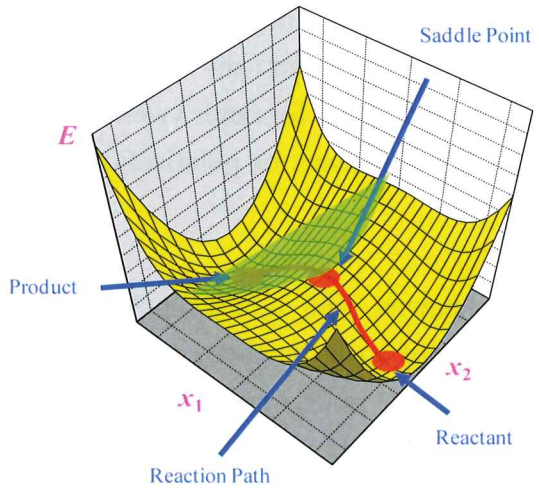

Figure 3.1 Representative potential energy surfaces.

Transition states of a chemical reaction is a first order saddle point on the potential energy surface. Molecular vibration frequencies and *Zero Point Energy* (ZPE) can be obtained from the force constants, which are the eigenvalues of the Hessian matrix formed from the second derivative of the energy according to the geometric coordinates. In the equilibrium geometries all frequency values are positive; only one virtual frequency corresponding to the reaction coordinate is observed in the transition state geometries.

In the PES calculations, molecular mechanic methods are often used to determine possible conformers of a molecule. Semiempirical methods can give a qualitative scheme of a reaction mechanism. Ab initio and DFT methods should be used to obtain quantitatively more accurate reaction PESs.

3.8 Solvent Effect

Solvation is related with the interaction between solvent and solute molecules, which will cause to changes in energy, stability, and molecular orientation. Thus, these variations, which depend on polarity, such as the electron distribution of the molecules, the reaction process, can also vary with the solvation. A suitable solvent permits kinetic and thermodynamic control over a chemical reaction. There are two different approaches in determining the effect of solvents in theoretical calculations. One approach is based on considering the solvent effects implicitly without including solvent molecules. The other one explicitly include solvent molecules to the calculation. the solvent is included as the continuity with the dielectric constant that it has. The Tomasi *polarized continuum model* (PCM) utilizes a van der Waals cavity created by interlocking atomic van der Waals radii scaled by an empirical factor, a detailed description of the electrostatic potential, and parameterizes the cavity/dispersion contributions based on the surface area.

3.9 Natural Bond Orbital Analysis (NBO)

Molecular electrostatic potential surface analysis is employed to determine the electronic charge density on a molecule. It is an influential method for defining the reactivity, structure activity and hydrogen bonds of molecular behaviors. NBO analysis generally helps to understand distribution of Lewis structures, bond structure, bond type, hybridization, charge, donor–acceptor interactions, etc.

NBO analysis, which provides a qualitative way to explain the relationship between nucleophilic or electrophilic center charges and reactivity, is a supportive analysis in elucidating the reaction mechanism. Natural bond orbital (NBO) methods can be derived from Hartree-Fock (HF), Density Functional Theory (DFT) and post-HF calculations. Generally, in the 3D molecular electrostatic potential surface maps, the red sections specify nucleophilic regions of high electron density whereas the blue sections display the electrophilic regions of lower electron density (Fleming, 1976; Weinhold and Landis, 1964).

4. EXPERIMENTAL AND COMPUTATIONAL DETAILS

4.1 Materials

The α-angelica lactone (Alfa Aesar, 98%), δ-valerolactone (Alfa Aesar, 98%, may contain polymer) and glycidol (Sigma Aldrich, 96%) were distilled under vacuum (0.5 mmHg) before use. Dichloromethane (Sigma Aldrich), methanol (Sigma Aldrich), tetrahydrofuran (Fluka), chloroform (Alfa Aesar), petroleum ether (Fluka), diethyl ether (Sigma Aldrich) were of analytic grade and were used as received. Toluene (Sigma Aldrich) was also dried under argon atmosphere and distilled prior to use. Tin (II) acetate (95%, $SnAcet_2$) and zinc (II) acetate (99.98%, $ZnAcet_2$) were obtained from Alfa Aesar. Cadmium acetate dihydrate (98%, $CdAcet_2.2H_2O$), lead (II) acetate trihydrate (95%, $PbAcet_2.3H_2O$), nickel (II) acetate tetrahydrate (98%, $NiAcet_2.4H_2O$) and cupper (II) acetate monohydrate (98%, $CuAcet_2.H_2O$) were procured from Merck. These compounds or salts were used without further purification. Triethylamine (≥99.0%) was obtained from Sigma-Aldrich. p-Toluenesulfonyl chloride (TsCl, 98%) and magnesium metal were purchased from Merck.

4.2 Methods

All reactions and manipulations were carried out using glovebox and conventional Schlenck tube techniques under argon atmosphere.

FTIR spectra were gotten with a Perkin Elmer Pyris 1 FTIR Spectrometer using KBr pellets.

^{1}H-NMR (400 MHz) and ^{13}C-NMR (100 MHz) spectra were taken in chloroform ($CDCl_3$) or dimethylsulfoxide (DMSO) as solvents containing TMS as internal standard with a Varian Unity 400 Spectrometer.

Molecular weight (M_n and M_w) of synthesized polymers were determined by gel permeation chromatography (GPC) on Viscotek HPLC system with a differential refractometer detector. THF served as the eluent at a flow rate of 1.0 mL/min. The molecular weights and polydispersities were reported versus monodisperse polystyrene standard.

Thermal gravimetric analyses of monomer, polymer or initiators were carried out using Perkin Elmer Pyris 1 TG/DTA under nitrogen flow (100mL/min) with 10 ^{0}C/min heating rate. The temperature range is approximate between 25 and 600 ^{0}C.

4.3 Computational methodology

The ROP mechanisms of cyclic monomers by using some selected initiators were computationally investigated in gas phase and solvent media. The geometry optimizations of all stationary points along the reaction pathways were performed with the DFT-B3LYP (Becke, 1993; Lee et al., 1988), B3LYP-D2 (Grimme, 2006), ωB97X-D (Chai and Head-Gordon, 2008), methods as coded in the Gaussian 09 computational chemistry suite (Frisch et al., 2010). The LanL2DZdp basis set and a relativistic electron core potential (ECP) developed by Hay and Wadt was added on metal atoms were employed throughout the study (Hay and Wadt, 1985; Wadt and Hay, 1985). In addition, the ROP mechanism of α-angelica lactone with $SnAcet_2$ were also investigated by the semiempirical methods (PM6 (Stewart, 2007), PM6-D3H4 (Řezáč and Hobza, 2012), PM7 (Stewart, 2013) implemented in MOPAC 2016 program (Stewart, 2016). All structures along the reaction pathway were characterized as minima and TSs with harmonic vibrational analyses. Besides, the transition state structures were connected with the corresponding reactants (intermediates) and products by exploiting intrinsic reaction coordinate (IRC) calculations (Hratchian and Schlegel, 2004). Effects of solvents, namely toluene, THF, DMF and DMSO, on the ROP mechanisms were incorporated with the Polarizable Continuum Model (PCM) (Tomasi et al., 2005). NBO analysis of initiators were performed with single point calculations of B3LYP, cam-B3LYP (Yanai et al., 2004) ωB97X-D, PBEPBE (Perdew et al., 1996), PBV86, HSEH1PBE (Heyd and Scuseria, 2004) MPW1PW91 (Adamo and Barone, 1998), M06, M062X, (Zhao and Truhlar, 2006, 2008) methods employing def2-TZVPPD basis set at the optimized geometries.

5. RESULT AND DISCUSSION

5.1 Polymerization of α-angelica lactone

Biodegradable, biocompatible poly(α-angelica lactone), PAL, can be polymerized through two possible pathways. One of them, as shown in Fig.5.1, is the ring-opening polymerization path1 which is provided formation of polyester and the other is ionic polymerization path2. However, although the double bond in the structure of the five-membered angelica lactone monomer decreases the stability of the ring structure, both polymerization methods are hampered by ring tension. In the literature, it is stated that the PAL obtained by vinyl polymerization is in the form of sticky, dark red solid and has low molecular weight (Chem.Rev., 2016).

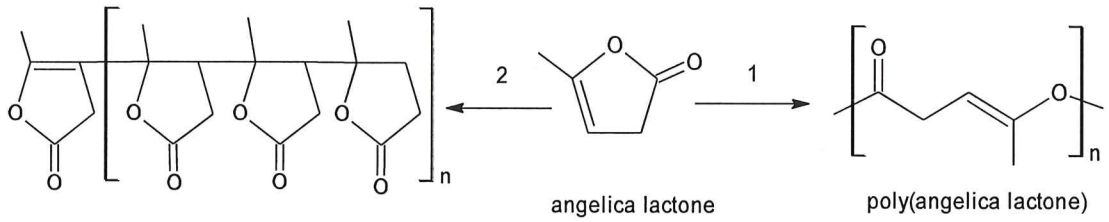

Figure 5.1 Possible polymerization reaction pathways for α-angelica lactone.

In some studies, it is thought that in the ring opening polymerization of the monomer, the obtained polymer is not completely polyester structure and the polymerization proceeds through vinyl groups (Danko and Mosnázek, 2017). The synthesis of the PAL has not yet been fully elucidated; therefore, the ROP of α-angelica lactone was investigated with an alternative initiator group in our study.

5.1.1 Ring Opening Polymerization of α-angelica lactone with $SnAcet_2$ or $ZnAcet_2$

α-angelica lactone (AL) was purified by vacuum distillation prior to use and kept under argon atmosphere at 4 ^{0}C. The determined amount of monomer ($5{,}5x10^{-3}$ mol) was charged into schlenck tube and then $SnAcet_2$ or $ZnAcet_2$ were added into the tube keeping with the monomer to initiator ratio (M/I; 300/1, 100/1) in glove box under argon atmosphere. Subsequently, the mixture was coupled to a vacuum gas line and mixed by adding dry toluene (1 ml) under argon atmosphere. Reaction is initiated by immersing in the oil bath which reaches the desired

temperature. Polymerization reactions were carried out at 110 °C and 130 °C for 30 hour under inert atmosphere. At the end of the reaction time, the flask was immersed in cold water and the mixture was exposed to air. Reaction products were purified by mixing in hexane. Then the product dried at room temperature in vacuum oven for 24 h. The polymer obtained was dark reddish color. The products were characterized by using FTIR, ^{1}H-NMR, GPC and TG methods. Schematic presentation of reaction was shown in Fig.5.2.

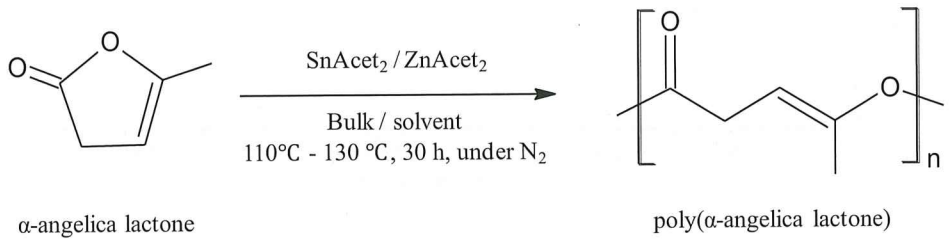

α-angelica lactone poly(α-angelica lactone)

Figure 5.2 The general scheme for ring opening polymerization of α-angelica lactone.

5.1.2 The Characterization Studies of PAL

As the structural analysis of the polymers shows no significant change depending on the initiator used, the characterization results for the polymer synthesized with the same kind initiator containing different metals are similar. For this reason, a common result is obtained for FTIR, ^{1}H-NMR and TG of each product.

The FTIR spectrums of the angelica lactone purified by vacuum distillation and the impurity remaining as a result of distillation were shown in Fig.5.3 The characteristic peak of the C=C- double bond was not observed in the substance separated as impurities. Therefore, it can be said that the monomer must be purified immediately before the experiment.

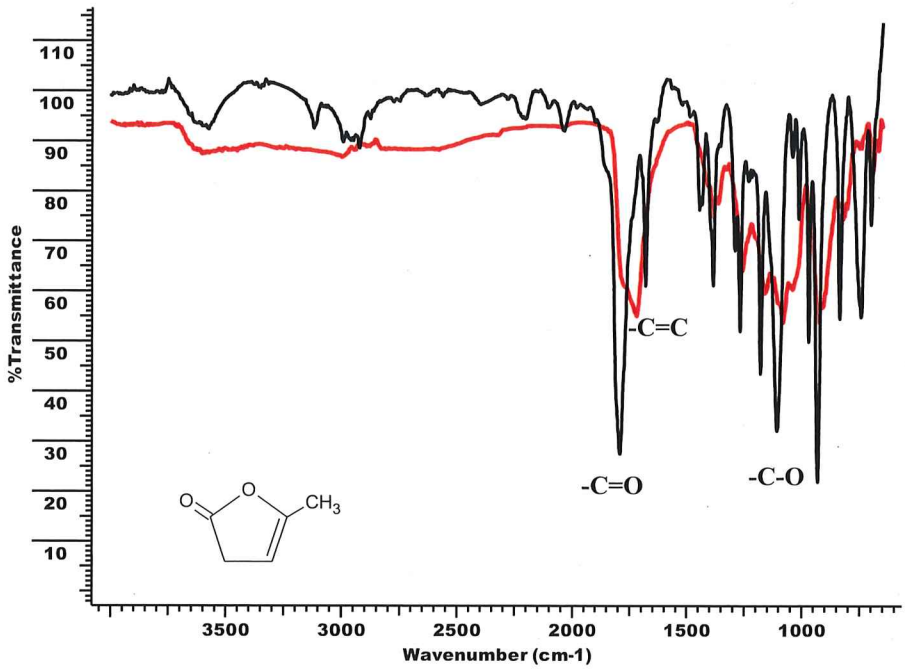

Figure 5.3 FTIR spectrum of distilled α-angelica lactone (black) and impurity of the monomer (red).

The characteristic peak of -C=O bond stretching, -C=C- double bond stretching and C-O-C band stretching were clearly observed at 1800 cm^{-1}, 1650 $cm^{-1}$and 1100 cm^{-1}, respectively in the FTIR spectrum of AL.

Similar peaks were obtained from FTIR spectrums of the monomer and the polymer because the same functional groups are also present in the structure of both. In FTIR spectrum of PAL (Fig.5.4.), the characteristic peak of -C=O bond stretching at 1760 cm^{-1} as a strong band was seen in the spectra. The absorption peak at about 1150 cm^{-1} was due to C-O-C stretching. The spectrum demonstrated that the -C=C peak was observable at 1600 cm^{-1}. It was observed that -C=C double bond intensity decreased when the FTIR spectrum of the PAL was analyzed. Furthermore, this indicated that the polymerization may proceeds over the double bond.

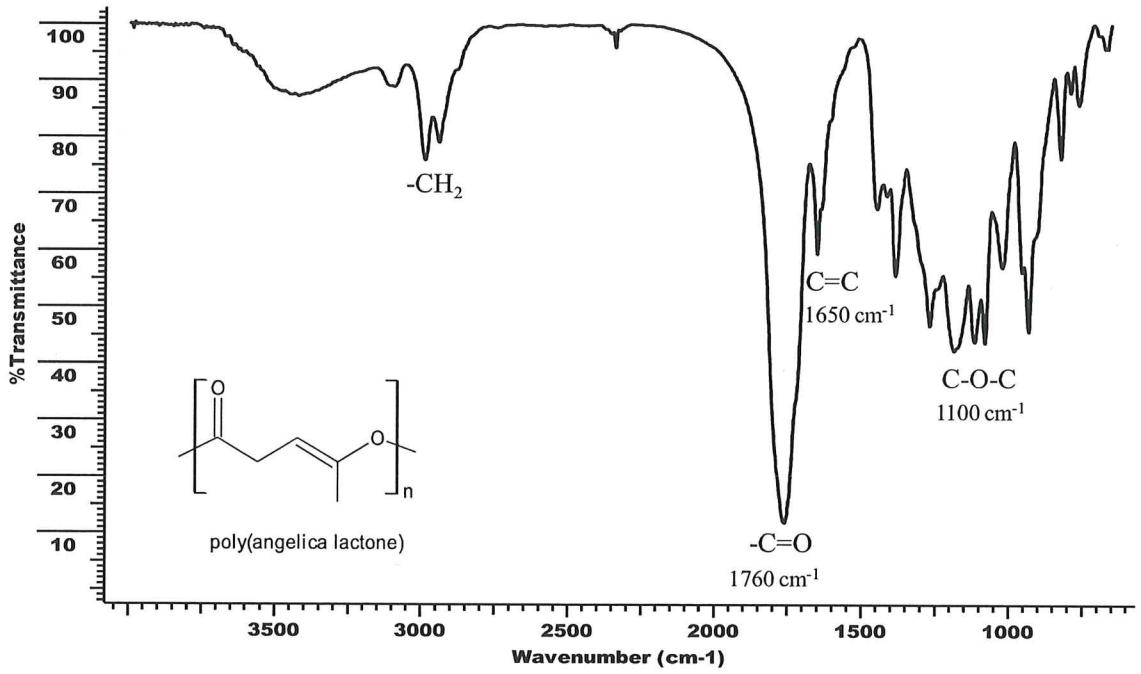

Figure 5.4 FTIR spectra of the poly(α-angelica lactone), PAL.

The ^{1}H-NMR spectrum of purified α-angelica lactone and PAL were shown in Fig.5.5 and 5.6, respectively. As expected, similar peaks were obtained in monomer and polymer. In monomer spectrum methyl protons peak (-CH_3) can be observed at 1.99 ppm. The peaks at 3.16 ppm and 5.11 ppm are assigned to the methylene (-CH_2-) and double bond (-CH=C) group protons, respectively. In polymer spectrum, the peak at 2.18 ppm was assigned to -CH_3 protons. The signals on 2.74 ppm were attributed to the -CH_2- group proton. The small peaks at 5.81 ppm and 6.10 were assigned to -CH=C double bond hydrogen. The decrease in peak intensity of -CH=C double bond hydrogen in the polymer spectrum indicates that the polymerization may proceed through both ionic polymerization and ring opening polymerization. In addition, peaks of the ionic polymerization product can be seen in the spectrum.

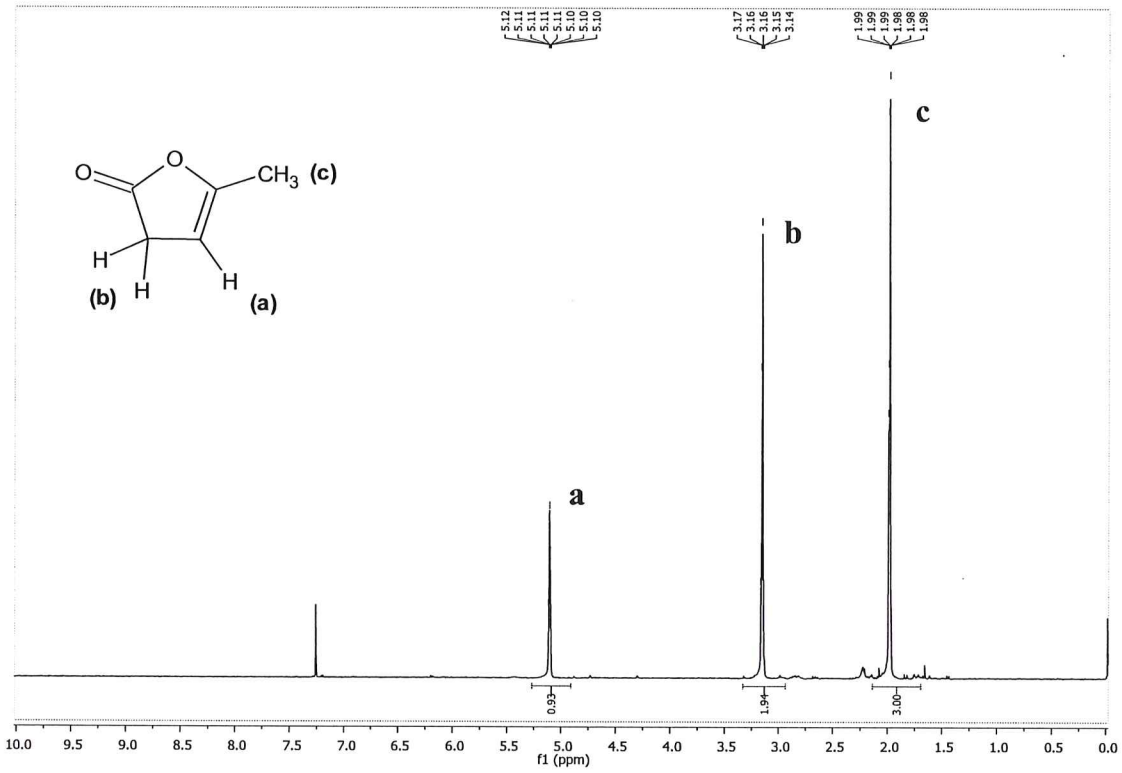

Figure 5.5 ^{1}H-NMR spectrum of the purified α-angelica lactone.

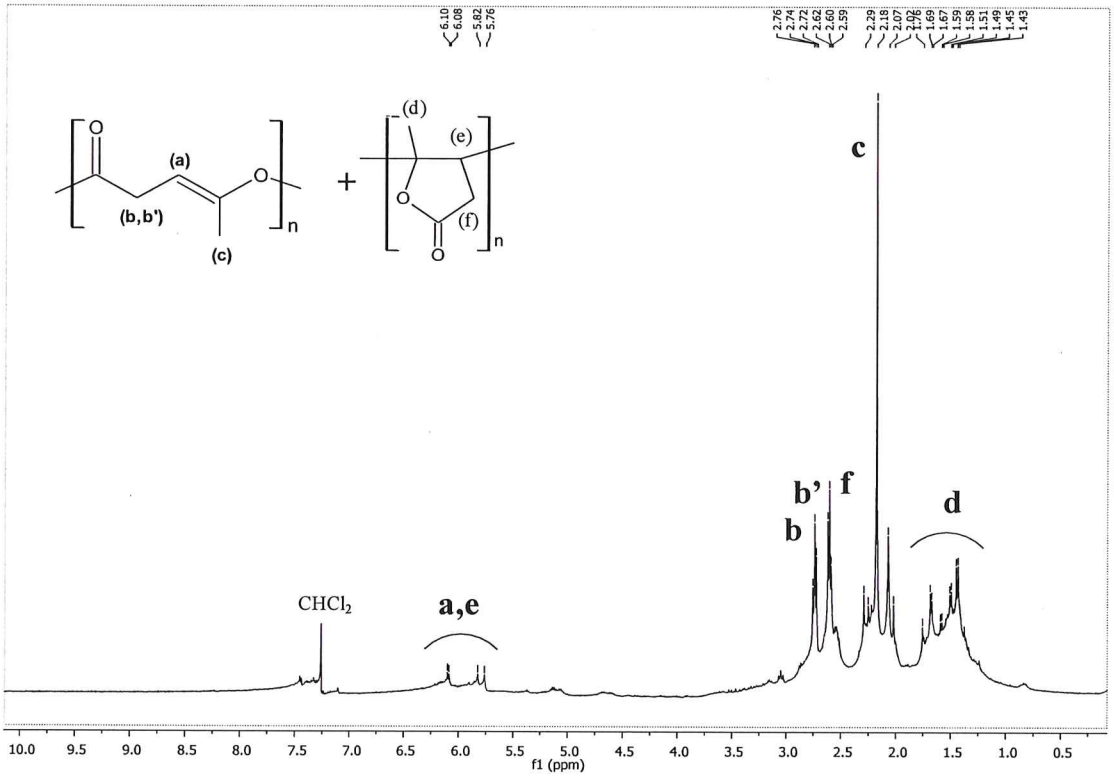

Figure 5.6 ^{1}H-NMR spectrum of the PAL.

The thermogravimetric analyses (TG) of the AL and PAL were carried out under nitrogen atmosphere and the thermogram was given in Fig.5.7 and 5.8., respectively. It was determined from the thermogram that the decomposition temperature of the monomer was between 50-125 °C in a single step. The maximum decomposition temperature is 110 °C.

According to the result, the polymer degrades in the range of 200-470 °C. Degradation takes place in more than one step. This shows that the polymer obtained was not only one structure. The remaining monomers not entering the reaction, or impurities in the medium, may have been formed the minor degradation steps. The maximum weight loss temperature is about 250-320 °C. The remaining part is about 20 percent. This can be carbonized organic material and inorganic materials.

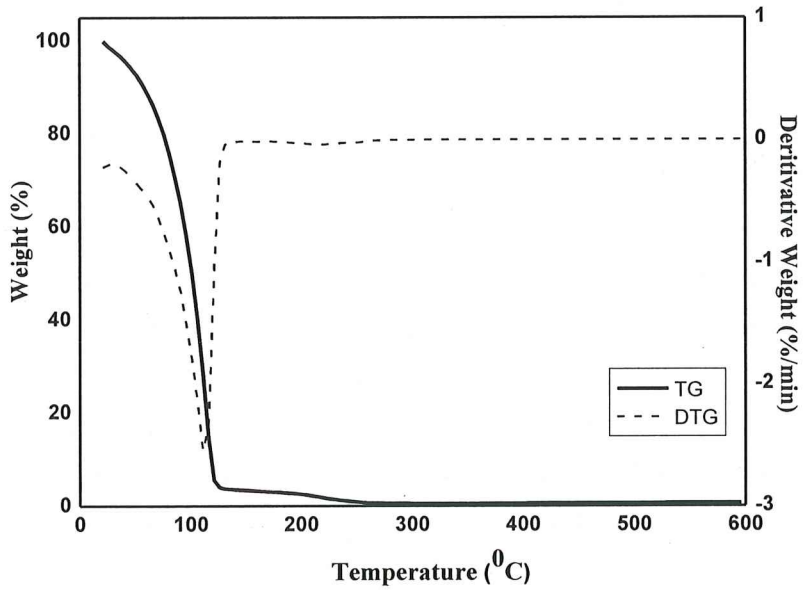

Figure 5.7 TG-DTG thermograms of the purified AL.

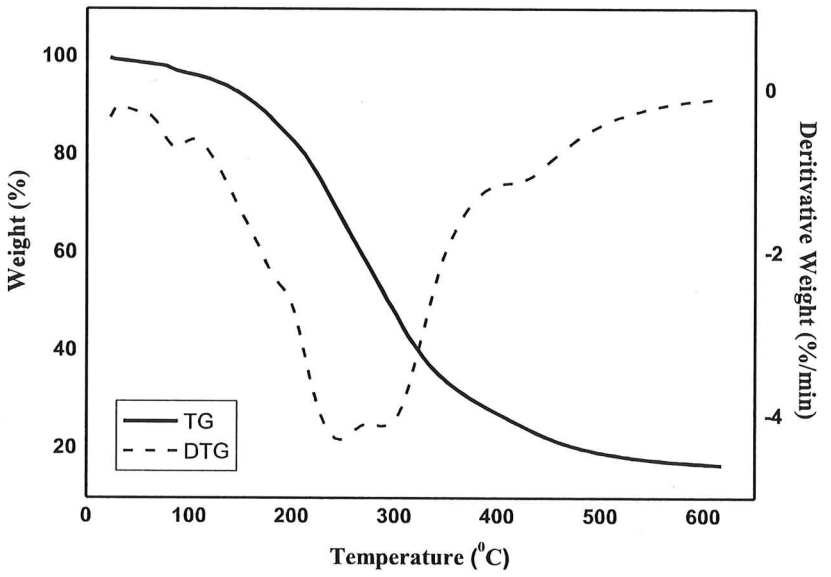

Figure 5.8 TG-DTG thermograms of the PAL.

GPC analysis of the polymer in THF was performed to determine the molecular weight. M_n, M_w, M_w/M_n values were obtained as a result of analysis. The molecular weights of the synthesized polymers were found to be between 1000 and 1500 g/mol. It was observed that the optimization studies made and using initiator with different metal did not lead to a significant change in the molecular weight. In the performed analyses, the presence of results of both the ring opening and the vinyl polymerization product shows that it is difficult to obtain high molecular weight PAL. Furthermore, it is considered that the PAL having polyester structure is not the main product in the polymer synthesized with $SnAcet_2$ and $ZnAcet_2$. For this reason, the reaction mechanism was investigated by computational methods.

5.1.3 Computational Study of ROP of α-angelica lactone with $SnAcet_2$

In the gas and solvent phases, the ROP mechanism of the α-angelica lactone with $SnAcet_2$ without a co-initiator was calculated with using the several semiempirical and DFT methods. The atomic charges and electrostatic potentials of α-angelica lactone and $SnAcet_2$ shown in Fig.5.9 were calculated at ωB97X-D/LanL2DZdp level. The varying bond lengths shown in Figure 1 play an important role in the polymerization reaction. As anticipated, the tin atom in the initiator and the carbonyl oxygen in the angelica lactone ring have the highest positive and

negative charges, respectively. Hence, the reaction begins with the interaction of these two oppositely charged atoms.

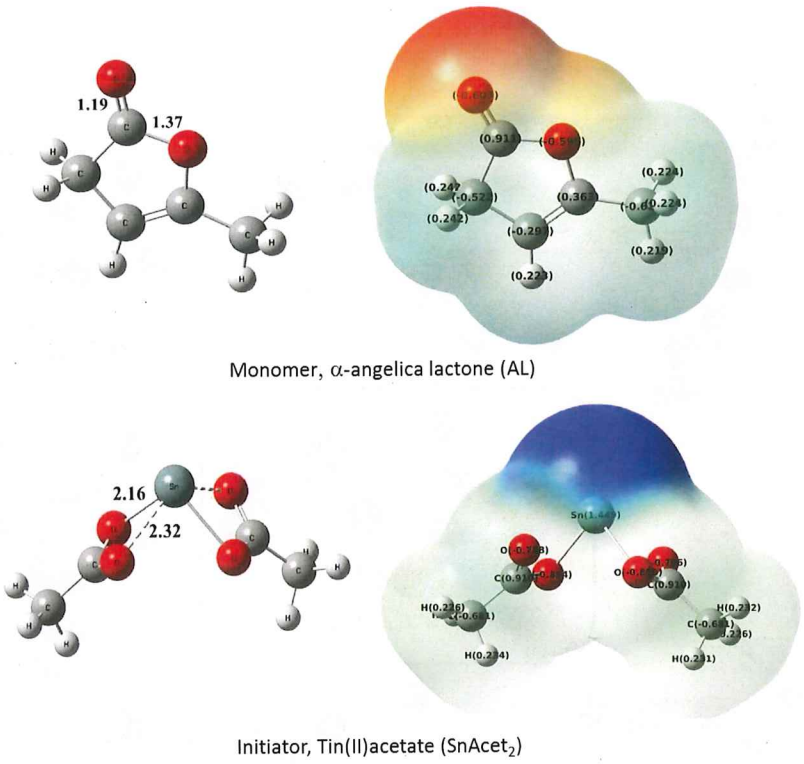

Figure 5.9 The geometries, electrostatic potentials and atomic charges of the monomer, AL, and initiator, $SnAcet_2$, obtained at ωB97X-D/LanL2DZdp level calculations.

.

5.1.3.1 ROP mechanism

In Figure 5.10, the studied coordination-insertion reaction mechanism for the polymerization is given. The initiation stage of the reaction mechanism consists of three barriers follow as TS1, TS_INT and TS2. In the first step, a stable complex forms via interaction between the monomer and initiator (complex) (Sn—O=C bond is 2.61 Å). The TS1 begins with the interaction between the tin atom in the initiator and the oxygen atom of the carbonyl group in the monomer (Sn—O=C bond is 2.10 Å) and also contain the formation of the bond between the carbonyl carbon in the monomer and the O atom of the acetoxy group (C—O bond is 1.71 Å). The bond distances of Sn—O=C and C—O have changed to 2.04 Å and 1.48 Å, respectively, in the intermediate structure (int1). The TS_INT barrier is caused by a low-energy conformational transformation occurred due to the distant (non-covalent) interactions in the structure. In the product structure obtained at the end of the ring opening step (TS2) of the monomer the O=C--O bond varies from 1.35

Å to 2.71 Å. Moreover, the Sn atom interacts with the other oxygen atom in the ring and binds to this oxygen with an acetate group.

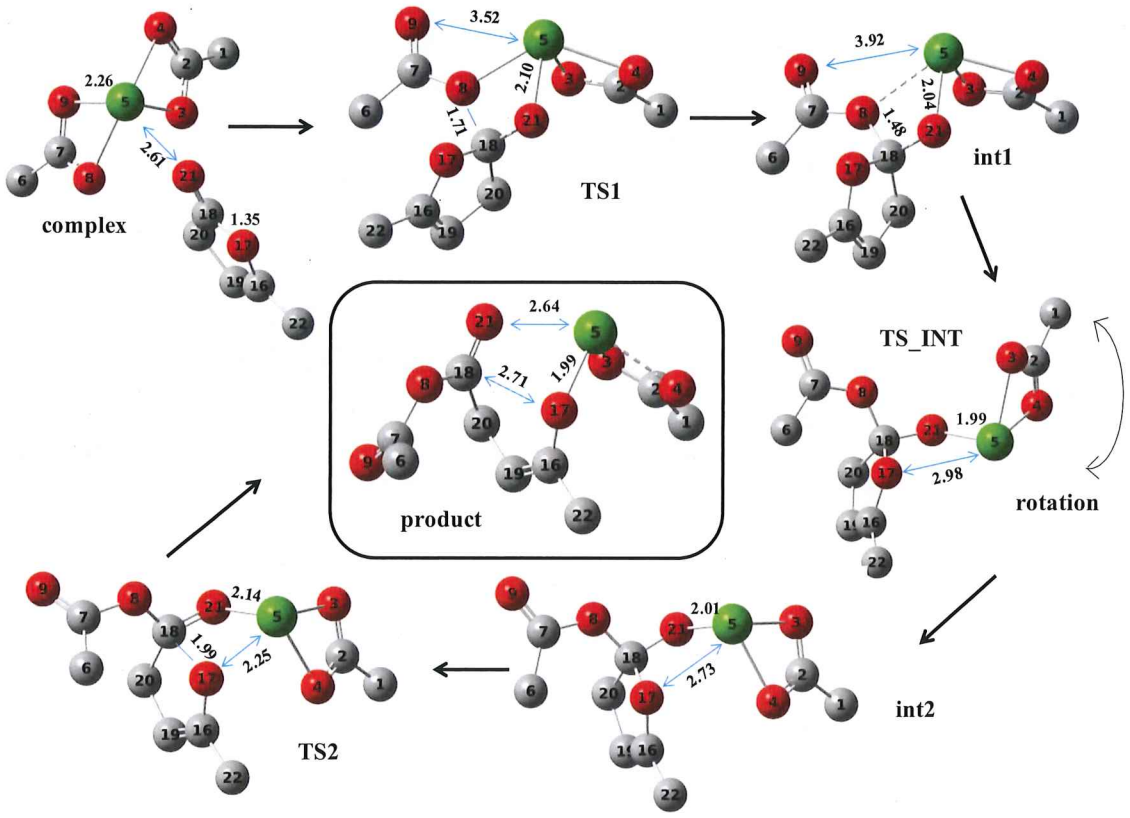

Figure 5.10 Initiation stage of the AL polymerization. Hydrogens are excluded. Distances are given in Å units. Oxygen, carbon and tin atoms are illustrated in red, gray and green, respectively.

5.1.3.2 Natural bond orbital analysis (NBO)

The NBO analysis leads to understand qualitatively of the relationship between electrophilic or nucleophilic center charges and reactivity. Therefore, the reaction is a supportive analysis for mechanism studies (Reed et al., 1988; Sattayanon et al., 2014). NBO analysis was carried out using ωB97X-D method with LanL2DZdp basis set in this study. Table 5.1 shows the atomic charges of some selected atoms playing an important role in the reaction mechanism. According to the data obtained from the NBO analysis, the oxygen atom of the carbonyl group in the monomer (O21) has a greater electron charge than the other oxygen atom (O17) in the structure. This explains why O21 attacks to the tin atom, the electrophilic center. While the nucleophilic property of O17 atom increases during

the reaction, the negative charge value of O21 atom decreases. This leads to attacking of the O17 atom to Sn atom in the ring opening step. In the formation step of the product, the positive charge on the Sn atom attains its maximum value. This increases the tendency of the tin atom to interact with another AL monomer, and thus explains obtaining lower barrier in the propagation stage than the initiation stage of the reaction.

Table 5.1 Calculated NBO atomic charges of stationary points on the reaction path obtained by ωB97X-D/LanL2DZdp.

	complex	TS1	int1	TS_INT	int2	TS2	product
Sn5*	1.468	1.491	1.485	1.474	1.478	1.488	1.513
O8*	-0.844	-0.826	-0.726	-0.643	-0.650	-0.625	-0.631
O17*	-0.579	-0.612	-0.639	-0.674	-0.692	-0.891	-1.022
C18	0.951	1.001	0.987	0.988	0.981	0.990	0.956
O21	-0.675	-0.918	-0.985	-1.003	-0.990	-0.859	-0.681

5.1.3.3 Performance Comparison of the methods

The performances of PM6, PM6-D3H4, PM7 and B3LYP, B3LYP-D2, ωB97X-D methods were compared with each other based on the experimental result (Table 5.2 and 5.3). As mentioned above, the initiation stage of the ROP mechanism occurs in three steps. It is seen that the largest one is the barrier of the third step when the barrier heights of these three steps are compared. The energy values and geometrical structures of TS1 and int1 involved in first step are found similar to each other, respectively. Therefore, TS1 cannot give off enough amount of energy so that int1 cannot pass over the third barrier. Taking all of these into account, the energy of the transition state structure of the third step was considered the polymerization reaction barrier.

Table 5.2 Calculated relative Gibbs free energy values (kcal/mol) of all points along the reaction path using the DFT methods.

	B3LYP	B3LYP-D2	ωB97X-D
reactant	-5.0 (4.9)[a]	-5.8 (4.5)	-1.3 (9.0)
complex	0.0 (0.0)	0.0 (0.0)	0.0 (0.0)
TS1	28.9 (25.0)	29.3 (26.1)	25.4 (22.3)
int1	27.5 (24.6)	28.6 (25.7)	22.8 (21.2)
TS_INT	-------[b]	31.7 (27.4)	28.8 (24.3)
int2	28.6 (24.0)	30.6 (26.9)	25.1 (22.2)
TS2	37.5 (32.7)	36.9 (32.9)	33.8 (30.2)
product	21.9 (20.4)	30.6 (28.7)	18.1 (16.6)

[a]The values of in parenthesis are enthalpy values in kcal/mol.
[b]TS_INT structure couldn't be located with the B3LYP method.

The value of the experimental activation barrier was determined as 26.3 kcal/mol by Chen et al., 2011. As given in the Table 5.2, even though the applied DFT methods in the study overestimate the reaction barrier value, the closest activation energy to the experimental one was found by ωB97X-D method as 30.2 kcal/mol. The B3LYP and its dispersion corrected version, B3LYP-D2, whose energy estimations for TSs and intermediate structures (int1 and int2) are very close to each other, show similar performances except for a conformational transition state structure (TS_INT), which has also been seen in some previous studies (Cheshmedzhieva et al., 2012), originating from the rotation of acetate group forming int2 from int1 (Fig.5.11). The methods involving empirical dispersion corrections, B3LYP-D2 and ωB97X-D, locate this TS_INT structure. However, we could not locate TS_INT with the B3LYP method, which suffers from lack of the dispersive interactions, in spite of our intense effort. This may be a good indicator of the fact that more accurate reaction potential energy surface can be obtained from the dispersion corrected methods. Consequently, the best

performing DFT functional for these types of calculations is found to be ωB97X-D since it can give more accurate results both qualitatively and quantitatively while B3LYP-D2 produce qualitatively better results compared to those of B3LYP.

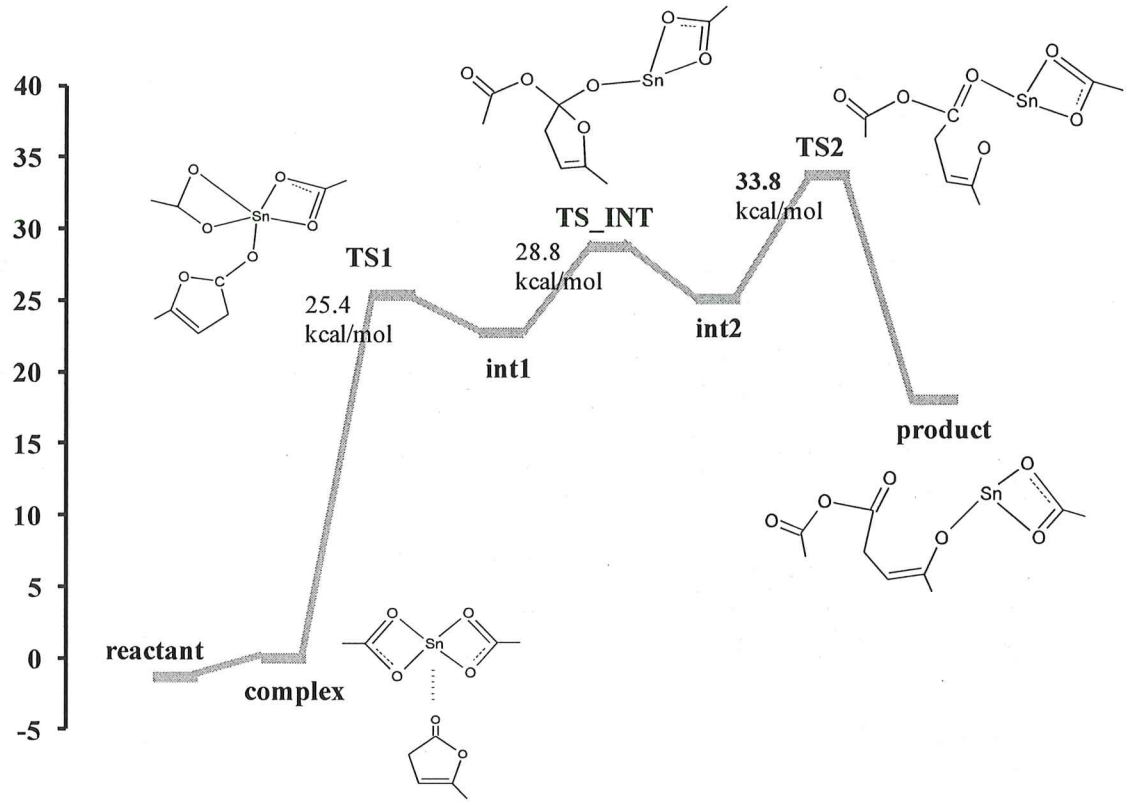

Figure 5.11 Gibbs free energy profile (in kcal/mol) for the initiation stage obtained by ωB97X-D/LanL2DZdp. All energies are relative to the complex.

Beside the semiempirical PM6 method, newly developed methods, PM6-D3H4 and PM7, which include non-covalent interactions, were also employed in this study. The most important advantage of these methods is that their computation times are considerably shorter than those of ab initio and DFT methods. The main purpose of employing semi empirical methods is to provide qualitatively correct energy profile for the reaction path and reasonable initial geometries of stationary points for higher level calculations (e.g. DFT). For this system, all of the semi empirical methods employed in this study considerably underestimate the reaction barrier. DFT methods predict that the energy difference between TS1 and int1 is very small. Conversely, both PM6 and PM7 methods estimate this energy difference considerably large. This means that the energy profile cannot be properly calculated by these two semi empirical methods. On the other hand,

PM6-D3H4 predicts the entire energy profile of the reaction qualitatively similar to that of the DFT.

Table 5.3 Calculated relative Gibbs free energy values (kcal/mol) of all points along the reaction path using the semiempirical methods.

	PM6	PM6-D3H4	PM7
reactant	-3.1 (8.3)[a]	-0.6 (10.9)	-3.1 (7.4)
complex	0.0 (0.0)	0.0 (0.0)	0.0 (0.0)
TS1	12.2 (9.4)	9.3 (8.9)	16.5 (15.2)
int1	2.3 (-0.5)	8.7 (7.4)	7.0 (2.0)
TS_INT	8.3 (3.1)	10.3 (9.2)	6.3 (5.7)
int2	7.0 (3.1)	8.9 (6.8)	9.8 (4.7)
TS2	13.4 (10.5)	11.1 (9.5)	20.4 (15.0)
product	6.6 (5.9)	6.6 (5.9)	4.3 (4.7)

[a]The values of in parenthesis are enthalpy values in kcal/mol.

5.1.3.4 Propagation stage

The propagation stage of the polymerization was also investigated and the interaction between the active chain and the new AL monomer was revealed. The movements of atoms in the propagation stage are rather similar to those in the initiation stage (Fig.5.12.). The structure called complex2 in this stage refers to the one formed between the product of the initiation stage and a new AL monomer. The activation barrier between the active chain and the new monomer (TS4) was found to be 14.5 kcal/mol (Fig.5.13). As the polymer chain formed a more stable structure as it grew, a lower barrier was obtained than the activation barrier at the initiation stage, as expected. This allows one more monomer to be added to the chain formed from molecules overcoming the barrier at the initiation of the reaction.

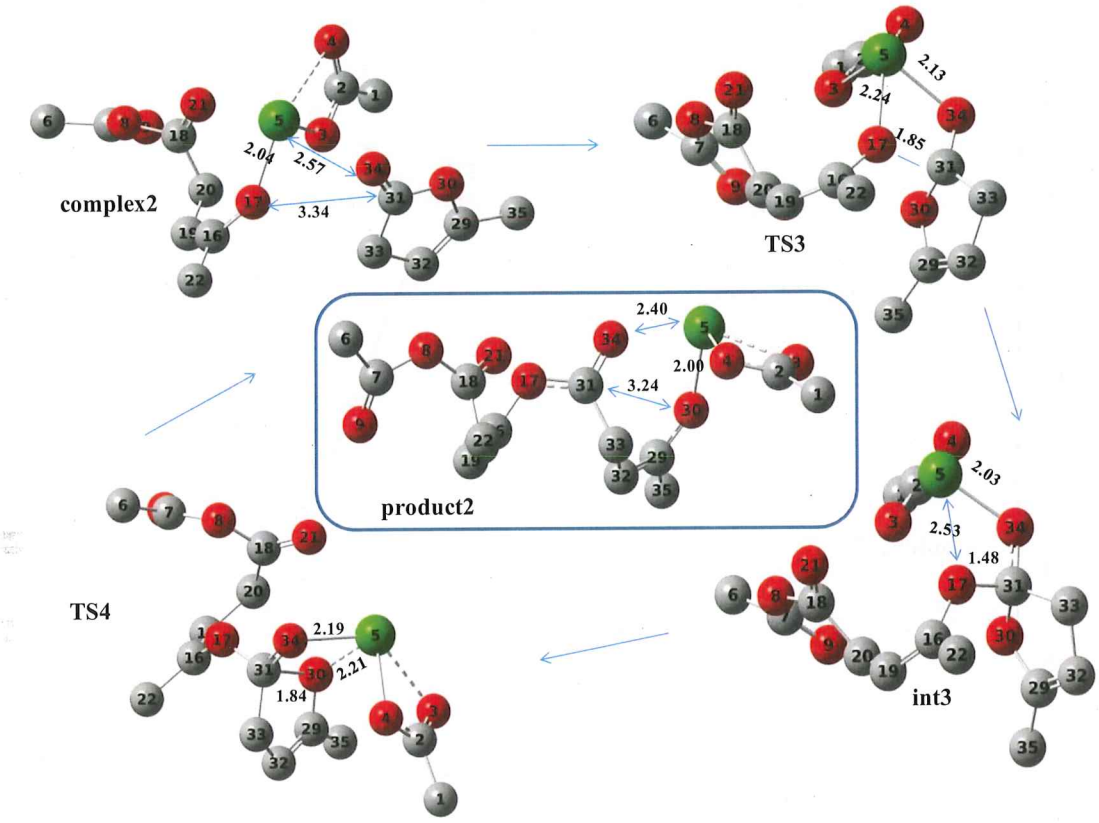

Figure 5.12 Propagation stage of the AL polymerization. Hydrogens are excluded. Distances are given in Å units. Oxygen, carbon and tin atoms are illustrated in red, gray and green, respectively.

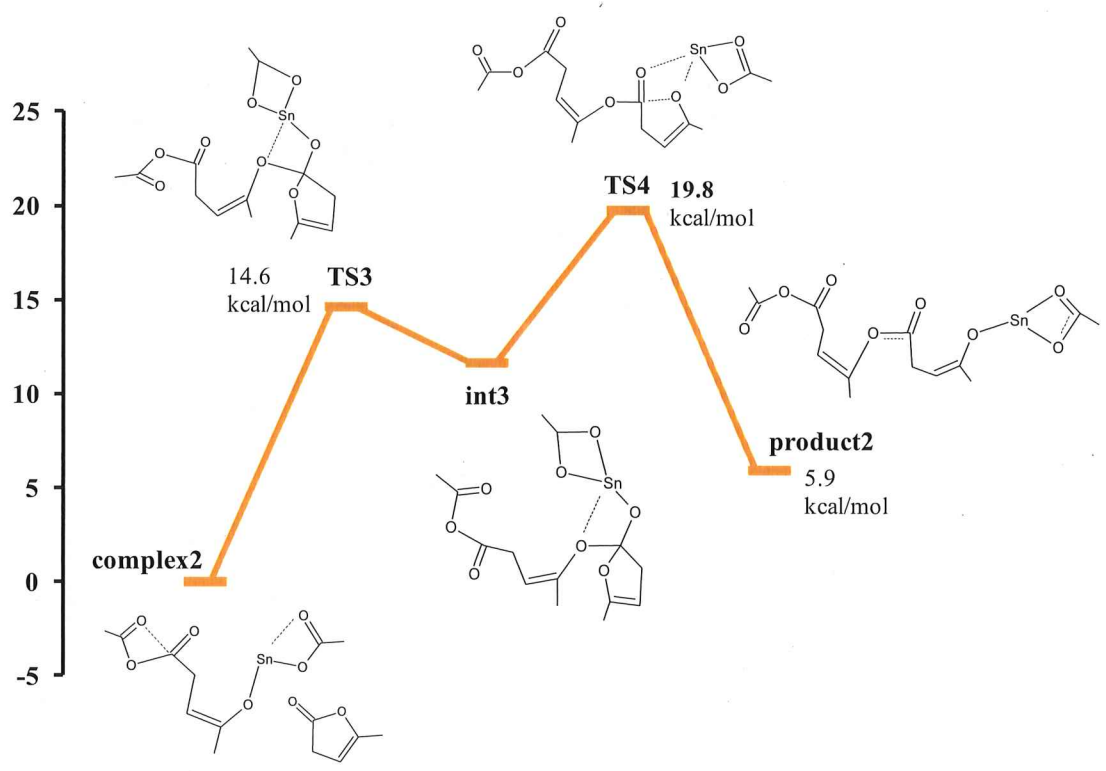

Figure 5.13 Gibbs free energy profile (in kcal/mol) for the propagation stage obtained by ωB97X-D/LanL2DZdp. All energies are relative to the complex.

5.1.3.5 Thermodynamics of α-AL polymerization

In a polymerization reaction, polymerizability (or spontaneity) is determined by Gibbs' free energy change of polymerization (ΔG_p), given in equation 5.1.

$$\Delta G_p = \Delta H_p - T\Delta S_p \qquad (5.1)$$

At a given temperature, ΔG_p must be negative for a spontaneous polymerization reaction. As seen from eq 1, the free energy change varies depending on two thermodynamic parameters; the enthalpy (ΔH_p) and entropy (ΔS_p) changes of polymerization. Ring size affects these values in the ring opening polymerization reactions of cyclic lactones. The magnitude of ΔH_p depends on the ring strain, whereas ΔS_p depends on the increased order of the system. These two thermodynamic parameters compete with each other in the opposite direction. The spontaneity of the reaction is mainly determined by the exothermicity magnitude of ΔH_p since the $-T\Delta S_p$ value always makes the free energy change increase due

to decrease in ΔS_p, depending on loss of translational degrees of freedom in polymerization reaction (Olsén et al., 2016). However, if the exothermicity of two different cyclic lactone reaction enthalpy changes is close to each other, then the change in entropy of polymerization will cause the differentiation in polymerizabilities of the monomers. As the translational degrees of freedom are lost as a result of polymerization, the value of the polymerization entropy change is determined by the rotational conformational degrees of freedom specified by the number of rotatable bonds contained in the polymer.

In this study, we obtained the polymerization enthalpy by subtracting the enthalpy of the monomer from the enthalpy difference between the product of the propagation stage and the product of the initiation stage with a slightly different point of view. Our approach differs from the routine enthalpy (Houk et al., 2008) calculations since it includes the effect of the initiator molecule (equation 5.2). In addition to that the **product2** and **product** does not include conformational relief unlike routine calculations. Chen et al. (2011) calculated the enthalpy of polymerization to be -6.36 kcal/mol while we calculated -1.4 kcal/mol. The reason for the relatively large difference between them is probably due to Chen and his colleagues using trimer and dimer structures of the monomer and calculating at a higher theoretical level than our calculations.

$$\Delta H_{polymerization} = (E_n - E_{n-1}) - E_M \tag{5.2}$$

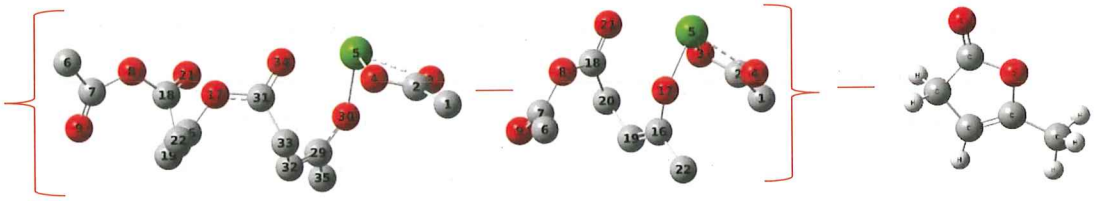

As the polymerization reaction proceeds, the exothermicity of the polymerization enthalpy decreases. Based on this, it can be predicted that the exothermic value of -6.36 kcal/mol will decrease. For poly(δ-valerolactone), PVL, which has a high molecular weight polymer in the literature and a negative ΔG_p, the ΔH_p value (-6.6 kcal/mol) is close to the polymerization enthalpy of AL. As the entropic factor is known to increase the free energy of the reaction, it can be predicted that the ΔG_p value of AL will either be very close to zero or positive. As mentioned above, this difference between the free energies changes of these two monomers

can be explained by the change of entropy as follows: Since the double bond free PVL is formed by the opening of six-membered rings, the rotation has a much higher degree of conformational freedom than poly(angelica lactone) PAL, which leads to less negative polymerization enthalpy change and a negative free energy value. However, PAL has a larger entropy change than that of PVL because it has a more rigid structure (not suitable for rotation), formed by the opening of five member rings consisting of double bonds, and this most likely leads to a positive ΔG_p value.

5.1.4 Computational Study of ROP of α-angelica lactone with $SnAcet_2.2H_2O$

Danko and Mosnázek (2017) have said that it is thermodynamically difficult to obtain high molecular weight by ring opening polymerization of five member angelica lactones. In addition, they suggested that an impurity like water in the system might increase the molecular weight of PAL which was synthesized by Chen et al. (2011). Therewith the reaction mechanism with $SnAcet_2$, which makes a coordination bond with two water molecules, was investigated computationally to be able to determine the effect of water on the initiator activity and the polymerization reaction.

The initiation and propagation stage for ring opening polymerization of α-angelica lactone was investigated by $SnAcet_2$ with water as a co-initiator. The determined activated monomer mechanism for the polymerization was shown in Fig.5.14. The initiation stage occurs in two steps (complex, TS1, int1, TS2, product) according to the calculations. As expected, there is an interaction between the tin atom in the initiator and the oxygen of carbonyl group in the monomer (Sn—O=C bond is 2.21 Å) at the TS1 structure. Besides, it contains the bond formation between the C atom of AL monomer and the O atom of the H_2O molecule (C—O bond is 1.83 Å). In the TS2 step, the O=C—O bond of AL break down from 1.53 Å to 2.76 Å. Also, the tin atom along with an acetate group and H_2O molecule move away from the carbonyl oxygen and bonds to the other oxygen atom in the ring. Due to the highest transition state energy value, the reaction barrier was determined as 12.9 kcal / mol (**TS1**).

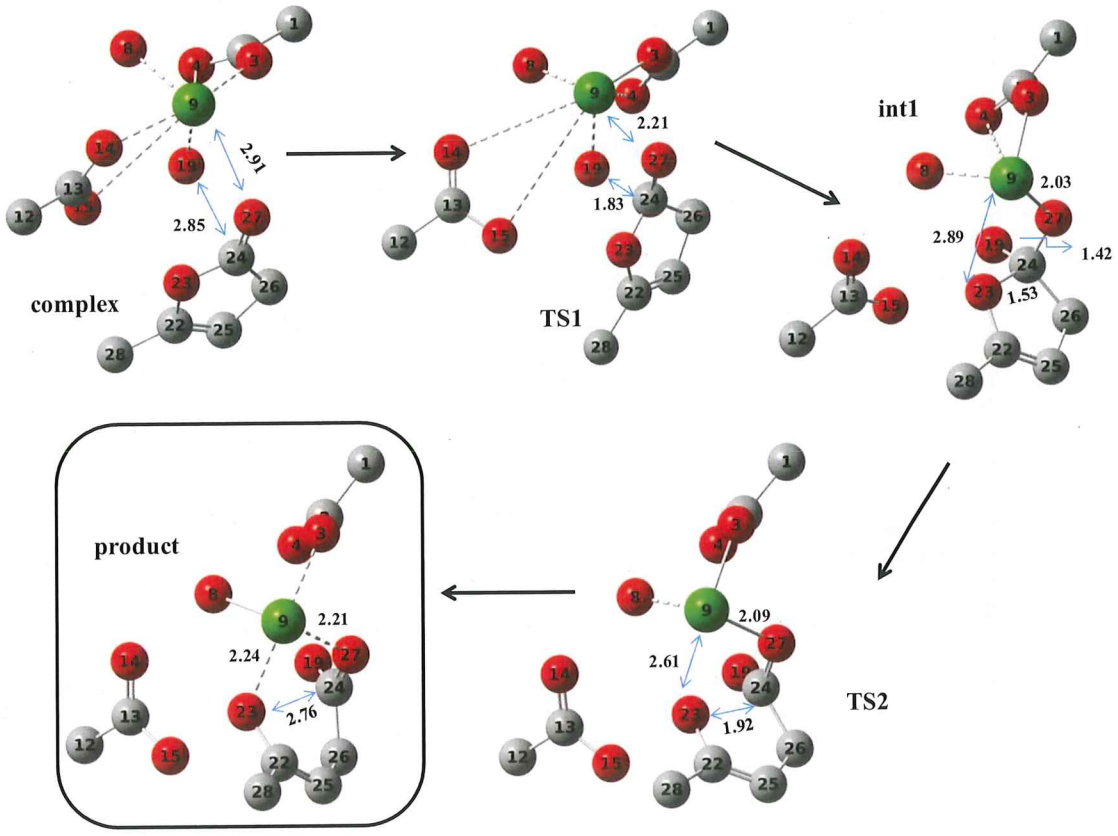

Figure 5.14 Initiation stage of the AL polymerization with $SnAcet_2.H_2O$. Hydrogens are excluded. Distances are given in Å units. Oxygen, carbon and tin atoms are illustrated in red, gray and green, respectively.

When the reaction energy profile (Fig.5.15) is examined it is seen that this reaction is an exothermic reaction and will spontaneously proceed towards product1. As shown in Table 5.4, the Gibbs free energy value of the product1 was found to be -3.9 kcal/mol. This result indicates that the initiation polymerization reaction results in a stable complex. A stable complex will not prefer to interact with a new AL monomer due to not acting as an active chain.

Table 5.4 Calculated relative Gibbs free energy values (kcal/mol) of all points along the initiation reaction path using the ωB97X-D/LanL2DZdp level.

	complex1	**TS1**	**int1**	**TS2**	**product1**
ωB97X-D	0.0	12.9 (10.6)[a]	0.5 (-1.9)	5.8 (2.3)	-3.9 (-6.6)

[a]The values of in parenthesis are enthalpy values in kcal/mol

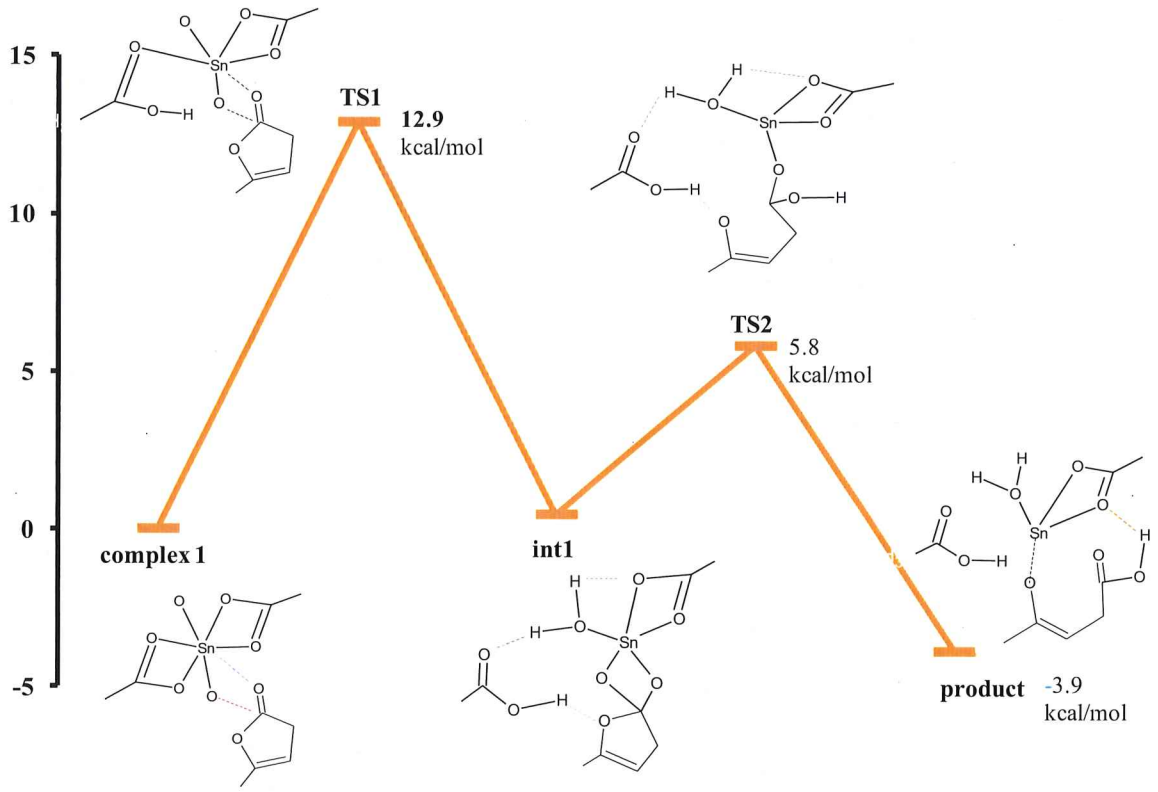

Figure 5.15 Gibbs free energy profile (in kcal/mol) for the initiation stage of ROP of AL using $SnAcet_2.2H_2O$ obtained by ωB97X-D/LanL2DZdp. All energies are relative to the complex.

5.1.4.1 Propagation stage

The propagation stage of the polymerization was also studied and two transition state points (TS3 and TS4) were found. Similar to the initiation polymerization stage, first an interaction occurs between the oxygen atom of the carbonyl group in the AL and the tin atom (the distance change from 3.35 Å to 2.16 Å). However, the reaction continues with the interaction between one of the oxygen atoms of the acetate group (O23) at the chain end and the carbonyl group carbon (C37) in the AL (Fig.5.16). Therefore, the water molecule, which is a co-initiator, plays an active role in the initiation stage but does not have a contribution to the polymerization reaction in the propagation stage. In this stage, the reaction proceeds through the active group in the chain end. According to the data the reaction barrier was determined as 21.8 kcal/mol (TS3). The TS4 containing the ring-opening step is lower than the TS3. Therefore, it can be said that the system is proceeding towards a stable complex formation.

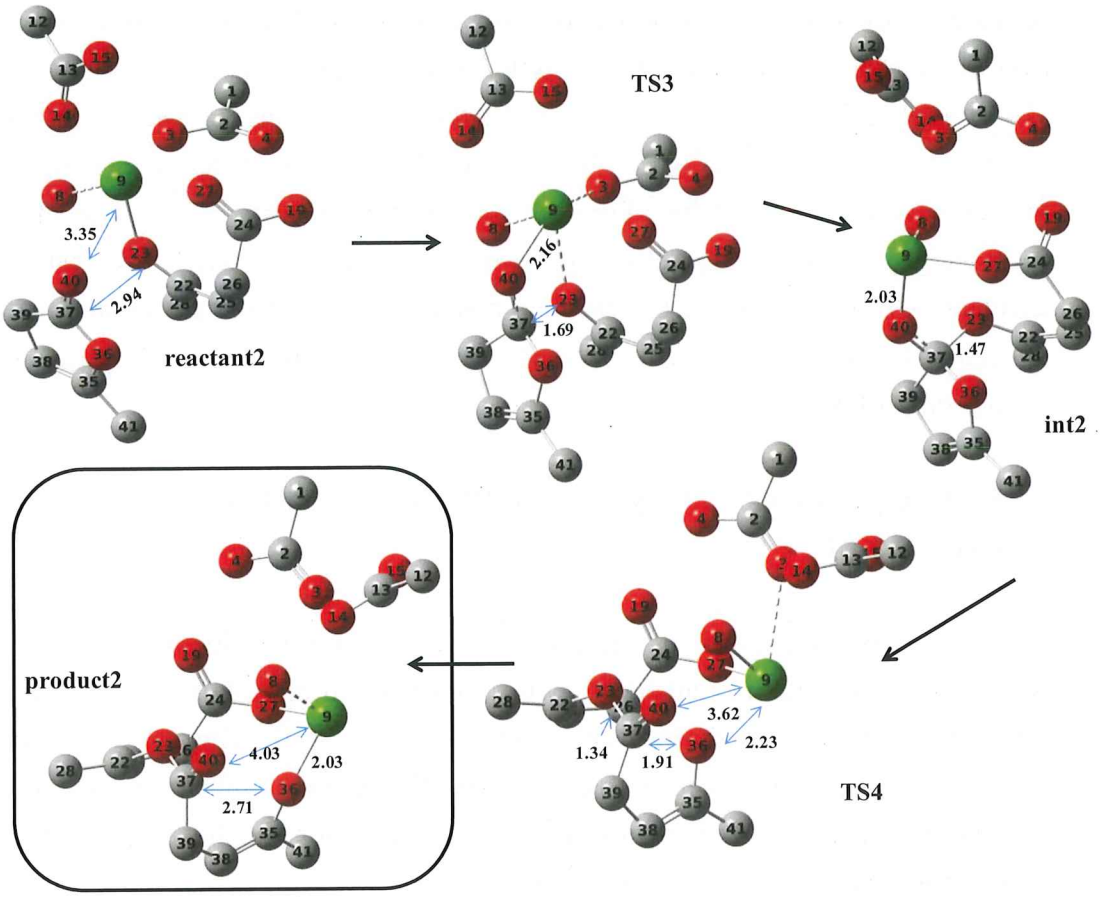

Figure 5.16 Propagation stage of the AL polymerization with $SnAcet_2.H_2O$. Hydrogens are excluded. Distances are given in Å units. Oxygen, carbon and tin atoms are illustrated in red, gray and green, respectively.

The following result can be seen when the results of initiation and propagation stage are compared. The activation barrier (TS3) obtained at the growth stage is greater than the activation barrier (TS1) obtained at the initiation stage. This indicates (Table 5.5) that it is kinetically difficult to add a new monomer to the active chain and that the resulting product will remain in the oligomer structure.

Table 5.5 Calculated relative Gibbs free energy values (kcal/mol) of all points along the propagation reaction path using the ωB97X-D/LanL2DZdp level.

	complex2	TS3	int2	TS4	product2
ωB97X-D	0.0	**21.8** (18.9)[a]	7.3 (5.5)	19.4 (16.2)	2.9 (1.3)

[a]The values of in parenthesis are enthalpy values in kcal/mol

In addition to these studies polymerization enthalpy of the system is obtained from enthalpy value of product1 and product2 according to Eq.5.2 and was found as -3.1 kcal/mol. The increased number of hydrogen bonds in the medium due to the water molecule increases the formation of the complex structure and makes the construction more stable. For this reason, the entropy of the system is decreasing. With the penalty effect of entropy to enthalpy, the Gibbs free energy exchange will be very close to zero or a positive value. This suggests that high molecular weight poly(α-angelica lactone) cannot be obtained using tin acetate in the presence of water.

5.1.5 Computational Study of ROP of α-angelica lactone with $SnAcet_2.2MeOH$

It is known that the effect of the acetoxy groups used as initiator in the ring opening polymerization is enhanced by the conversion to the alkoxide group with interaction with alcohol in the medium (Ryner et al., 2001) Thus, the initiation stage of polymerization mechanism for α-angelica lactone with tin acetate was studied in the presence of methanol (Fig.5.17.). The reason for choosing methanol as an alcohol is to shorten the calculation time.

According to the calculations, it was determined that the reaction was exothermic and had two activation barriers (TS1 and TS2) (Fig.5.18). The activation energy value of the reaction was found to be 17.3 kcal/mol since the value of the TS2 barrier containing the ring opening was lower than that of the TS1 barrier (Table 5.6). In addition, a stable complex was obtained as a result of the reaction (-2.5 kcal/mol). This result is qualitatively similar to the polymerization reaction which was used water as a co-initiator. Therefore, the propagation stage of the polymerization reaction has not been studied.

Table 5.6 Calculated relative Gibbs free energy values (kcal/mol) of all points along the initiation reaction path using the ωB97X-D/LanL2DZdp level.

	complex1	**TS1**	**int1**	**TS2**	**product1**
ωB97X-D	0.0	17.3 (14.8)[a]	8.5 (5.6)	13.0 (10.2)	-2.5 (-4.9)

[a]The values of in parenthesis are enthalpy values in kcal/mol

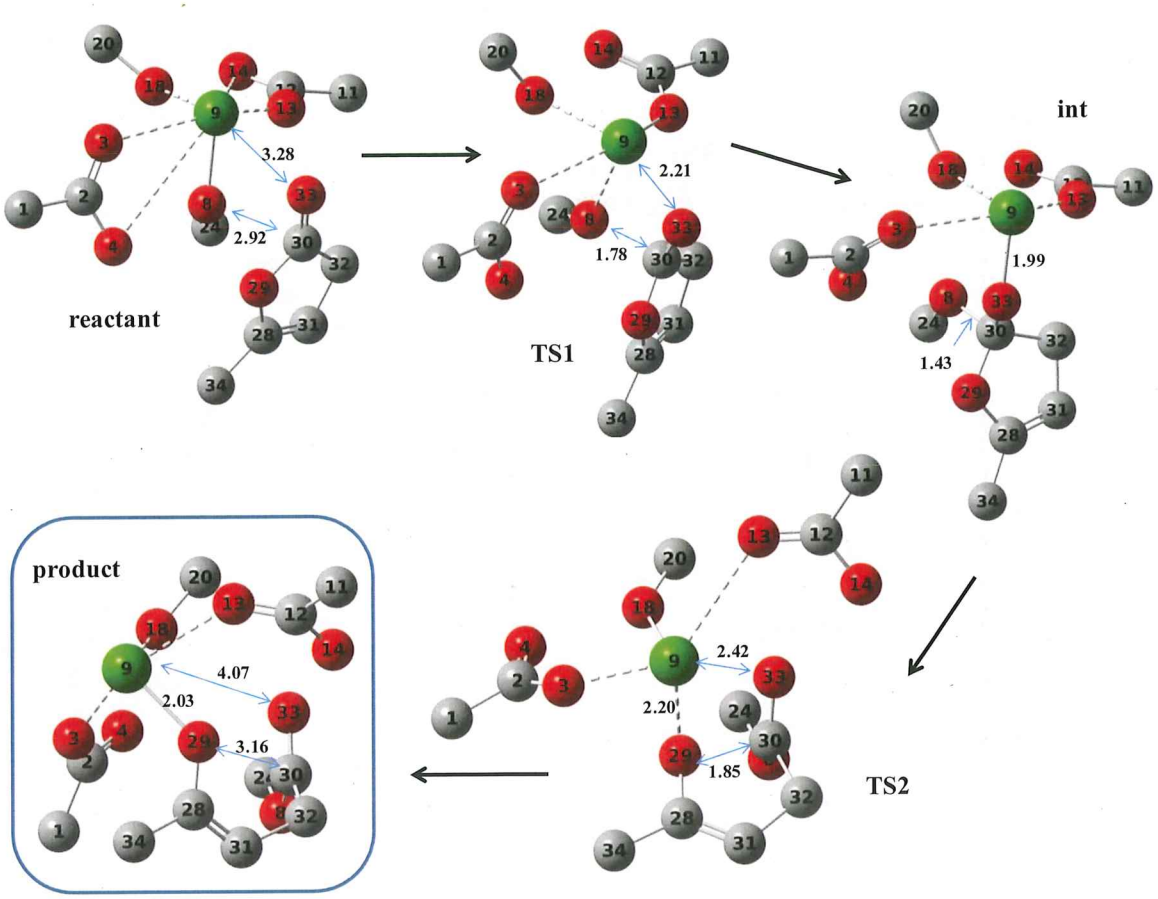

Figure 5.17 Initiation stage of the AL polymerization with $SnAcet_2.2MeOH$. Hydrogens are excluded. Distances are given in Å units. Oxygen, carbon and tin atoms are illustrated in red, gray and green, respectively.

As a result; in the ring opening polymerization reaction of α-angelica lactone with tin acetoxy groups, it has been demonstrated that substances such as alcohol or water acting as co-initiators have not positively effect on the reaction and that high molecular weight PAL synthesis is difficult.

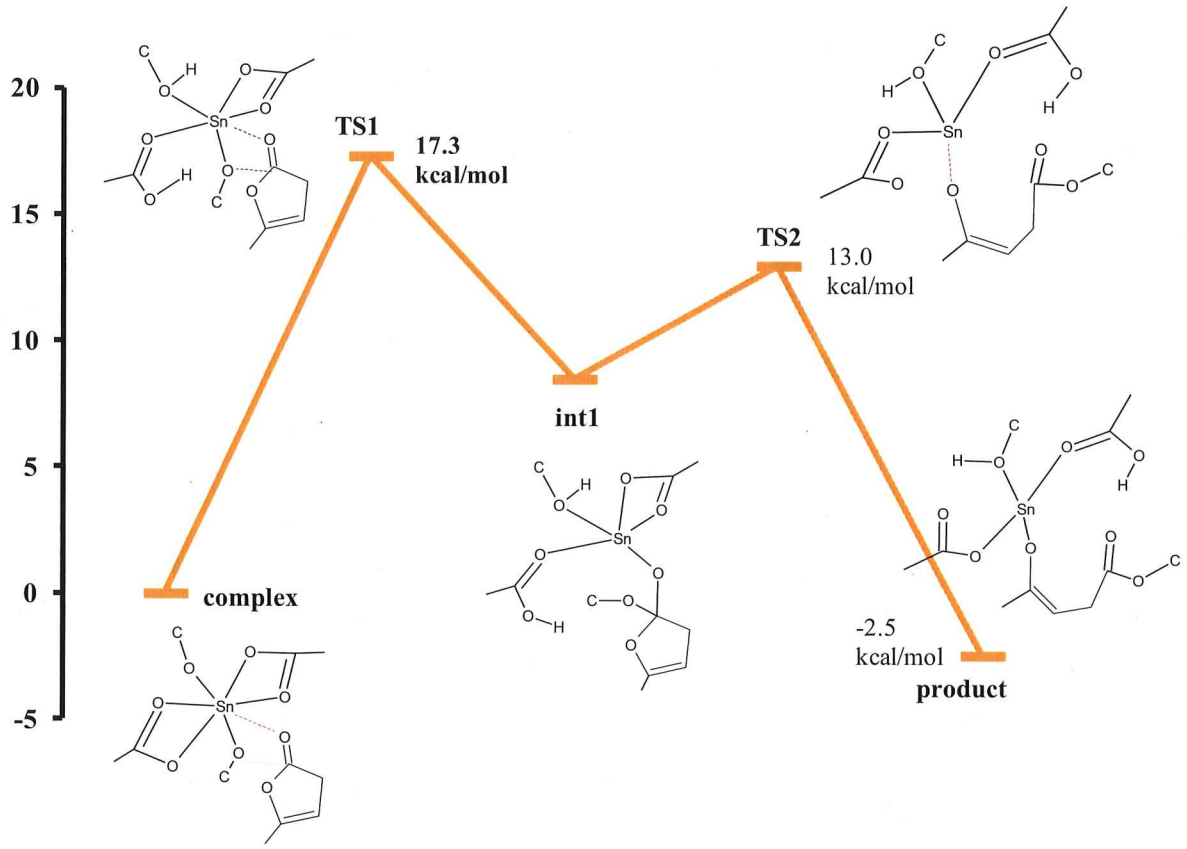

Figure 5.18 Gibbs free energy profile (in kcal/mol) for the initiation stage of ROP of AL using $SnAcet_2$.2MeOH obtained by ωB97X-D/LanL2DZdp. All energies are relative to the complex.

5.1.6 Ionic polymerization of α-angelica lactone with $SnAcet_2$

In the previous section, it is indicated that the reaction in the synthesis of poly(angelica lactone) can proceed in two ways (ionic and ring opening polymerizations). Comparison of activation barriers for both types of reaction is an important point in the interpretation of the product structure. Tin acetate is predicted to have Lewis acidity when an acetate group is separated from its structure (Nijenhuis et al., 1992) and in this case, the reaction can proceed through vinyl polymerization (Marvel et al., 1939; Delidovich et al., 2016). Therefore, vinyl polymerization of angelica lactone in the presence of tin acetate was also studied at ωB97X-D/LanL2DZdp level. When the atomic charges of the angelica lactone were calculated, the charge of carbon atom in the ring (in Fig.5.19, the carbon atom corresponding to C12) was found to be -0.297 (Fig.5.9). Thus, it has been found that the vinyl polymerization proceeding through the double bond starts with interaction between the active complex and the carbon atom (**C**H=C), which has nucleophilic center property (Fig.5.19). Reaction barrier was found as

24.78 kcal/mol (Fig.5.20). Obtaining a barrier of less than about 5 kcal/mol from the ring-opening polymerization reaction barrier indicates that the reaction may proceed through both paths.

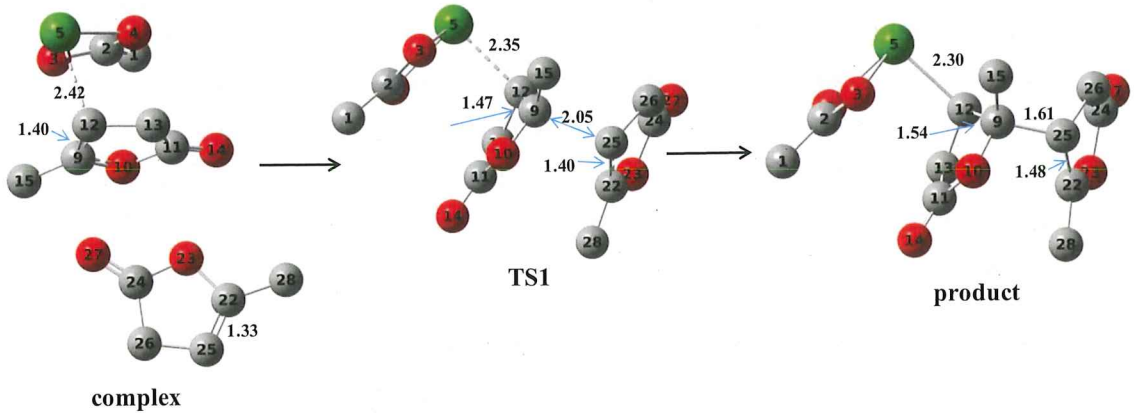

Figure 5.19 Ionic polymerization of AL with $SnAcet^+$ complex. Hydrogens are excluded. Distances are given in Å units. Oxygen, carbon and tin atoms are illustrated in red, gray and green, respectively.

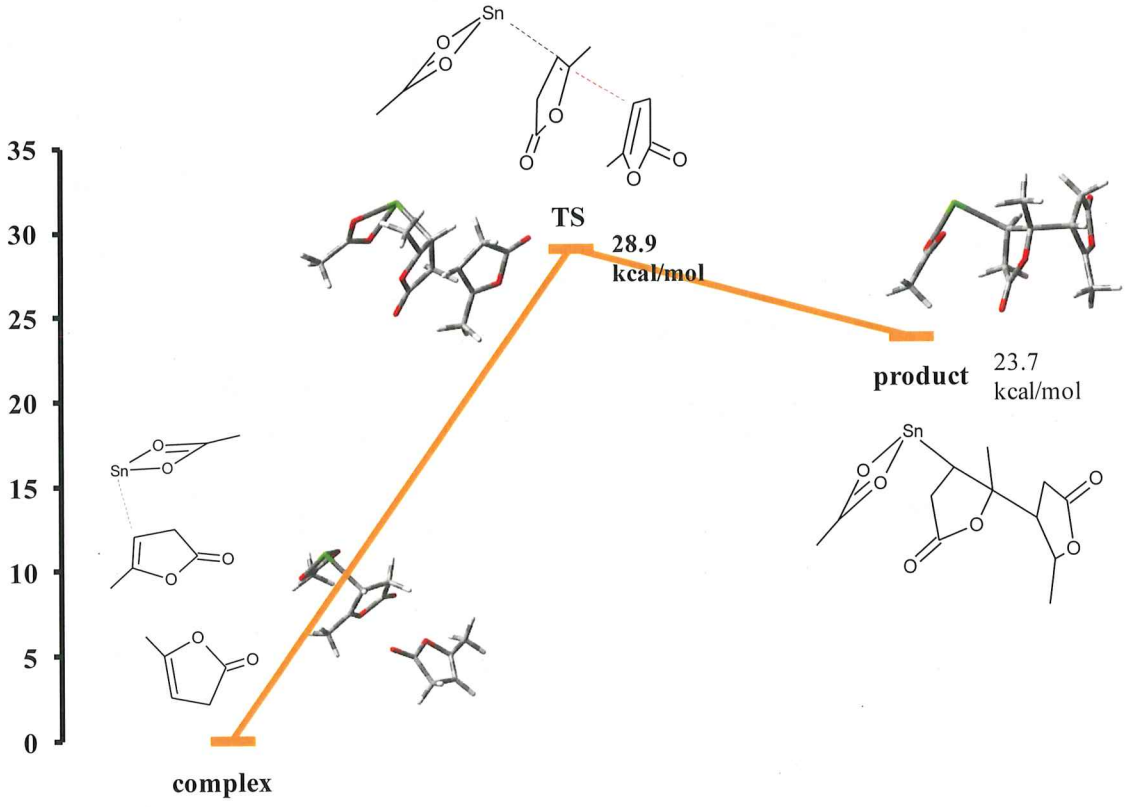

Figure 5.20 Gibbs free energy profile (in kcal/mol) for vinyl polymerization of AL obtained by ωB97X-D/LanL2DZdp. All energies are relative to the rectant.

5.1.7 Computational Study of ROP of α-angelica lactone with Zinc(II)acetate, ($ZnAcet_2$)

5.1.7.1. Initiation Stage

In the synthesis of such biodegradable polymers, the research for biocompatible metal-containing initiators continues. In this sense, the tendency towards complexes containing zinc, magnesium, calcium and iron is remarkable. Although there have been many studies with zinc-containing structures in recent times, there is not much work in the presence of zinc acetate. This knowledge was steered us to the zinc complex for investigate the metal effect, which is actively play role in the initiation and propagation stages of the ring opening polymerization reaction.

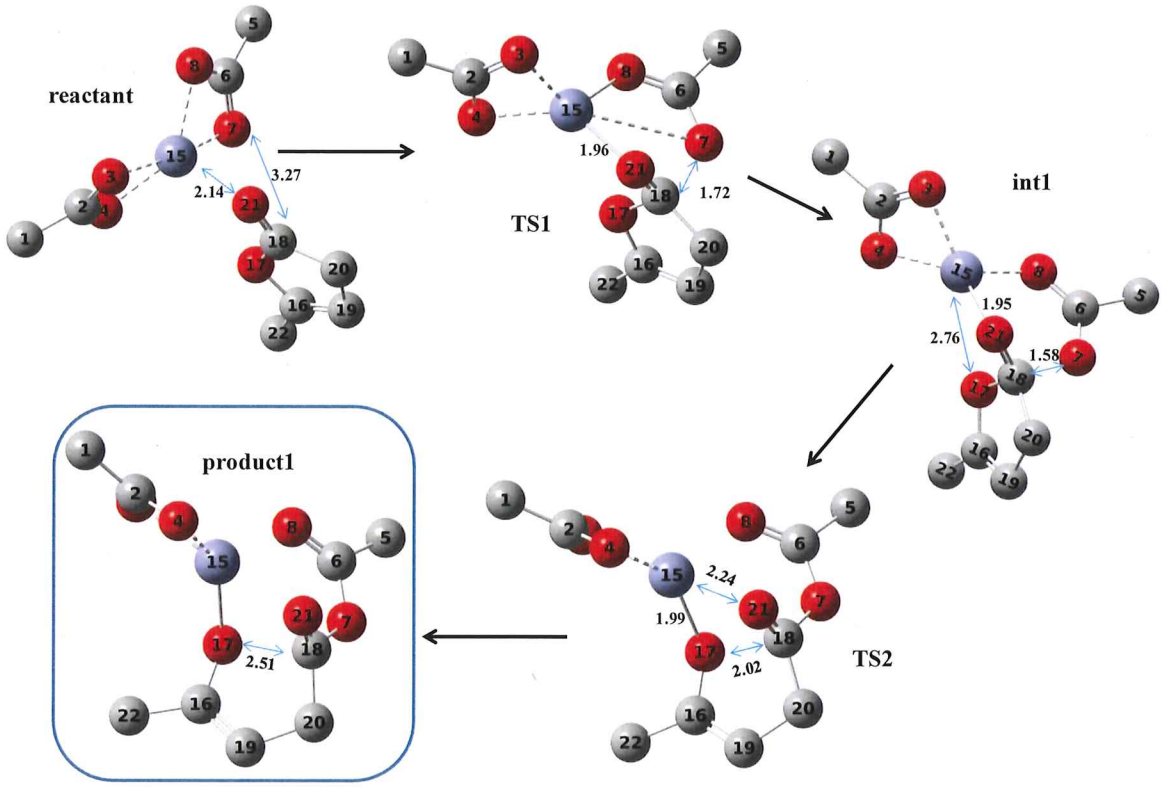

Figure 5.21 Initiation stage of the AL polymerization with $ZnAcet_2$. Hydrogens are excluded. Distances are given in Å units. Oxygen, carbon and zinc atoms are illustrated in red, gray and purple, respectively.

The initiation and propagation stages for ROP of α-angelica lactone with $ZnAcet_2$ were computationally studied at the ωB97X-D/LanL2DZdp level (Fig.5.21.).

According to the data acquired, there is no influence on the polymerization reaction mechanism steps of metal exchange as expected. On the other hand, two activation barriers called TS1 and TS2 was obtained (Fig.5.22).

Table 5.7 Calculated relative Gibbs free energy values (kcal/mol) of all points along the initiation reaction path using the ωB97XD/LanL2DZdp level.

	complex1	**TS1**	**int1**	**TS2**	**product1**
ωB97X-D	0.0	14.3 (10.8)[a]	14.1 (11.3)	23.4 (19.9)	20.9 (18.8)

[a]The values of in parenthesis are enthalpy values in kcal/mol

The reaction activation barrier was determined to be 19.9 kcal/mol (TS2) (Table 5.7). When the reaction initiation step mechanism between tin acetate and zinc acetate is examined, it is expected that the polymerization should be more efficient in the presence of zinc acetate. Because there are about 10 kcal / mol difference between the two reaction barriers.

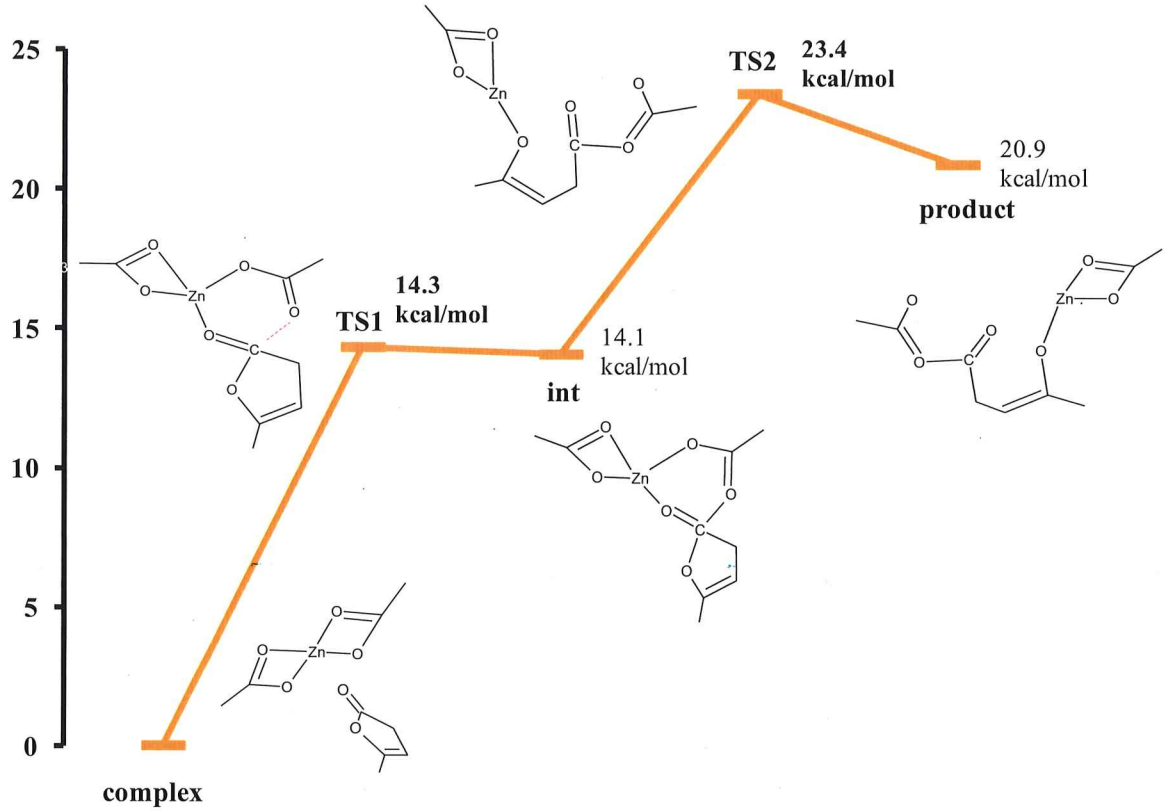

Figure 5.22 Gibbs free energy profile (in kcal/mol) for the initiation stage of ROP of AL using $ZnAcet_2$ obtained by ωB97X-D/LanL2DZdp. All energies are relative to the complex.

5.1.7.2 Propagation stage

The propagation stage was studied at ωB97X-D/LanL2DZdp level for complete investigation of the polymerization reaction of α-angelica lactone in the presence of $ZnAcet_2$, (Fig.5.23). The activation barrier of stage which contains the adding a new monomer to the active chain was determinate as 12.9 kcal/mol (Table 5.8). However, the energy values of stationary point TS3, int2 and TS4 at the potential energy surface are almost the same. (12.4, 12.9, 12.9 kcal/mol, respectively).

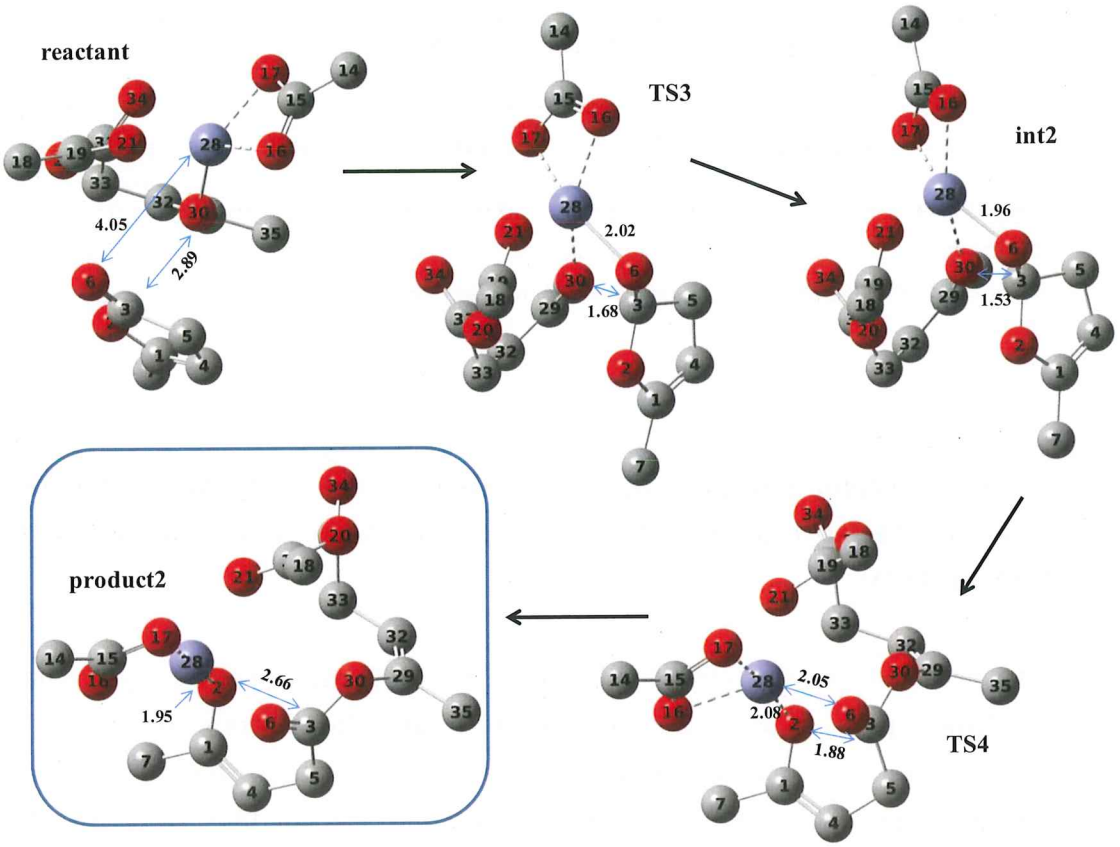

Figure 5.23 Propagation stage of the AL polymerization with $ZnAcet_2$. Hydrogens are excluded. Distances are given in Å units. Oxygen, carbon and zinc atoms are illustrated in red, gray and purple, respectively.

The Hammond hypothesis states that if two consecutive stable structures in a reaction mechanism, such as the transition state structure and the intermediate, are close to each other in terms of energy, small molecular rearrangements are sufficient for their conversion to each other. A further importance of this postulate is that it allows discussion of the transition state structure in terms of reactants, intermediates and products. In our case, since the TS structures resembles to intermediates they are said to be the "late" transition structures. Hence, it can be concluded that the TS structures and intermediates are in equilibrium with each other, they do not release energy during transformation.

Table 5.8 Calculated relative Gibbs free energy values (kcal/mol) of all points along the propagation reaction path using the ωB97X-D/LanL2DZdp level.

	complex2	TS3	int2	TS4	product2
ωB97X-D	0.0	14.4 (12.4)[a]	13.9 (12.9)	16.3 (12.9)	9.0 (7.2)

[a]The values of in parenthesis are enthalpy values in kcal/mol

5.2 Ring Opening Polymerization of δ-valero lactone Using Acetats Contain Different Metal ($SnAcet_2$, $PbAcet_2.3H_2O$, $CdAcet_2.2H_2O$, $NiAcet_2.4H_2O$, $CuAcet_2.H_2O$)

δ-valerolactone (δVL) was dried over CaH_2 and then purified by vacuum distillation prior to use. $2{,}6x10^{-3}$ mol δVL and the determined amount of monomer for 50/1, 100/1, 300/1, 450/1, 600/1 (M/I) ratios were charged into schlenck tube in glovebox and placed in the gas-vacuum line. After that, the reaction mixture dissolved in dry toluene. Polymerizations were carried out different temperature, time and monomer-initiator ratio. At the end of the reaction period, the flask was dipped in liquid nitrogen to terminate the reaction. The product was dissolved in minimum quantity of dichloromethane after that the mixture was precipitated by dropwise addition to methanol. The white precipitate was centrifuged and dried in a vacuum at room condition. The poly (δ-valerolactone) (PVL) with broad high molecular weight range was obtained at high yield.

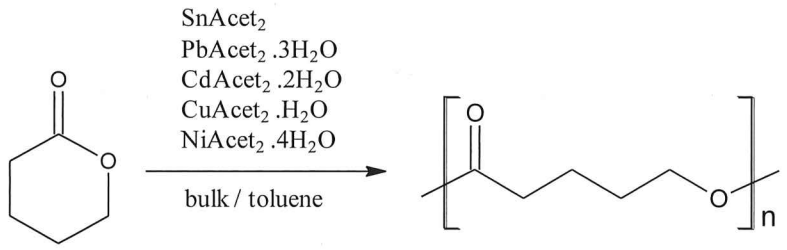

δ-valerolactone poly(δ-valerolactone)

Figure 5.24 General reaction scheme for ring opening polymerization of δ-valerolactone.

5.2.1 Synthesis of poly(δ-valerolactone) with $SnAcet_2$

Tin complexes in ring opening polymerization are commonly used because of their high catalytic activity and low racemization properties. However, polyester synthesis using tin acetate has not been found in the literature so far. Therefore, the ROP of δ-VL was performed with $SnAcet_2$ as an initiator in toluene medium. A lot of experiments were carried out in order to determine the optimum polymerization conditions. Table 5.9 illustrates the reaction conditions studied, the molecular weight (M_n and M_w) of the polymer obtained and the polymerization yield.

Table 5.9 Optimization studies for ROP of δ-valerolactone with $SnAcet_2$.

Entry	Temperature (^{0}C)	Time (h)	M/I	Mn (g/mol)	Mw (g/mol)	Mw/Mn	Yield %
1	110	8	300	14670	29040	1.98	90
2	**130**	**8**	**300**	**20818**	**33168**	**1.59**	**85**
3	140	8	300	17010	23301	1.37	75
4	130	4	300	16302	27335	1.68	73
5	130	12	300	14418	28403	1.97	70
6	130	18	300	11223	21211	1.89	46
7	130	8	450	15769	25861	1.64	63
8	130	8	600	8250	23022	1.46	67
9	130	8	100	12480	21590	1.73	80

The polymerization reactions were realized at 110, 130 and 140 °C for 8 hours at monomer/initiator ratio is 300 to decide the optimum reaction temperature and other variables were kept constant (Fig.5.25.). The molecular weight increased with increasing temperature up to 130 °C, and then the polymerization yield and

the molecular weight decreased at higher temperatures. It is known that, in ROP reaction, increased temperature can be caused to depolymerization and it can decreases the polymerization yield due to the ceiling temperature effect (Wang et al., 2004). So the optimum reaction temperature was determined as 130 °C.

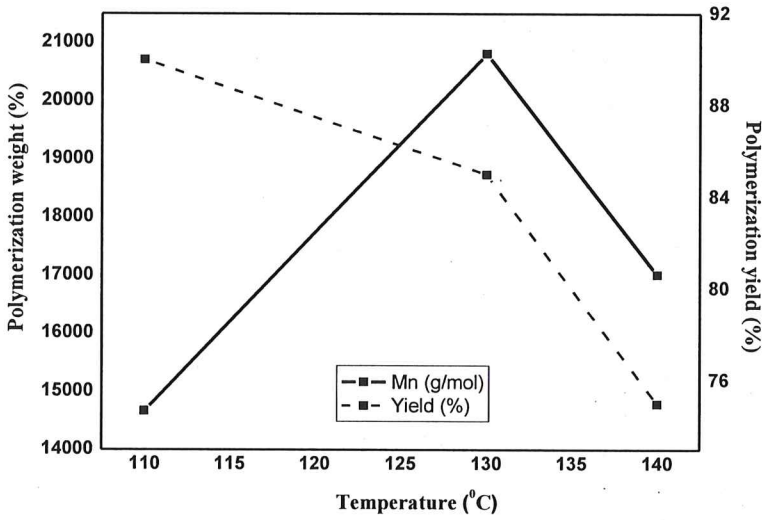

Figure 5.25 The effect of temperature on molecular weight and polymerization yield of PVL with $SnAcet_2$ at 8 h, 300/1, monomer/initiator ratio.

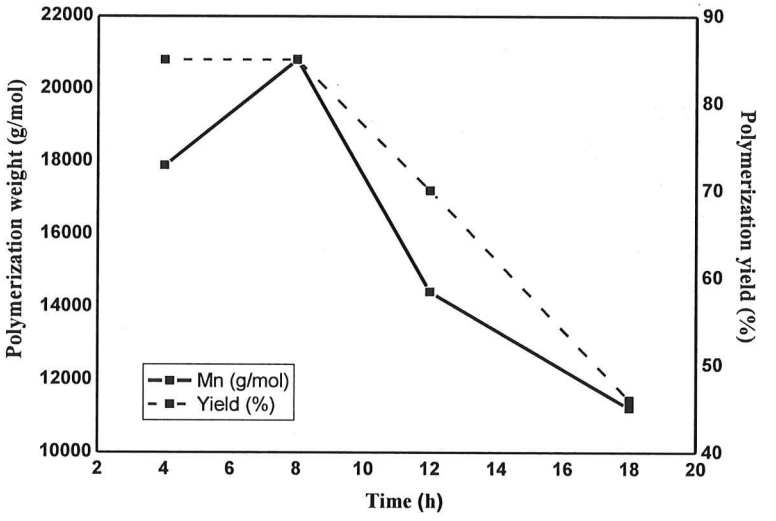

Figure 5.26 The effect of time on molecular weight and polymerization yield of PVL with $SnAcet_2$ at 130°C, 300/1, monomer/initiator ratio.

Fig.5.26 shows the influence of polymerization time on the molecular weight and yield of PVL. Experiments were carried out for 2, 4, 8, 12, 18 and 24 hours at 130°C and 300/1 monomer/initiator ratio. It is found that increasing the reaction time from 4 hours to 8 hours did not change the polymerization yield however it increased the molecular weight. The reaction time of more than 8 hours decreased both the yield and the molecular weight. This may be attributed to transesterification and side reactions occurring during long reaction times. Hence the optimum reaction time was identified as 8 hours.

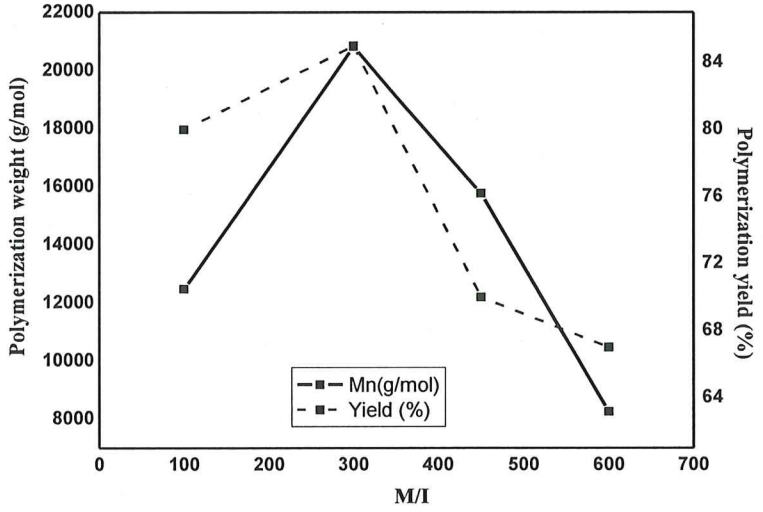

Figure 5.27 The effect monomer/initiator ratio on molecular weight and polymerization yield of PVL with $SnAcet_2$ at 130°C, 8 h.

The PVL was synthesized for 100/1, 300/1, 450/1 and 600/1 monomer/initiator ratio (M/I) conditions at 130 °C and 8 hours to assessment of optimum monomer/initiator ratio. Fig.5.27 shows that the M/I ratio has a similar effect on both the molecular weight and the polymerization yield. The highest molecular weight (20818 g/mol) was obtained at 300/1, M/I, ratio with 85% polymerization yield. In cases of the M/I ratio is lower (100/1) and higher (600/1), the decreasing in the yield and the molecular weight can be explained as follows: Increasing in initiator concentration may result in more chain ends, which may lead to the formation of shorter polymer chains. Contrary to this, decreasing in initiator concentration may cause to produce less active chain sites. It is therefore important to find the optimum value.

5.2.2 Synthesis of poly(δ-valerolactone) with $PbAcet_2.3H_2O$

In the periodic table, the Pb atom is located in the same group with the Sn atom (just below it). Therefore, the lead acetate ($PbAcet_2.3H_2O$) complex was tested as an initiator to determine whether it has a similar efficiency with the $SnAcet_2$ complex on the polymerization process or not.

The experiments were carried out at different time, temperature and monomer/initiator ratio for the evaluation of optimum polymerization conditions. The data obtained are shown in Table 5.10.

Table 5.10 Optimization studies for ROP of δ-valerolactone with $PbAcet_2.3H_2O$.

Entry	Temperature (^{0}C)	Time (h)	M/I	Mn (g/mol)	Mw (g/mol)	Mw/Mn	Yield %
1	110	8	300	3691	4216	1.14	10
2	130	8	300	5954	8912	1.50	60
3	**140**	**8**	**300**	**19425**	**34980**	**1.80**	**91**
4	150	8	300	16036	35154	2.19	79
5	160	8	300	11748	22170	1.89	79
6	140	4	300	20495	46701	2.28	64
7	140	2	300	14133	27073	1.92	43
8	140	12	300	13306	27119	2.04	81
9	140	18	300	8178	16241	1.99	50
10	140	8	450	13289	23717	1.78	65
11	140	8	600	14863	28953	1.95	70
12	140	8	100	9025	21993	2.44	55

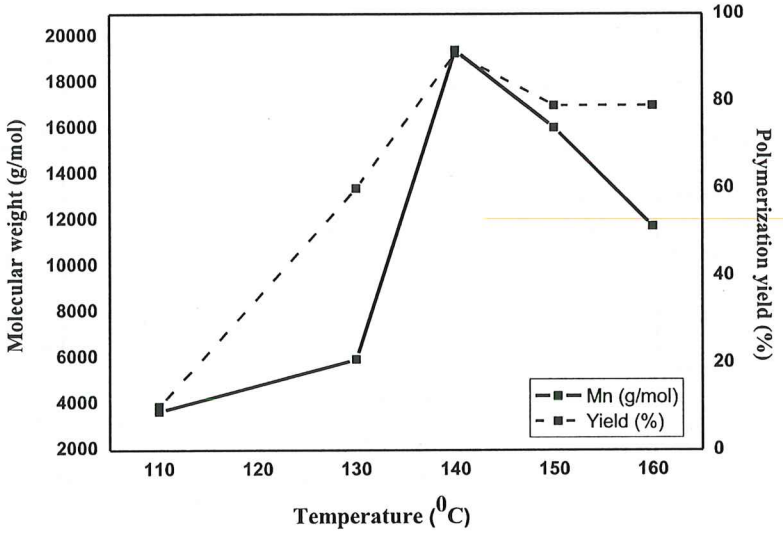

Figure 5.28 The effect of temperature on molecular weight and polymerization yield of PVL with $PbAcet_2.3H_2O$ at 8 h, 300/1 monomer/initiator ratio.

In order to determine the best reaction temperature, the polymer was synthesized at 110, 130, 140, 150, 160 °C for 8 hours at 300/1, M/I ratio and the highest molecular weight was obtained at 140 °C (Fig.5.28). The polymerization yield increased rapidly with increasing temperature up to 140 °C and then it decreased at 150 °C and remaining constant at higher temperature. The molecular weight increased stepwise with increasing temperature up to 150 °C, and decreased at higher temperatures. It is thought that higher temperature may be caused to chain breakage.

The polymerization reactions were performed for 2, 4, 8, 12, 18 hours at constant M/I as 300/1 to observe the effect of the time on the polymerization (Fig.5.29). The highest molecular weight is obtained at 4 hours but polymerization yield (64%) was low at this condition. Therefore, when both the yield and the molecular weight were considered together, the best reaction time was determined as 8 hours.

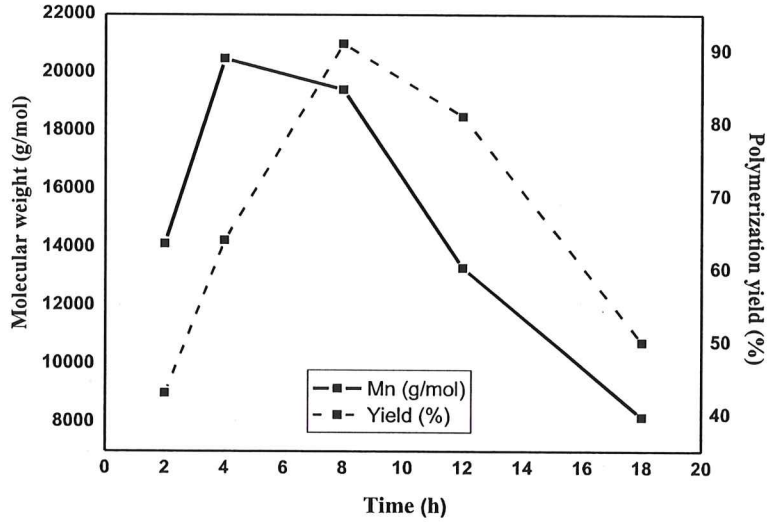

Figure 5.29 The effect of time on molecular weight and polymerization yield of PVL with $PbAcet_2.3H_2O$ at 130 °C, 300/1 monomer/initiator ratio.

The PVL was synthesized for 100/1, 300/1, 450/1 and 600/1 at 140 ^{0}C, for 8 hours for the purpose of the optimum monomer/initiator ratio. Fig.5.30 shows that the monomer/initiator ratios affect the polymerization yield and molecular weight in the same manner. The optimum M/I ratio was identified as 300/1.

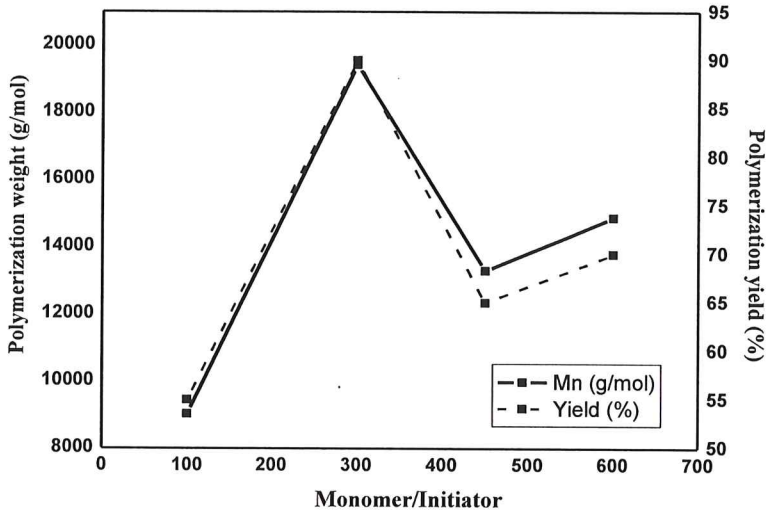

Figure 5.30 The effect of M/I ratio on molecular weight and polymerization yield of PVL with $PbAcet_2.3H_2O$ at 130 °C, 8 h.

5.2.3 Synthesis of poly(δ-valerolactone) with $CdAcet_2.2H_2O$

Another metal atom selected to compare the initiator activity of the acetate complexes containing different metals is cadmium. Cadmium acetate used in only a few studies in the literature has not been tried for polymerization of δ-valerolactone. One of the reasons of choosing the Cadmium atom is the fact that it is in the same group (just below it) with the zinc atom which is very popular recently.

An optimization study was conducted to find the reaction condition giving the highest molecular weight and polymerization yield. Table 5.11 contains the molecular weight, polymerization yield, and poly dispersity index (PDI) obtained under several reaction conditions.

Table 5.11 Optimization studies for ROP of δ-valerolactone with $CdAcet_2.2H_2O$.

Entry	Temperature (^{0}C)	Time (h)	M/I	Mn (g/mol)	Mw (g/mol)	Mw/Mn	Yield %
1	140	8	300	14532	25138	1.73	32
2	150	8	300	36971	68278	1.85	92
3	160	8	300	31465	69058	2.19	76
4	**150**	**4**	**300**	**45438**	**87249**	**1.92**	**91**
5	150	2	300	22777	52673	2.31	73
6	150	12	300	41643	81661	1.96	88
7	150	18	300	40690	73464	1.80	87
8	150	4	600	35241	85515	2.43	79
9	150	4	100	48595	86503	1.78	70
10	150	4	50	4952	6048	1.22	37

Experiments were carried out at 140, 150 and 160 °C for 4 hours at 300/1 monomer/initiator ratio to determine the best polymerization temperature. Fig.5.31 shows that the effect of increasing temperature on molecular weight and

yield is the same. The value of both parameter increases up to 150 °C and then decrease with increasing temperature due to the thermal decomposition of the monomer.

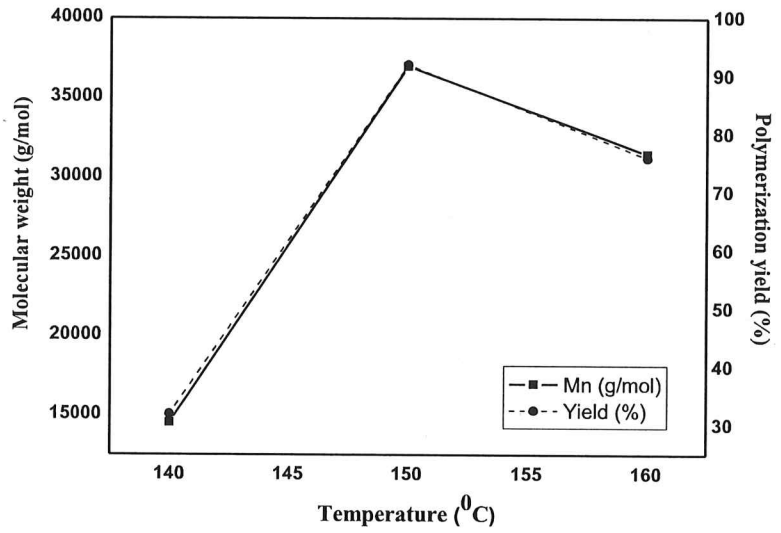

Figure 5.31 The effect of temperature on molecular weight and polymerization yield of PVL with $CdAcet_2 .2H_2O$ at 4 h, 300/1, monomer/initiator ratio.

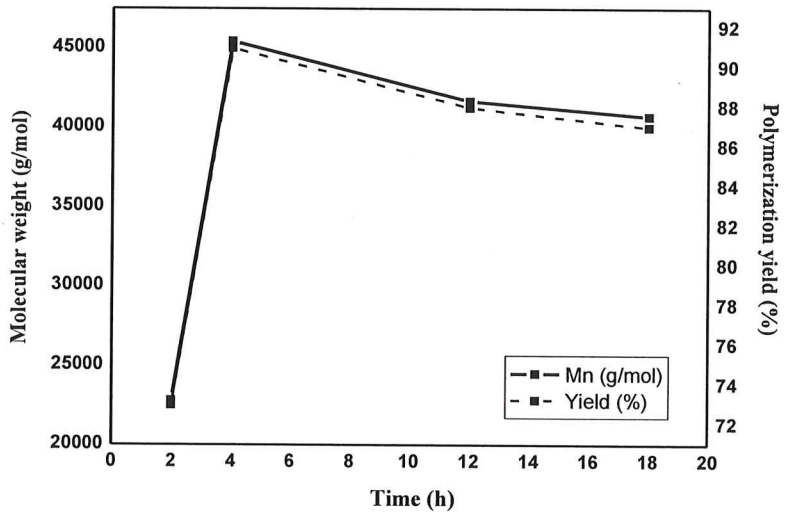

Figure 5.32 The effect of time on molecular weight and polymerization yield of PVL with $CdAcet_2 .2H_2O$ at 150 °C, 300/1, monomer/initiator ratio.

The effect of reaction time on the molecular weight and the yield was given in Fig.5.32. Several experiment were carried out for 2, 4, 8, 12 and 18 hours at 150 °C and 300/1, M/I ratio to find the optimum reaction time. It can be seen that, higher molecular weight PVL (45438 g/mol) was obtained in a shorter time when using cadmium acetate as initiator compared with other acetate complexes. This shows that cadmium acetate has a high efficiency as an initiator. It was determined that the change in reaction period parameters has almost the same effect on the molecular weight and polymerization yield.

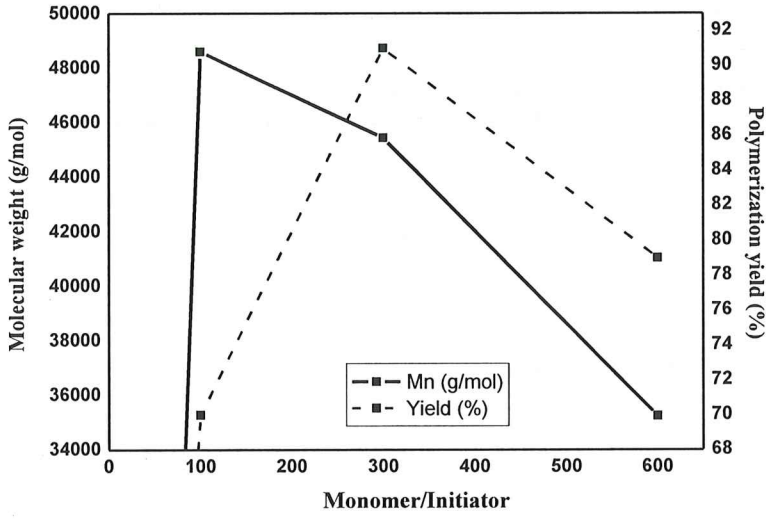

Figure 5.33 The effect of monomer/initiator ratio on molecular weight and polymerization yield of PVL with $CdAcet_2 .2H_2O$ at 150 °C, 4 h.

In order to reveal the effect of the monomer/initiator ratio on the polymerization, PVL was synthesized at 150 °C for 4 hours with rates of 50/1, 100/1, 300/1 and 600/1. As seen from Fig.5.33, the molecular weight increases with increasing concentration of the initiator up to 50/1, M/I ratio. The high initiator ratio is most likely to result in the formation of many oligomer structures because of the fact that it forms too many active ends. The separation of these formed oligomers in the purification step can result in lower polymerization yield. However, when the polymerization yield and molecular weight are taken into account, the optimum ratio is determined as 300/1.

5.2.4 Synthesis of poly(δ-valerolactone) with $NiAcet_2.4H_2O$

It has been investigated whether nickel metal having lower toxic effects could or could not be a new alternative initiator for the ring-opening polymerization. In the polymerization studies of PVL with $NiAcet_2.4H_2O$ complex, a much lower molecular weight and lower polymerization yield were obtained. The optimization results are given in Table 5.12.

Table 5.12 Optimization studies for ROP of δ-valerolactone with $NiAcet_2.4H_2O$.

Entry	Temperature (^{0}C)	Time (h)	M/I	Mn (g/mol)	Mw (g/mol)	Mw/Mn	Yield %
1	130	8	300	——	——	——	——
2	150	8	300	5124	5710	1.11	21
3	160	8	300	5033	7258	1.44	16
4	150	4	300	3164	4366	1.38	10
5	150	12	300	5750	9142	1.59	30
6	150	18	300	6704	10250	1.53	44
8	150	18	600	2150	2730	1.27	7
9	**150**	**18**	**100**	**10891**	**17639**	**1.62**	**82**
10	150	18	50	4480	6164	1.38	65

The polymer was synthesized at 130, 150 and 160 ^{0}C for 8 hours at 300/1, M/I ratio, and the working temperature was determined as 150 ^{0}C. The polymer could not be obtained at 130 °C and there was also no significant difference in the molecular weight of synthesized polymer at 150 °C and 160 °C (Fig.5.34).

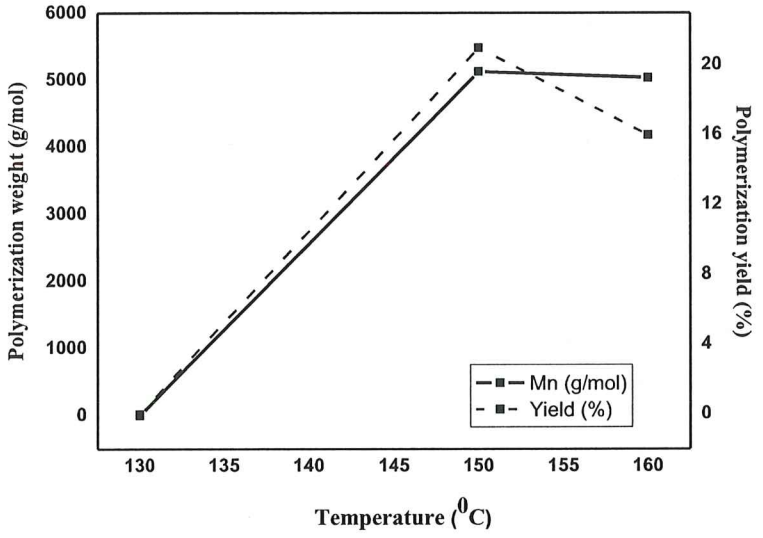

Figure 5.34 The effect of temperature on molecular weight and polymerization yield of PVL with $NiAcet_2.4H_2O$ at 18 h, 100/1, monomer/initiator ratio.

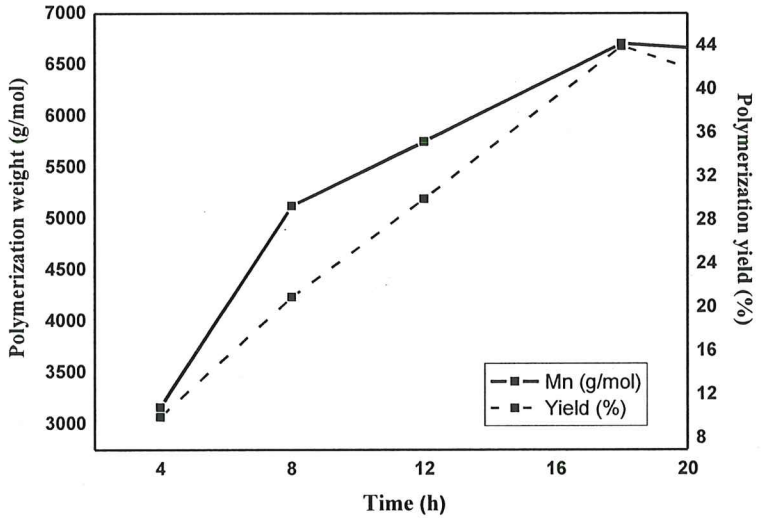

Figure 5.35 The effect of time on molecular weight and polymerization yield of PVL with $NiAcet_2.4H_2O$ at 150 °C, 100/1, monomer/initiator ratio.

Fig.5.35 shows the relationship between the polymerization time and the molecular weight, as well as, polymerization yield of the PVL. The reactions were executed for 4, 8, 12, 18 and 24 hours at 150 °C and 300/1 ratio for the evaluation

of optimum polymerization time. As seen from the Figure 5, both parameters increase up to 18 hours, but then they started to decrease in the longer reaction period.

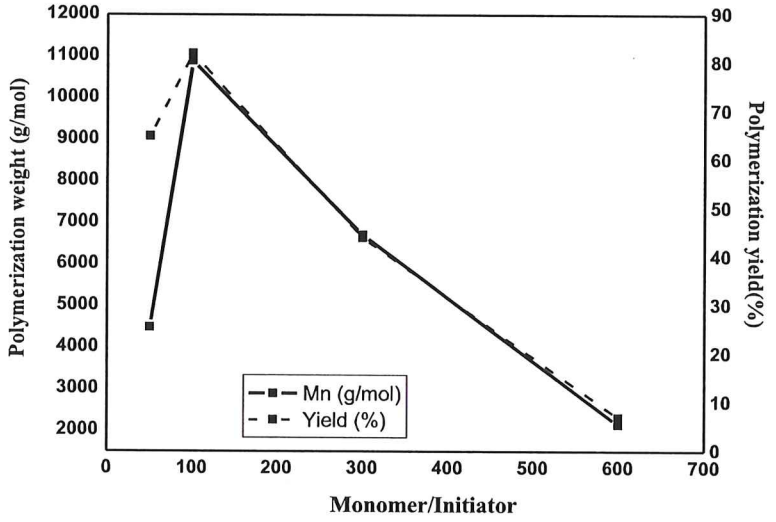

Figure 5.36 The effect of M/I on molecular weight and polymerization yield of of PVL with $NiAcet_2.4H_2O$ at 150 °C, 18 h.

The polymerization reaction of PVL was carried out for 50/1, 100/1, 300/1 and 600/1 monomer/initiator ratio at 150 °C, 18 h for assessment of the optimum initiator ratio. From Fig.5.36, the best M/I ratio was identified as 100/1. Both the molecular weight and the polymerization yield were increased with increasing initiator concentration up to 50/1 ratio. The increase in polymerization efficiency is also surprising. However, in the light of all these results, it has been shown that $NiAcet_2.4H_2O$ in terms of molecular weight is not an effective initiator for ring opening polymerization of δVL.

5.2.5 Synthesis of poly(δ-valerolactone) with $CuAcet_2.H_2O$

PVL was synthesized using $CuAcet_2.H_2O$ to compare the activity of acetate complexes containing different metals (Ni and Cu) in the same period. As seen from Table 5.13, the polymerization yields of obtained polymers are extremely low. For this reason, the molecular weight of each optimization condition could not be analyzed by GPC and the optimization graphs could not be drawn. The highest polymerization yield was obtained as 25% at 150 ^{0}C, 8 hours and 100/1

monomer/initiator ratio condition (M_n= 5755 g/mol). Surprisingly, the highest molecular weight of the polymer was found to be 19411 g/mol in spite of very low polymerization yield. These interesting results will also be discussed in the next section including theoretical studies.

Table 5.13 Optimization studies for ROP of δ-valerolactone with $CuAcet_2$. H_2O.

Entry	Temperature (^{0}C)	Time (h)	M/I	Yield %
1	110	8	300	——
2	140	8	300	2
3	**150**	**8**	**300**	**10**
4	160	8	300	9
5	150	4	300	5
6	150	2	300	3
7	150	12	300	8
8	150	18	300	7
9	150	8	600	4
10	150	8	100	25

5.2.6 Characterization of poly(δ-valerolactone), PVL

Characterization results for the product which was obtained using different metal containing initiators does not change due to the having same structure and same functional groups. Therefore the analysis results were given for the polymer with the highest molecular weight that is synthesized at 150 °C, 4 h, and 300/1, M /I ratio using $CdAcet_2.2H_2O$.

FTIR-ATR spectra of poly(δ-valerolactone) was given at Fig.5.37 and expected peaks were observed. The spectrum showed the following bands: 2850 cm^{-1} (-

CH_2- stretching), 1700 cm^{-1} (C=O ester bond stretching), 1150 cm^{-1} (CO-O ester bond stretching).

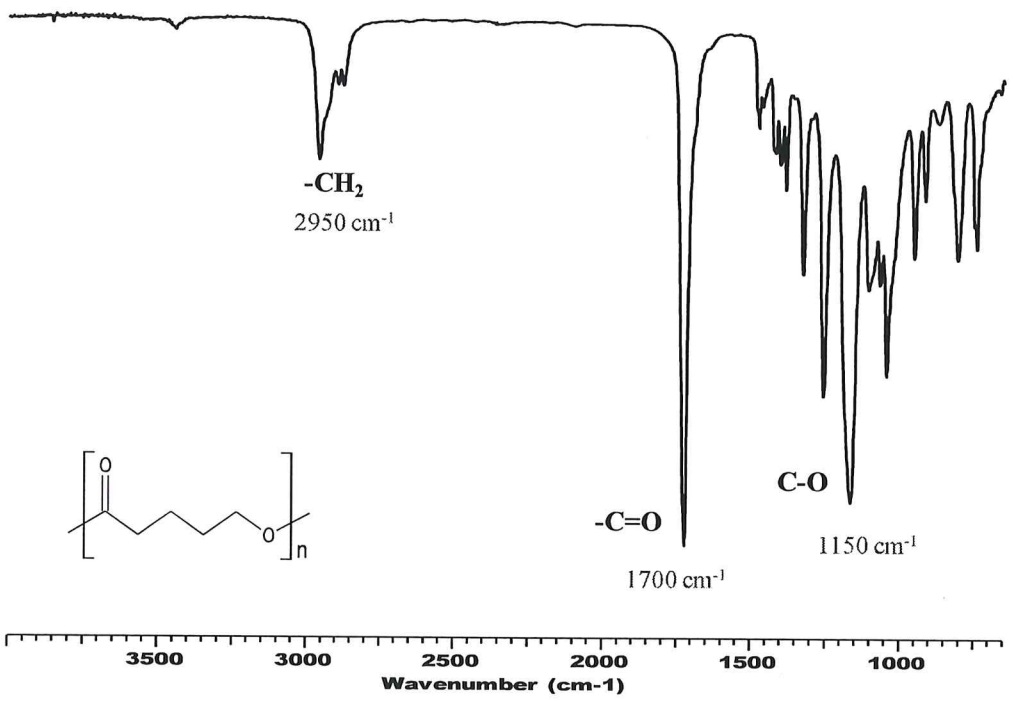

Figure 5.37 FTIR spectrum of poly(δ-valerolactone).

The ^{1}H-NMR spectra of distilled δ-valerolactone and PVL was given in Fig.5.38 and 5.39. As a result of the ring-opening reaction, the expected peaks in both spectra are the same. However, in the spectrum of the polymer, it was detected that the polymer peaks shifted to a lower region according to the monomer peak.

In monomer spectra the peaks at 1.85 ppm (m, 4H), 2.52 ppm (t, 2H) and 4.31 ppm (t, 4H) indicated the $COCH_2\mathbf{CH_2}CH_2CH_2O$–, $CO\mathbf{CH_2}$– and –$\mathbf{CH_2}O$ group, respectively. As designated in Figure x, the spectrum confirmed the structure of PVL as follows: 1.69 (m, $–COCH_2\mathbf{CH_2}CH_2CH_2O–$), 2.33 (t, $–CO\mathbf{CH_2}–$), 3.64 (t, $–CH_2OH$ end group), 4.07 (t, –$\mathbf{CH_2}O$).

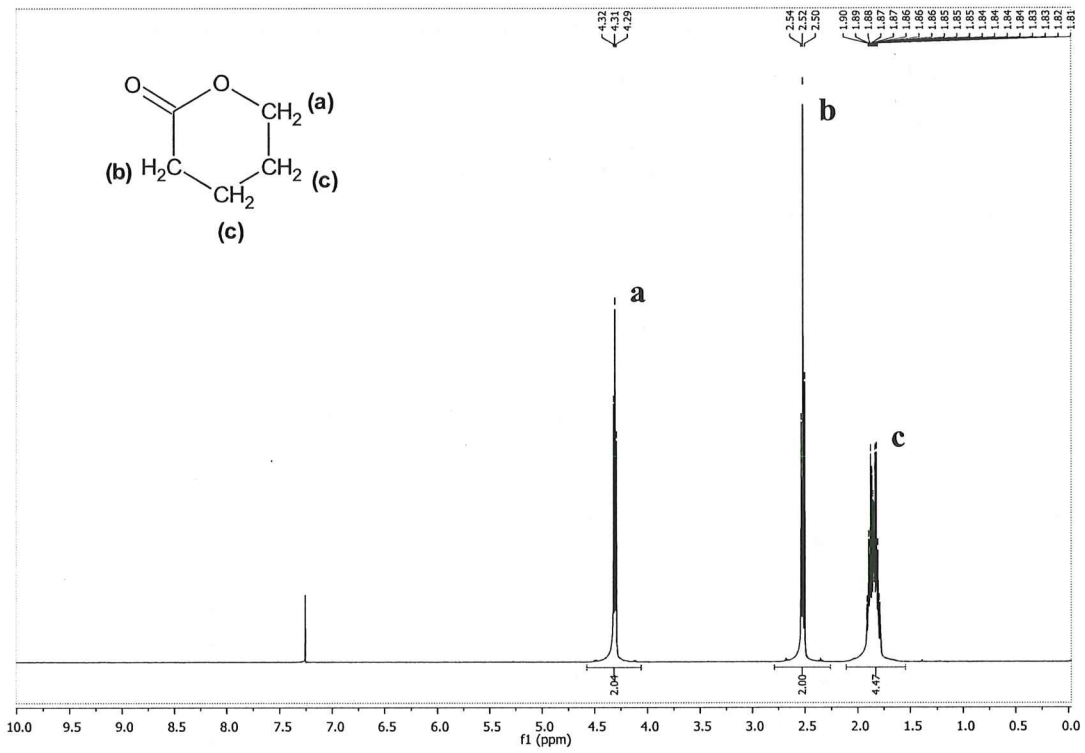

Figure 5.38 ^{1}H-NMR spectrum of purified δ-valerolactone.

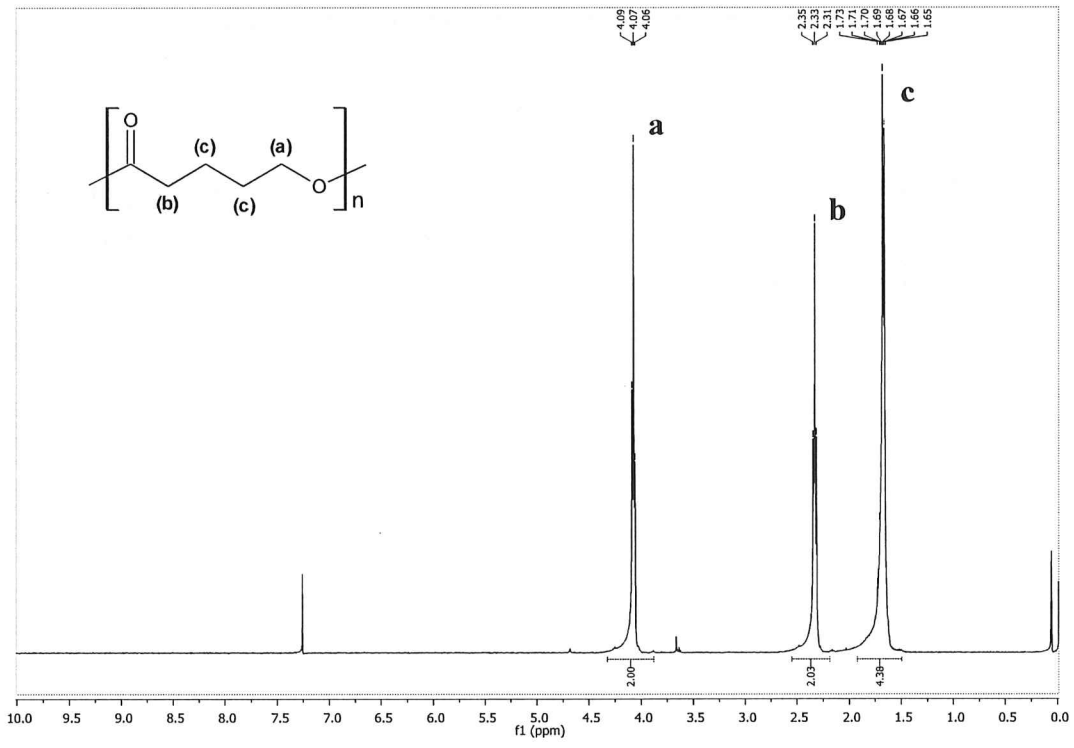

Figure 5.39 ^{1}H-NMR spectrum of poly(δ-valerolactone).

Thermal stability of polymer investigated and the thermogram was given at Fig.5.40. It could be said that PVL is stable up to 220 °C. It was fully degraded at 320 °C at one step and at 600 °C nearly 1.5 % weight lost was seen. It is thought that this remaining amount is most probably the metal compound coming from the initiator that binds to the polymer structure.

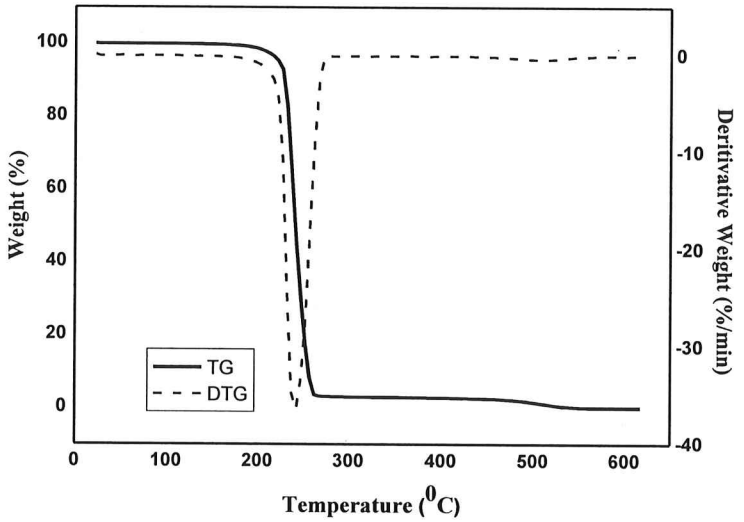

Figure 5.40 TG thermogram of poly(δ-valerolactone).

It can be seen that the thermal stability of the polymer is considerably increased about 150 ^{0}C when the thermal properties of the monomer and the polymer are compared (Fig.5.41.).

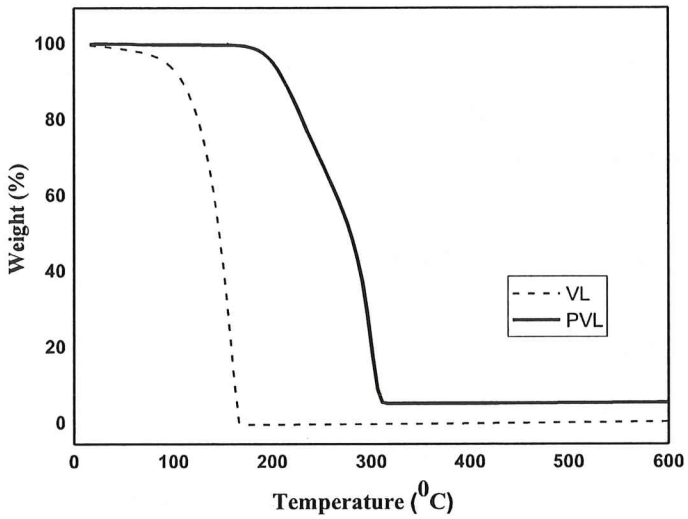

Figure 5.41 TG thermogram of δ-valerolactone and poly(δ-valerolactone).

In the DSC analysis was performed, the glass transition temperature (t_g) of the polymer was determined to be 54 °C (Fig.5.42.).

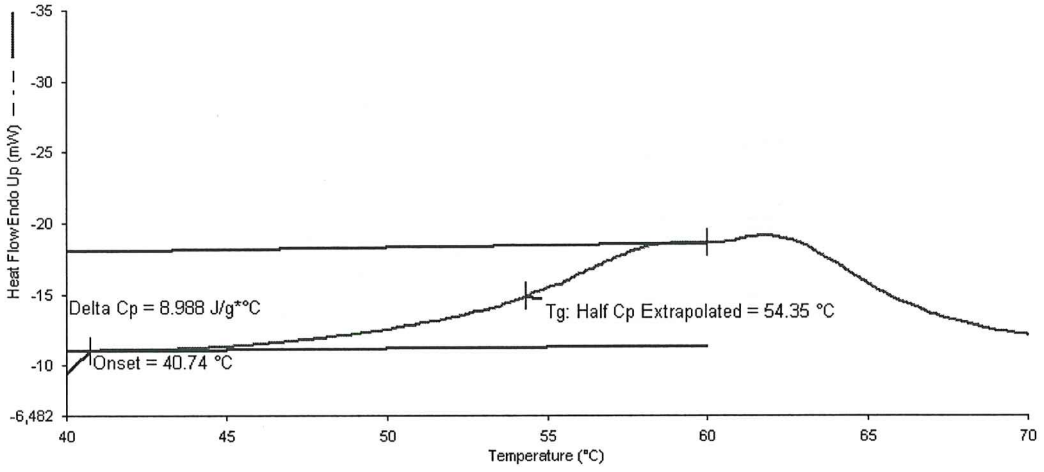

Figure 5.42 DSC thermogram of poly(δ-valerolactone).

5.2.7 Cytotoxicity Assay

Cytotoxicity test was carried out for poly(δ-valerolactone) synthesized with $SnAcet_2$, $CdAcet_2.2H_2O$ and $PbAcet_2.3H_2O$ initiators which contain toxic metal. It was investigated whether they were suitable or not for cell application.

Polymers (0,1 g/ml) and polyethylene, used for negative control (0,1 g/ml) were extracted in serum-free Dulbecco's Modified Eagle's medium (DMEM) at 37 °C for 24 hours. The cytotoxicity of polymers treated BHK-21 cell lines were determined by using colorimetric MTT assay [(3-(4,5-dimethylthia zol-2-yl)-2,5-diphenyltetrazolium bromide] (Monteiro-Riviere, Inman, and Zhang 2009). For MTT assay, $1x10^5$ cells/ml were initially seeded into 96-well microtiter plates. After the overnight incubation, the culture medium was replaced with different concentration of the polymer extracts (1:1, 1:2, 1:4, 1:8). After 72 hours incubation period, cell viability was evaluated with MTT test via measuring the absorbance at 570 nm using spectrophotometer. Then, MTT medium was removed and DMSO was added as a positive control. Three replicates were performed for each experiment.

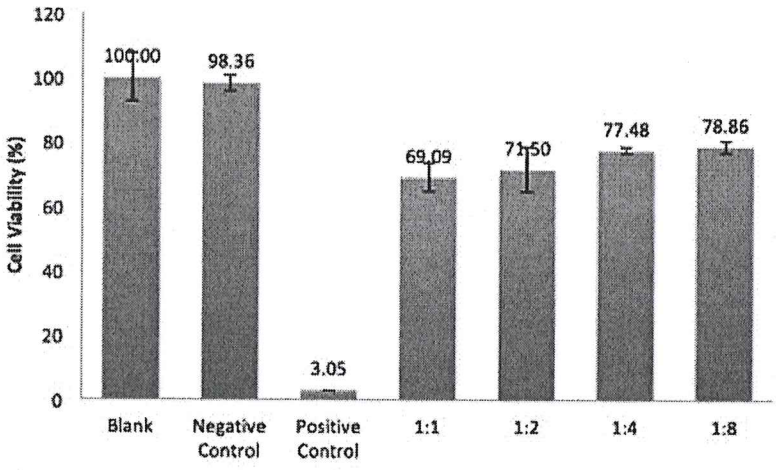

Figure 5.43 Viability of BHK-21 cells after an incubation time of 72 hours with various concentration of PVL extract synthesized using $SnAcet_2$.

Cell viability was found to be below 70% in the performed MTT analysis using a 1: 1 dilution ratio for PVL synthesized with tin acetate. Thus, it was determined that this concentration had a cytotoxic effect in regard to cell death, but did not

show cytotoxic effect in terms of cell death at other extraction concentrations of polymer (Fig.5.43).

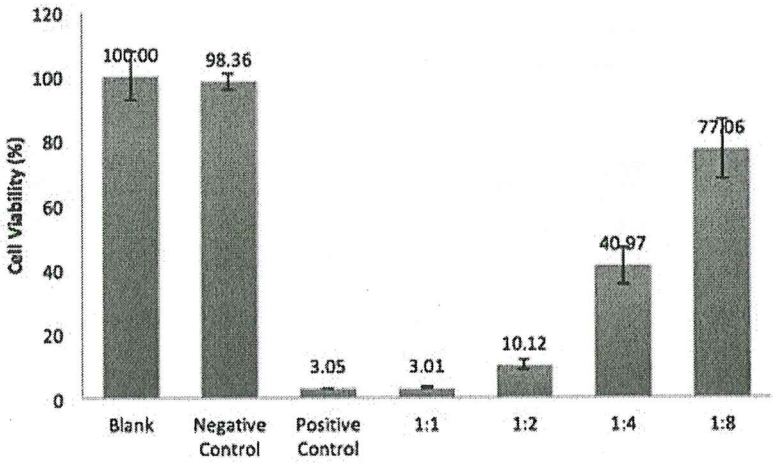

Figure 5.44 Viability of BHK-21 cells after an incubation time of 72 hours with various concentration of PVL extract synthesized using $CdAcet_2.2H_2O$.

As seen from Fig.5.44, since the cell viability of the PVL material synthesized with Cadmium acetate was over 70% in the MTT analysis performed for 1: 8 extraction medium, it was determined that this concentration did not show cytotoxic effect in terms of cell death. However it was found that PVL has cytotoxic effect in terms of cell death at its other extraction concentrations (for 1:1, 1:2 and 1:4)

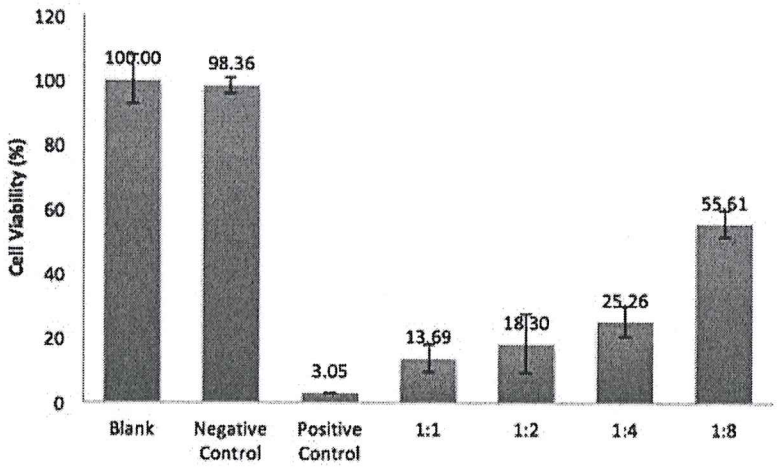

Figure 5.45 Viability of BHK-21 cells after an incubation time of 72 hours with various concentration of PVL extract synthesized using $PbAcet_2.3H_2O$.

As the cell viability in the MTT analysis performed with all concentrations of the extraction medium of the PVL synthesized with lead acetate was below 70%, it was determined that this material had cytotoxic effect in terms of cell death (Fig.5.45).

5.2.8 Theoretical study of PVL

5.2.8.1 Coordination Insertion Mechanism for ROP of δVL

In a theoretical study, Ryner et al. revealed that the rate determining step for the coordination-addition reaction of lactide is the ring opening step. In addition, theoretically calculated ring opening polymerization barriers of lactide, dioxane and glycolide were compared in another publication of the authors, and in these studies it was shown that the rate determining step of the reaction and the reaction energy profile change depends on the structure of the lactone monomers, as well as the structure of initiator. Thus, theoretical studies make it possible to be able to gain a better understanding on the processes of the ring opening polymerization mechanism for different cyclic monomers and different initiators.

To the best of our knowledge, there are no theoretical studies on the ring opening polymerization of δ-valerolactone initiated by $SnAcet_2$ reported so far. Therefore, we carried on a detailed computational study for the initiation stage of ring polymerization reaction process in the gas phase and in toluene medium, since it is revealed that the reaction can experimentally proceed with or without solvent. The most stable geometry and electrostatic potential surface of δ-valerolactone are shown in Fig.5.46.

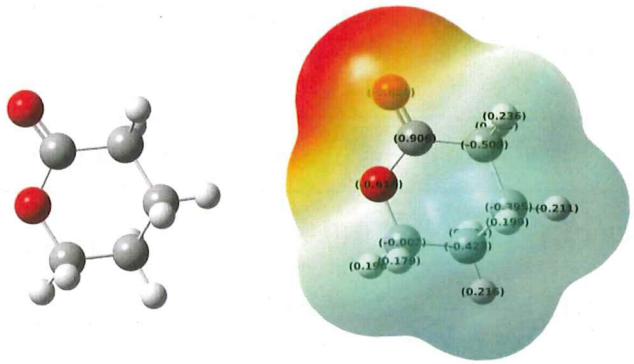

Figure 5.46 Optimum geometry and electrostatic potential surface of δ-valerolactone.

The optimized geometries of all stages along the reaction coordinate and corresponding energies for each step of the reaction were calculated at ωB97X-D/LanL2DZdp level of theory (Fig.5.47 and 5.48, respectively). The ROP mechanism of δVL is a five-step mechanism. The reaction starts with the interaction between the carbonyl oxygen (O3) and the metal (C=O----Sn 2.16 Å), which is the first step (TS1) for the coordination-insertion mechanism, and then occurs a complex (int1) (C=O—Sn 1.34 Å). This step also contains the bond formation as a result of interaction between acetyl oxygen (O5) and carbonyl carbon (O5---C=O 1.49 Å). Generally, in the ring opening polymerization, the bond breaking step constitutes the reaction barrier. In the mechanism, this process begins with the interaction between tin (Sn) and oxygen (O21) in the ring. It can be said that the TS_INT1 and TS_INT2 barriers which occur from result of this interaction can be originated from the rearrangement of monomer structure. The bond between tin and endocyclic oxygen (O21) causes the bond between carbonyl carbon (C2) and O21 to stretch, and then this cause the ring opening. Consequently, TS2, (energy of 28.9 kcal/mol relative to the reactant complex) that

belongs to the opening of the bond between C2 and O21, constitutes the activation barrier of the reaction because it is the highest energy step on the reaction potential energy surface (PES). To investigate the solvent effect on the activation barrier the PCM calculations were performed in toluene medium to be able to mimic experimental conditions. The energy of TS2 were found to be 29.02 kcal/mol in toluene medium. This result shows that there is no significant effect of the solvent on the reaction barrier (Table 5.14).

Table 5.14 Calculated relative Gibbs free energy values (kcal/mol) of all points along the reaction path at ωB97X-D/LanL2DZdp level in gas phase and toluene medium.

	gas phase	**toluene**
complex	0.0 (0.0)[a]	0.0 (0.0)[a]
TS0	7.2 (6.8)	5.3 (4.5)
int1	2.2 (2.2)	1.0 (0.6)
TS1	16.1 (13.3)	16.3 (12.8)
int2	10.9 (7.7)	11.5 (7.1)
TS_INT	18.6 (14.9)	19.0 (14.1)
int3	14.0 (11.3)	15.0 (10.6)
TS_INT2	19.6 (15.1)	20.4 (14.6)
int4	17.5 (15.3)	17.9 (14.7)
TS2	**28.9 (26.2)**	**29.3 (25.7)**
product	19.7 (19.9)	20.5 (19.1)

[a]The values of in parenthesis are enthalpy values in kcal/mol.

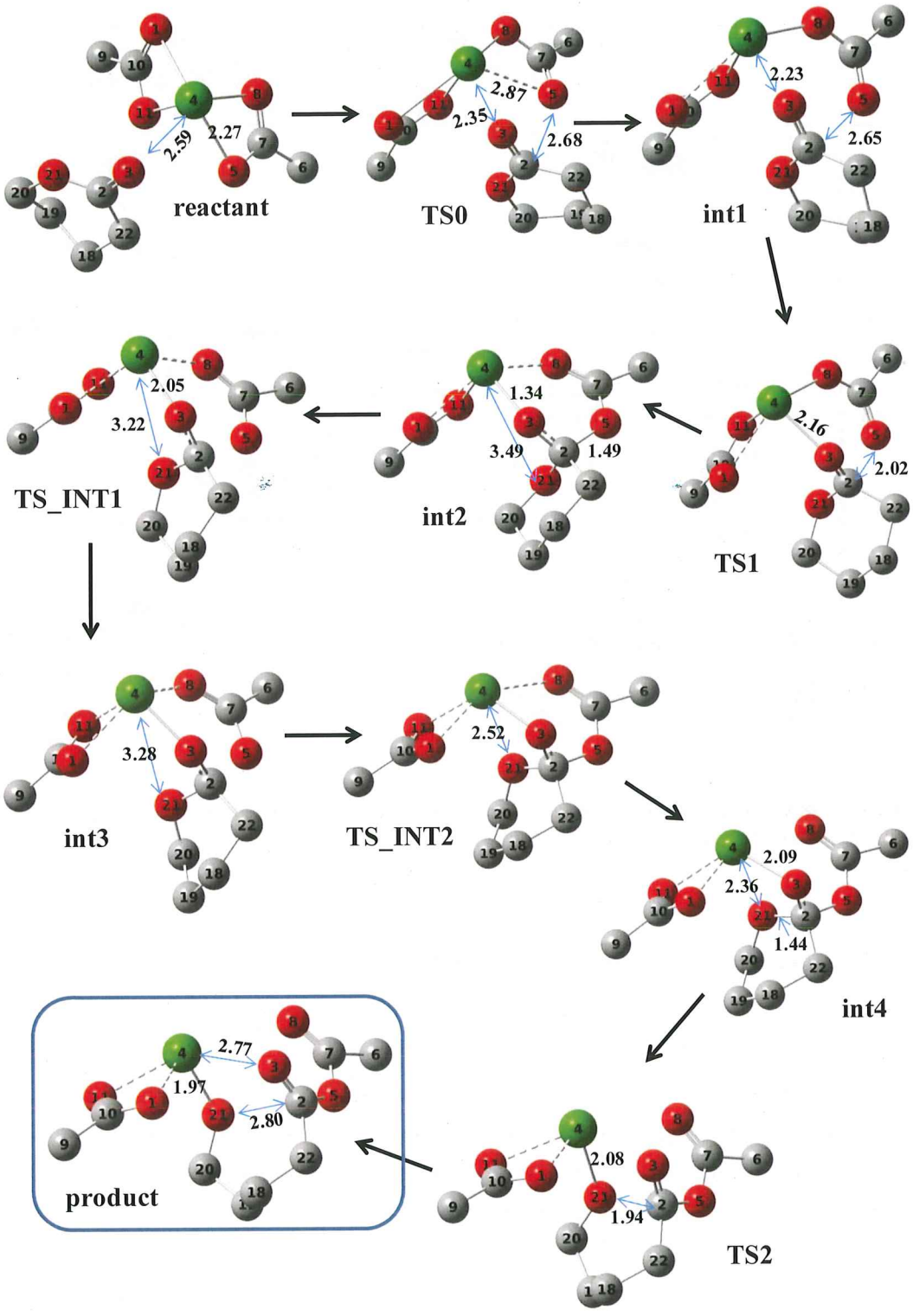

Figure 5.47 The initiation stage of coordination-insertion polymerization of δ-valerolactone with $SnAcet_2$. Bond lengths are given in Å. Hydrogens are not included. Oxygen, carbon and tin atoms are illustrated in red, gray and green, respectively.

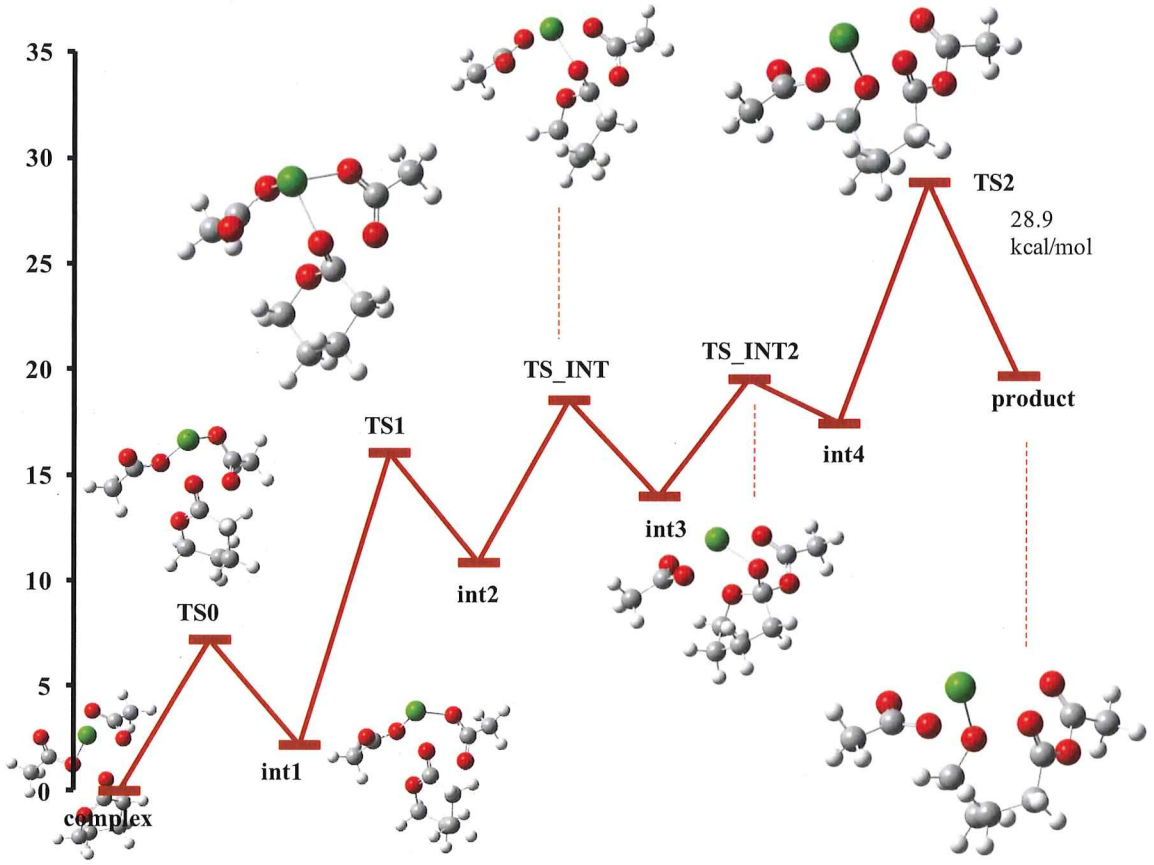

Figure 5.48 Gibbs free energy profile (in kcal/mol) for the initiation stage obtained by ωB97X-D/LanL2DZdp. All energies are relative to the complex.

5.2.9 NBO and LUMO Analysis of Initiators

Electrophilicity of metal center located at initiator plays an important role in the ring opening polymerization of cyclic lactones since it attracts oxygen atom of carbonyl group of cyclic lactone (Sattayanon et al., 2015). In addition, the metal complex having the lowest energy LUMO among the metal-containing initiators used in polyester synthesis has a greater tendency to make bond with the carbonyl oxygen in the monomer. The ring opening step of lactones involves formation a bond between the endocyclic oxygen and the initiator metal. In this case a lower reaction barrier can be obtained with an initiator having low LUMO. Besides, it is compatible with the experimental results that the more electrophilic initiators polymerize the cyclic esters faster (Schenck et al., 2002). Thus, determination of atomic charges on metal centers (via NBO analysis) are taken into account together with LUMO energy comparisons of initiator complexes (LUMO analysis) might help choosing a good initiator.

In the present study, the efficiencies of $SnAcet_2$, $PbAcet_2.3H_2O$, $CdAcet_2.2H_2O$, $NiAcet_2.4H_2O$ and $CuAcet_2.H_2O$ complexes that was used as initiators for PVL synthesis were computationally investigated. The stable structures and atomic charges on metallic centers (via NBO analysis) of these metal complexes were initially optimized at MP2/LanL2DZdp level. Thermogravimetric analysis and physical chemistry handbook data were used to determine how many water molecules connected to acetate complexes containing water at reaction temperature. The electronic properties of all species were, then, determined with single point calculations of B3LYP, cam-B3LYP, ωB97X-D, PBEPBE, PBV86, HSEH1PBE, MPW1PW91, M06, M062X methods employing def2-TZVPPD basis set at the optimized geometries.

Tables X and Y tabulate NBO analysis and LUMO energies of acetate complexes with different metals calculated at various DFT methods employing def2-TZVPPD basis set, respectively. Considering the experimental results and the calculated values together, it is thought that the high molecular weight of the polymer is related to the initiator with low LUMO energy value and the polymerization efficiency is related to the positivity of the NBO charge of the metal in the initiator complex. However, in the initiation of the polymerization reaction, it can be said that the high electropositivity of the metal is the main determinant factor.

The PVL synthesized with tin and lead acetate have similar molecular weights and polymerization yields. The methods satisfying these trends (similar molecular weights and polymerization yields) should give similar NBO charges and LUMO energies that are close to each other. As seen from Tables 5.15 and 5.16, the B3LYP method is the method that best fits to these criteria. The PVL synthesized with lead and cadmium acetate have similar polymerization yields but very different molecular weights. The methods satisfying these trends (similar molecular weights and polymerization yields) should give similar NBO charges but LUMO energies that are extremely different from each other. Accordingly, the B3LYP and M06 methods are the methods that best fits to these criteria. Copper acetate is different from other complexes in terms of electronic structure since it contains an unpaired electron (doublet spin state).

Table 5.15 NBO charges for metals of acetate complexes calculated at various DFT methods employing def2-TZVPPD basis set

Metal of complex	Mn (g/mol)[a]	Yield %[b]	B3LYP	CAM-B3LYP	ωB97X-D	PBEPBE	PBV86	HSEH1PBE	MPW1PW91	M06	M062X
Sn	20818	85	1.370	1.396	1.395	1.305	1.302	1.367	1.371	1.393	1.456
Pb	19425	91	1.442	1.473	1.477	1.376	1.372	1.443	1.449	1.464	1.537
Cd	45438	91	1.407	1.438	1.436	1.327	1.318	1.415	1.424	1.402	1.494
Cu	19411	10	1.151	1.203	1.201	1.015	1.008	1.182	1.192	1.125	1.351
Ni	6704	44	0.921	0.961	0.968	0.758	0.761	0.931	0.944	0.898	1.066

a) The obtained highest molecular weight (Mn) of PVL obtained by GPC at 300/1, monomer/initiator ratio.

b) The polymerization yield for the obtained highest molecular weight PVL.

Table 5.16 LUMO energies of acetate complexes with different metals calculated at various DFT methods employing def2-TZVPPD basis set

Metal of complex	Mn (g/mol)[a]	Yield %[b]	B3LYP	CAM-B3LYP	ωB97X-D	PBEPBE	PBV86	HSEH1PBE	MPW1PW91	M06	M062X
Sn	20818	85	-29.17	-3.51	13.58	-41.50	-43.10	-32.43	-23.65	-28.98	-7.49
Pb	19425	91	-28.26	-3.97	14.11	-39.63	-40.83	-30.96	-22.39	-30.47	-8.53
Cd	45438	91	-31.93	-6.73	13.49	-43.91	-44.54	-33.22	-25.22	-35.69	-13.72
Cu	19411	10	-24.29	6.18	23.61	-41.94	-43.54	-26.54	-18.03	-23.36	-2.86
Ni	6704	44	-60.59	-25.58	-8.72	-89.21	-90.61	-63.30	-53.39	-58.81	-17.46

a) The obtained highest molecular weight (Mn) of PVL obtained by GPC at 300/1, monomer/initiator ratio.

b) The polymerization yield for the obtained highest molecular weight PVL.

The calculations of these types of complexes require unrestricted formalism. Therefore, the DFT methods employed may not give the accurate and reliable results. Although the nickel complex has a very low LUMO energy (a desired property), it is not a suitable initiator for high molecular weight PVL synthesis due to its rather low electrophilicity compared to the others. However, the methods that give these desired properties (low LUMO and NBO charge) are B3LYP and M06. Considering all these, the methods that give the closest trends to the experimental results in determining the effectiveness of metal complexes are the B3LYP and M06 methods. Between these two methods B3LYP performs slightly better than M06.

It is revealed that the molecular weight differentiations of the PVLs that were synthesized with aforementioned initiators can be explained by the joint evaluation of NBO and LUMO analyzes. Therefore, these analyses can help to discover a good initiator leading to a high molecular weight polymer.

5.3 Synthesis of Poly(δ-valerolactone-co-glycidol) Poly(δVL-co-PG)

Recently, polyglycidol, which contains hydroxyl functional group and exhibits hydrophilic property, is of interest. The monomer obtained from glycerol dehydration is an important alternative to petroleum-based polymers in this respect (Petchsuk et al., 2009). Polyglycidol, which has a linear or branched structure that can be polymerized by anionic or cationic ring opening polymerization, was first studied in 1966. The hyper-branched structure and biological inertness properties of polyglycidol provide that it is a preferred material for the synthesis of the copolymerization (Pitet et al., 2007; Gottschalk et al., 2007). The study for copolymerization of glycidol and δ-valerolactone is still absent in the literature. Therefore, we investigated synthesis of poly(δ-valerolactone-co-glycidol) with different ratios (Fig.5.49).

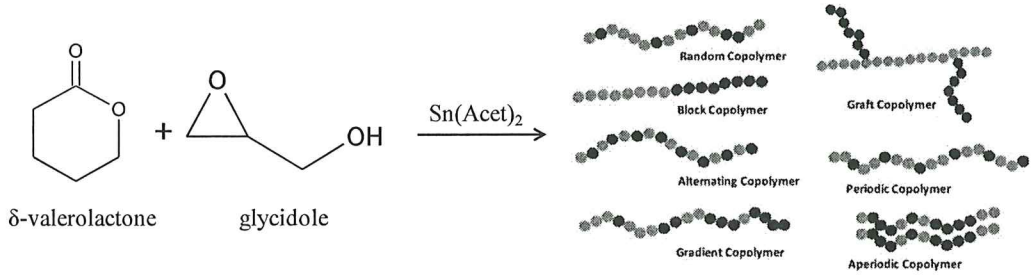

Figure 5.49 The general representation for copolymerization of δ-valerolactone and glycidol.

5.3.1 Reaction Conditions

A series of δ-valerolactone/glycidol copolymer at several compositions including mol: mol as (4:1), (2:1) and (1:1) δVL/GL feed ratios, were synthesized. Initially the monomers were purified by vacuum distillation. For typical ROP polymerization experiment, $2{,}6x10^{-3}$ δVL and glycidol in different molar ratios were injected into the schelenk tube under argon atmosphere. Subsequently, $SnAcet_2$ was added in a molar ratio of 300/1 of the monomers. The mixture was dissolved in added dry toluene. The reaction was performed at 130°C under an inert atmosphere for 18 hours. The copolymers were purified by mixing with ether and then dried in vacuum at 50 ^{0}C. Due to the solubility problems of the obtained products, characterization was only performed with FTIR and TG analysis.

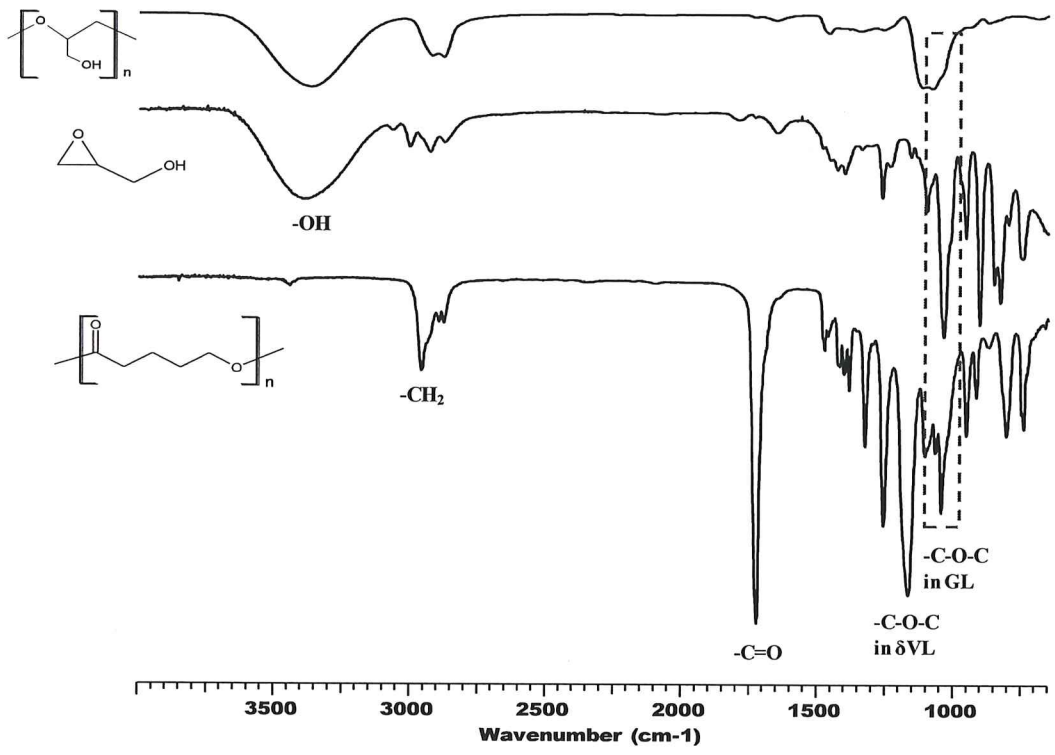

Figure 5.50 FTIR spectrum of polyglycidol, glycidol and poly(δ-valerolactone).

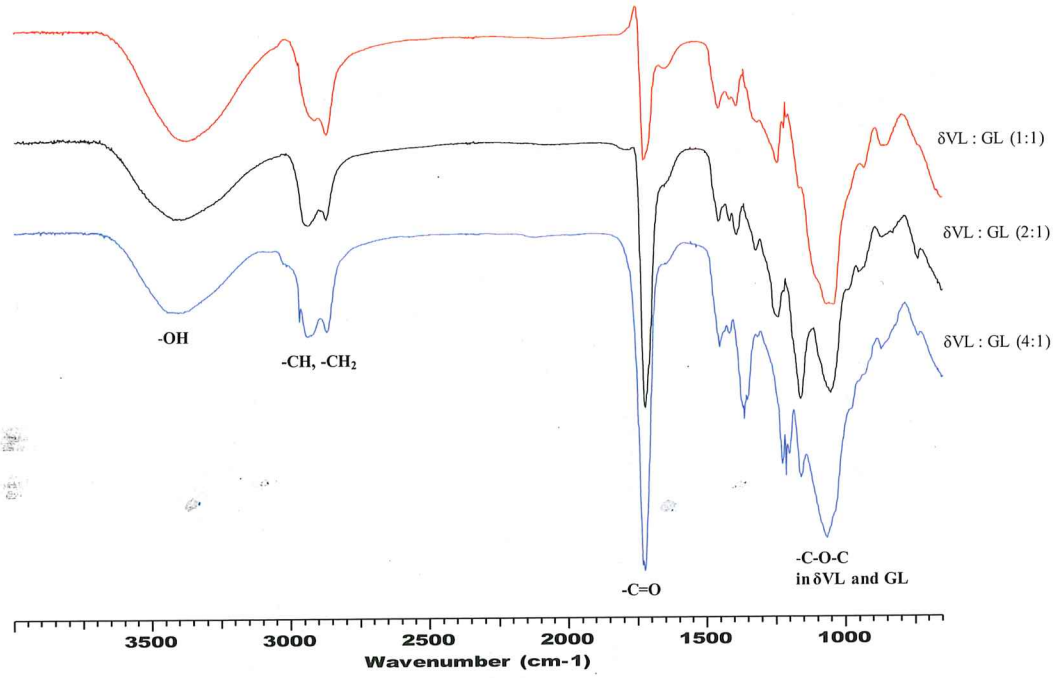

Figure 5.51 FTIR spectrum of poly(δ-valerolactone-co-glycidol) with different composition (1:1, 2:1, 4:1).

FTIR spectra of synthesized homopolymers (polyglycidol, PVL) and copolymers at various compositions were given at Fig.5.50 and 5.51, respectively. Generally, the characteristic –OH stretching band at 3450 cm^{-1} and C–O–C stretching band at 1050 cm^{-1} evidenced glycidol units presence. The C=O stretching band at 1650 cm^{-1} and the C-O stretching band at 1150 cm^{-1} belong to the poly(δ-valerolactone). Also, the peaks belong to –CH and $–CH_2$ group are located at 2800-2950 cm^{-1}. However, as the monomer ratios changed, the characteristic C-O peak found in glycidole and δ-valerolactone structure appeared to be one shoulder or two shoulders. This shows that the chemical structure of the resulting copolymers changes with respect to monomer compositions. The presence of broad and one-shoulder C-O peak in FTIR spectrum of δVL/GL (1:1) was revealed that it may be a cross-linked copolymer.

The thermal properties of poly(δ-valerolactone) and polyglycidol (PGL) were used to interpret the thermal properties of the synthesized poly(δVL-co-PGL) structures. It was demonstrated in Fig.5.52 again that the PVL decomposed at 300 °C and at one step. Furthermore, degradation temperature area of PGL was found between 330-400 °C and it can be seen from Fig.5.52 that the degradation occurred

in one step. The maximum degradation temperature was also determined as 380 °C.

Furthermore, Fig.5.53 shows the DSC curve of polyglycidol. The glass transition temperature of the polymer was determined to be 96 °C.

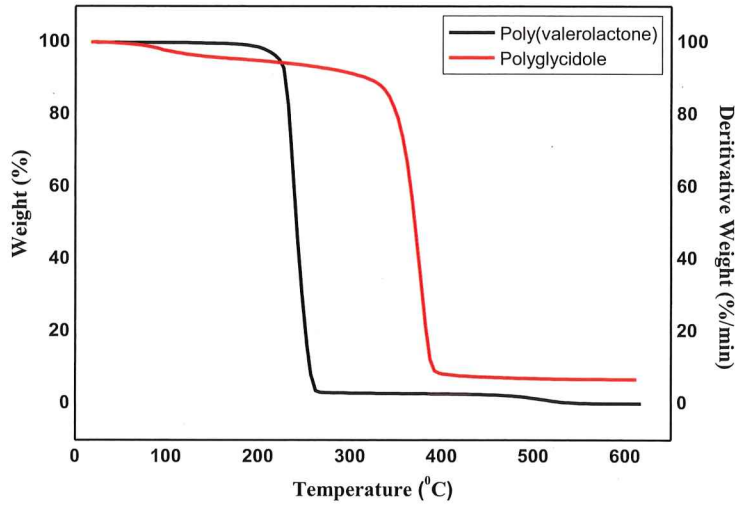

Figure 5.52 TG thermogram of poly(δ-valerolactone) and polyglycidol.

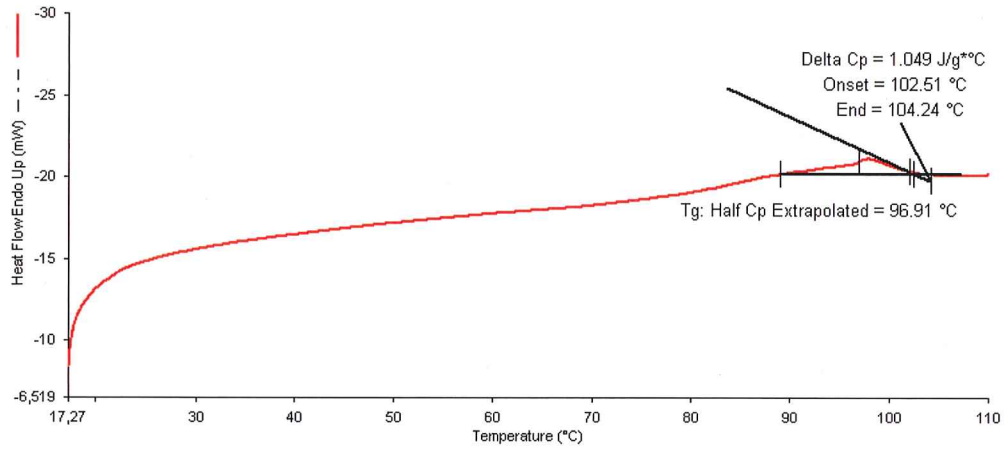

Figure 5.53 DSC thermogram of polyglycidol.

Thermogravimetric analyses (TG-DTG) of random copolymers with various compositions were performed and the thermograms were given at Fig.5.54 and 5.55, respectively. The thermograms clearly indicate that the thermal properties of the copolymer change according to its composition. In addition, the degradation steps at 300 and 380 °C in the thermogram can be interpreted as PVL and PGL structures, respectively.

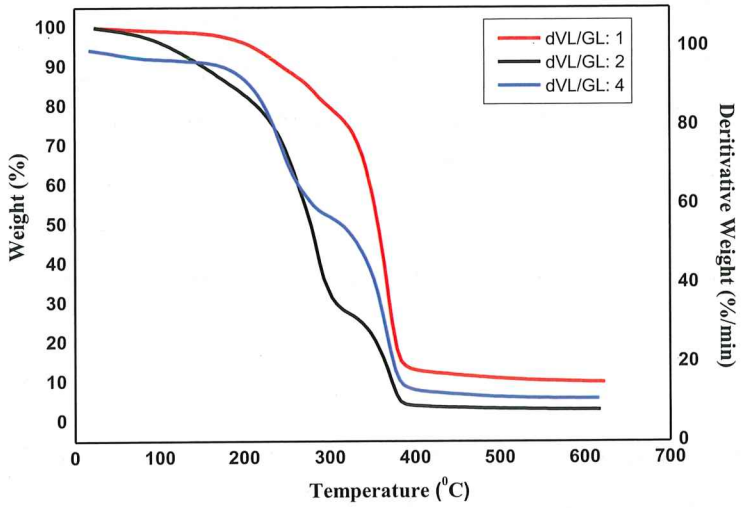

Figure 5.54 TG thermogram of poly(δ-valerolactone-co-glycidol) with different composition (1:1, 2:1, 4:1).

When the thermal behaviors of poly(δVL-co-GL), (1:1) and poly(δVL-co-GL), (4:1) copolymers were examined, it can be said that the structure may be cross-linked block copolymer structure. Because the synthesized copolymers have solubility problems. In the ring-opening copolymerization, the ratios in the monomer mixture were not reflected in the copolymer composition. This is a feature of the ring-opening copolymerization process and shows that it is different from the radicalic or ionic copolymerization processes. The ring opening copolymerization reactions do not match the copolymerization equation (Odian, 2004). Despite partial dissolution in DMSO and acetone, it was not sufficient for NMR analysis.

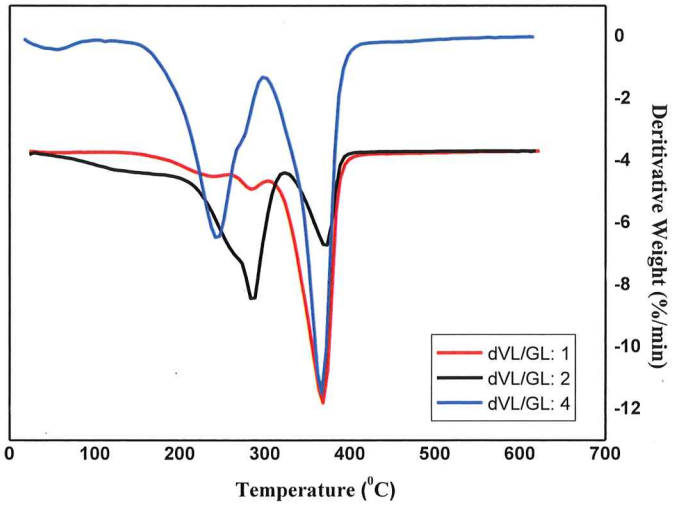

Figure 5.55 DTG thermogram of poly(δ-valerolactone-co-glycidol) with different composition (1:1, 2:1, 4:1).

When the DSC curve of the copolymer is examined, it is seen that the glass transition temperature of the product is 66 °C (Fig.5.56). This value is, as expected, between the glass transition temperatures of the homopolymer structures of both monomers.

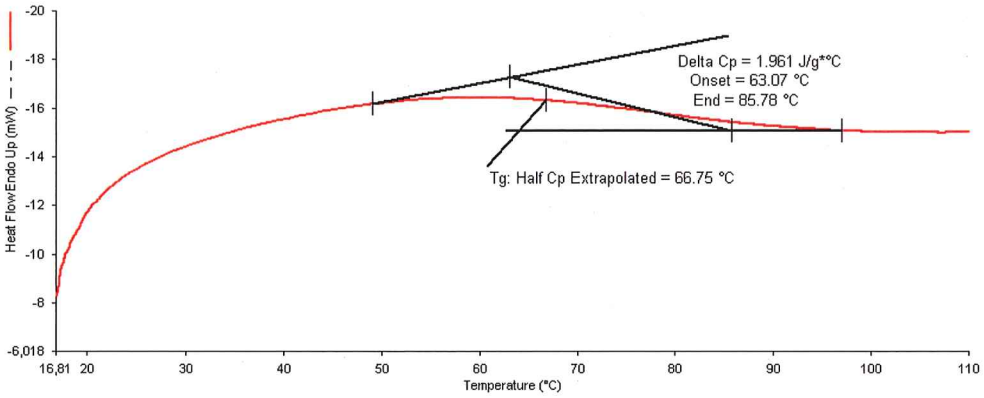

Figure 5.56 DSC thermogram of poly(δ-valerolactone-co-glycidol), (4:1).

5.3.2 Synthesis of Block Poly(δ-valerolactone-b-glycidol) (PVL-b-PGL)

Because of the problem of the dissolution of the products obtained as a result of the random copolymerization synthesis, controlled block copolymerization was also tried. The overall reaction procedure is the same. The only difference is that the initiator and δ-valerolactone are mixed at 130 °C for a while before adding glycidol. 3:1 (mol:mol), δVL:GL feed ratio, was studied. Unlike the random copolymers obtained, it is soluble in DMSO. The structure obtained was elucidated by FTIR, TG and additionally ^{1}H-NMR.

When the FTIR spectrum (Fig.5.57) of the obtained copolymer was investigated, characteristic peaks of both monomers are observed. The –OH stretching and –C–O stretching peaks of glycidol are located at 3500 cm^{-1} and 1050 cm^{-1}, respectively. The C=O stretching band at 1650 cm^{-1} and the C–O stretching band at 1150 cm^{-1} concern with the δ-valerolactone.

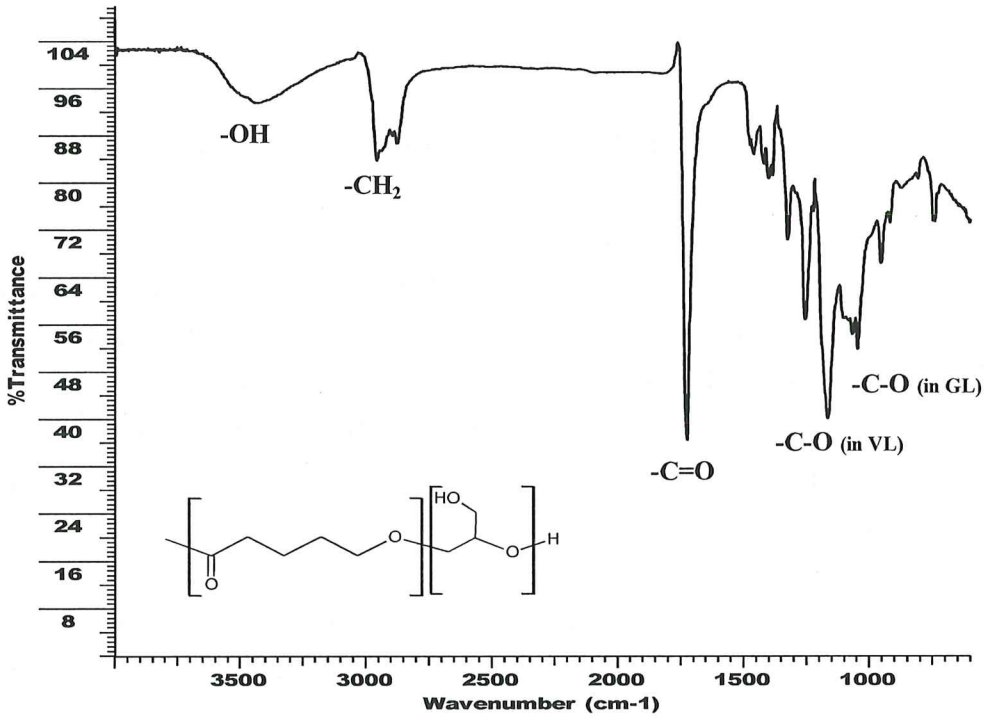

Figure 5.57 The FTIR spectrum of (PVL-b-PG), (3:1).

The chemical structure of copolymer was determined by ^{1}H-NMR in DMSO. Fig.5.58 belong to 60/40 δVL/GL copolymer ^{1}H-NMR spectrum. The peaks at

4.07 (a), 2.36 (c) and 1.57 (b) ppm associated with OC-CH_2, O=C-CH_2 and CH_2-CH_2, respectively. The broadly overlapping peaks in the 3.2-4 ppm range belong to the -CH and -CH_2 groups of the glycidol structure.

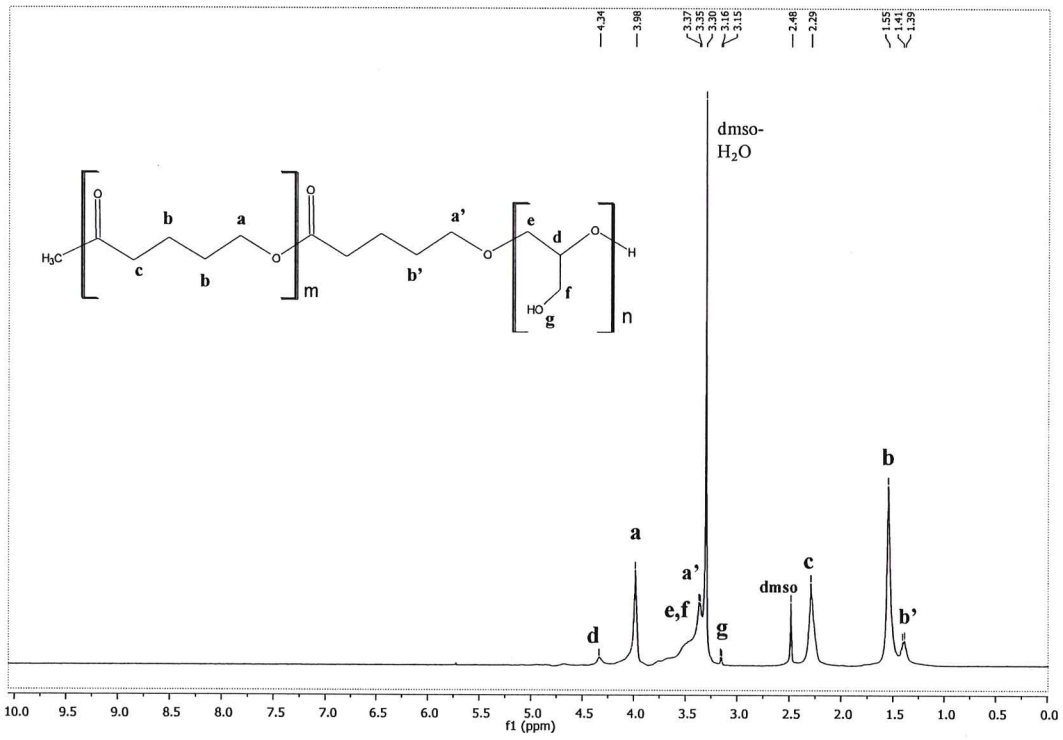

Figure 5.58 The ^{1}H-NMR spectrum of (PVL-b-PG), (3:1).

Fig.5.59 shows the TG and DTG curves of the synthesized block copolymer. It was determined that degradation takes place between 250 and 420 °C in two steps. The maximum degradation curves at 300 °C and 380 °C are related to structure of PVL and PGL, respectively. It is also seen that 70% of the copolymer is poly (δ-valerolactone). Therefore, it can be thought that this is the reason for the structure to become soluble.

The molecular weight of block copolymer was measured by GPC in THF. The number average molecular weight was obtained as nearly 3500-4000 g/mol.

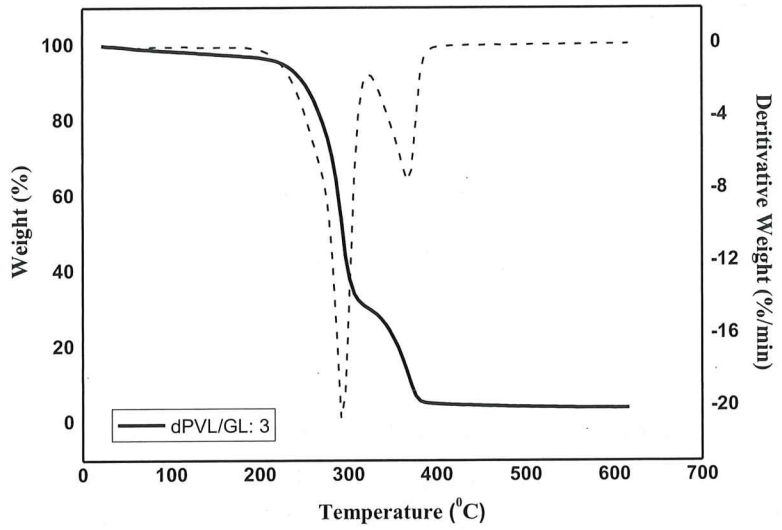

Figure 5.59 The TG thermogram of (PVL-b-PG), (3:1).

5.3.3 Synthesis of Tosylate Glycidol (TsGL)

The aim of tosylation of glycidol was to protection functional group for synthesize soluble and not cross-linked poly(δ-valerolactone-co-glycidol). Furthermore, the reason for the selection of tosylate as a protecting group is frequently used in displacement reactions. Thus, the -OH group in the structure can be converted to other functional groups such as $-N_3$.

Triethylamine (0.009 mol) and glycidol (0.007 mol) was added into balloon, then cooled to 0^0C by stirring in dichloromethane (10 ml) under the inert atmosphere. p-Toluensulfonyl chloride (0.007 mol) was slowly added into the mixture and stirred overnight. It was checked by TLC technique that the starting materials did not remain. The precipitate was separated; the organic phase was washed with HCI, saturated solution of Na_2CO_3 and the pH was arranged to neutral. Organic phase dried over $MgSO_4$ and dried under vacuum. The product dissolved in diethyl ether and crystallized in petroleum ether (Marvanova et al., 2016). TLC technique is used to control the impurity of the product (ethyl acetate/petroleum ether 1:1). The structure was illuminated by FTIR, ^{1}H-NMR and ^{13}C-NMR. The structure of TsGL was given in Fig.5.60.

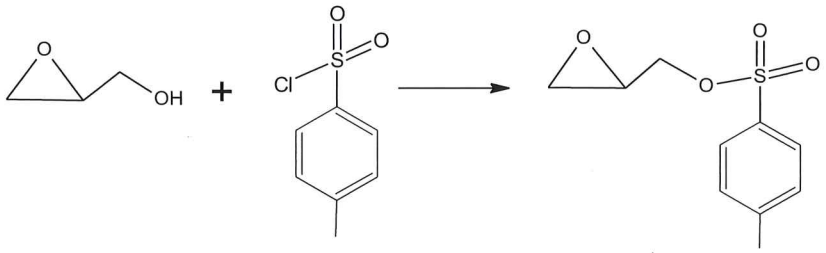

Figure 5.60 Tosylation of glycidol,TsGL, in DCM, at 0 ℃, overnight.

Fig.5.61 indicates FTIR spectrum of the glycidol and Tosyl-glycidol. The characteristic peak of –OH bond and C–O–C etheric peak was obtained at 3356 cm^{-1} and 1043 cm^{-1}, respectively. $–CH_2$ and –CH peak was gotten at 2700-2800 cm^{-1}. It is seen that in the FTIR spectrum of the structure obtained by protecting the –OH bond with the tosyl group, the –OH bond disappeared and the new tosyl group peaks were added. The characteristic peak assignment for the FTIR spectrum of the Ts-GL is as follows: S=O stretching band at 1358 cm^{-1}, -SOOOC and –OTs stretching bands at 1180 cm^{-1} and 661 cm^{-1}, respectively.

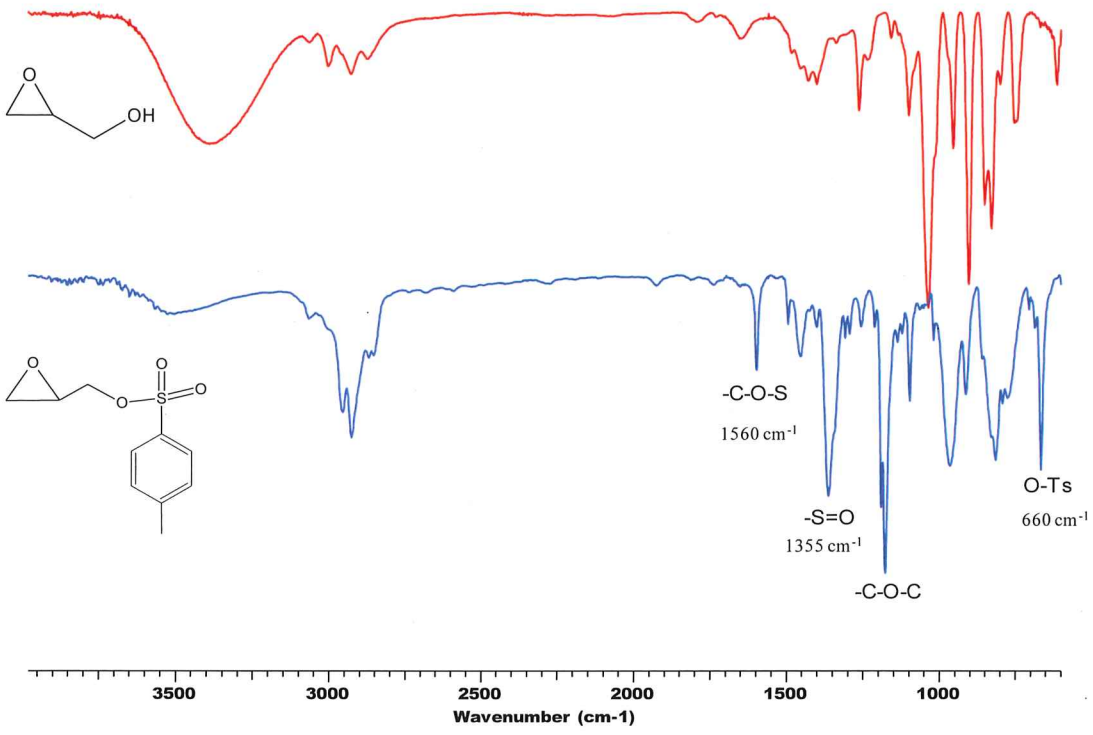

Figure 5.61 FTIR spectrum of glycidol and tosyl- glycidol.

The ^{1}H-NMR and ^{13}C-NMR spectrums of TsGL were given in the Figure 5.62 and 5.63. The doublet peaks at 7.85 ppm and 7.34 ppm were assigned to Ar-$H^{2,6}$ and Ar-$H^{3,5}$ that was represented as **f** and **g**, respectively. The doublet doublet peaks at 4.25 ppm and 3.95 ppm were designated to Ts-OCH_2 (showed as **a,b**). The signals on 3.25 ppm, 2.80 ppm and 2.60 ppm were appointed to CH-oxiran (multiply), CH_2-oxiran (triplet) and CH_2-oxiran (doublet). The peaks were termed as **c, e and d,** respectively. The singlet peak at 2.42 ppm was assigned to Ar-CH_3 (**h**).

^{1}H-NMR ($CDCl_3$), δ (ppm): 7.85 (d, 2H, Ar-$H^{2,6}$, **f**), 7.34 (d, 2H, Ar-$H^{3,5}$, **g**), 4.25 (dd, 1H, Ts-OCH_2, **a**), 3.95 (dd, 1H, Ts-OCH_2, **b**), 3.25 (m, 1H, CH-oxiran, **c**), 2.80 (t, 1H, CH_2-oxiran, **e),** 2.60 (dd, 1H, CH_2-oxiran, **d**) 2.42 (s, 3H, Ar-CH_3, **h**).

^{13}C-NMR ($CDCl_3$), δ (ppm): 145.12 (Ar-$C^{2,6}$, **e**), 133.18 (Ar-$C^{3,5}$, **d**), 130.05 (Ts-OCH_2, **g**), 128.15 (Ts-OCH_2, **f**), 70.58 (CH-oxiran, **c**), 48.65 (CH_2-oxiran, **b),** 44.10 (CH_2-oxiran, **a**) 21.02 (Ar-CH_3, **h**).

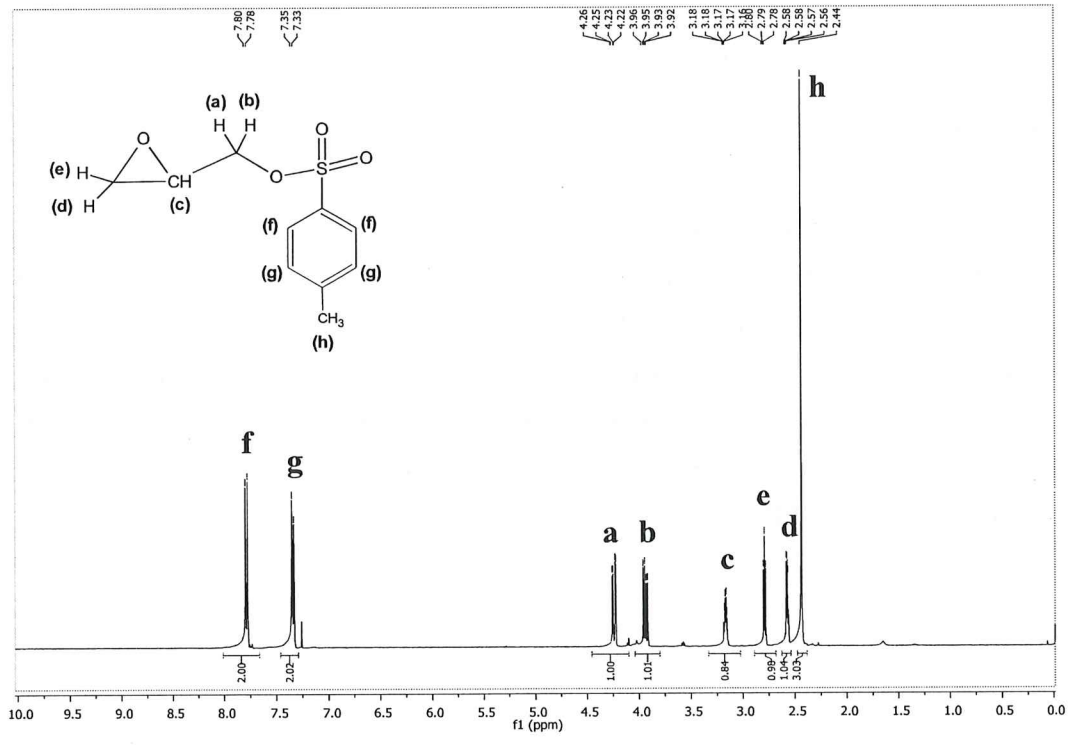

Figure 5.62 ^{1}H-NMR for TsGL.

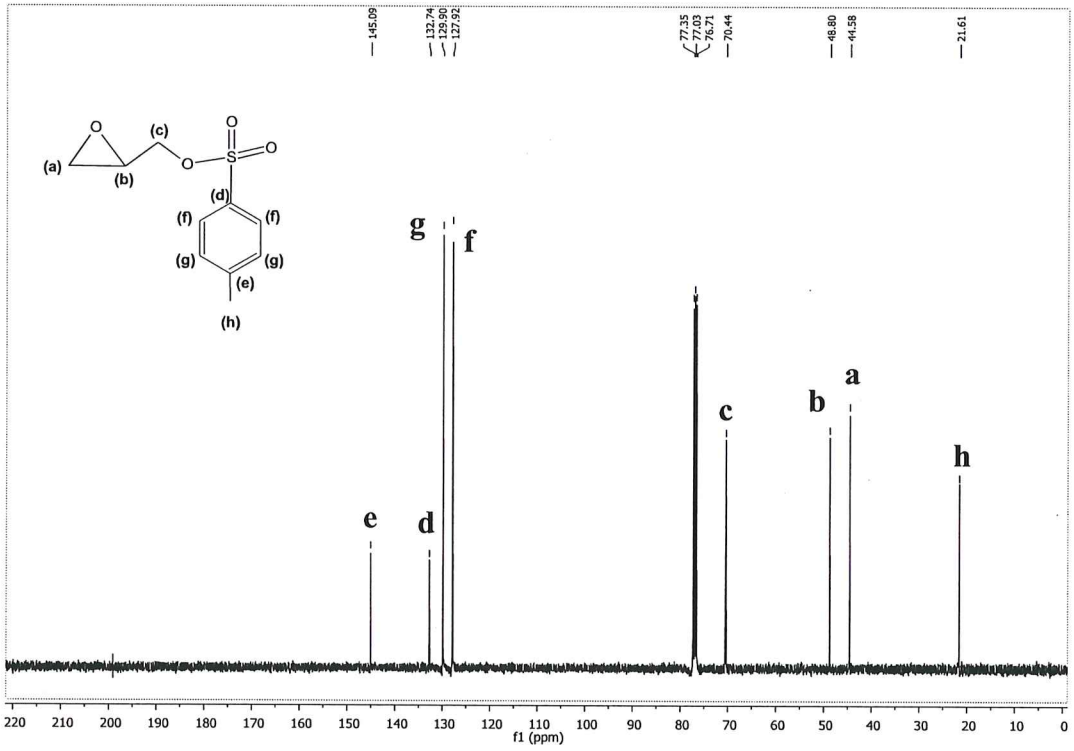

Figure 5.63 ^{13}C-NMR for TsGL.

5.3.3.1 The Copolymerization of TsGL with δVL

Firstly, the TsGL (0.007 mol) was added into the balloon and vacuumed for half an hour. Then freshly purified δVL (0.021 mol) was added under argon atmosphere. In glove box, the $SnAcet_2$ was weighed and added into the balloon. The reaction was continued for 12 hours at 130 °C (Fig.5.64). The reaction was stopped with immediate temperature reduction. Then the product was purified by precipitation in methanol and dried under vacuum. The product was characterized by FTIR and ^{1}H-NMR.

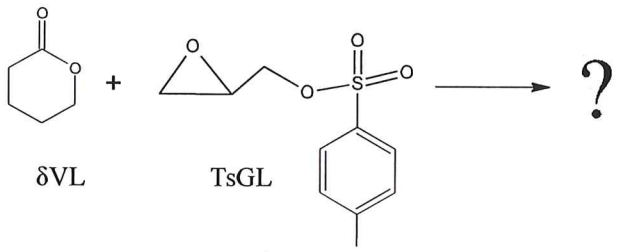

Figure 5.64 General scheme for copolymerization of δVL and TsGL.

The FTIR spectrum of copolymer of TsGL with δ-valerolactone was presented at Fig.5.65. It was expected that the peaks of both monomers was found in the spectrum. The characteristic –C=O stretching band of the PVL was obtained at 1725 cm^{-1} and the peak at 1160 cm^{-1} was attributed to the –C–O group. The characteristic bands assignment for the FTIR spectrum of the Ts-GL were as follows: S=O stretching band at 1358 cm^{-1}, –SOOOC and –OTs stretching bands at 1036 cm^{-1} and 661 cm^{-1}, respectively.

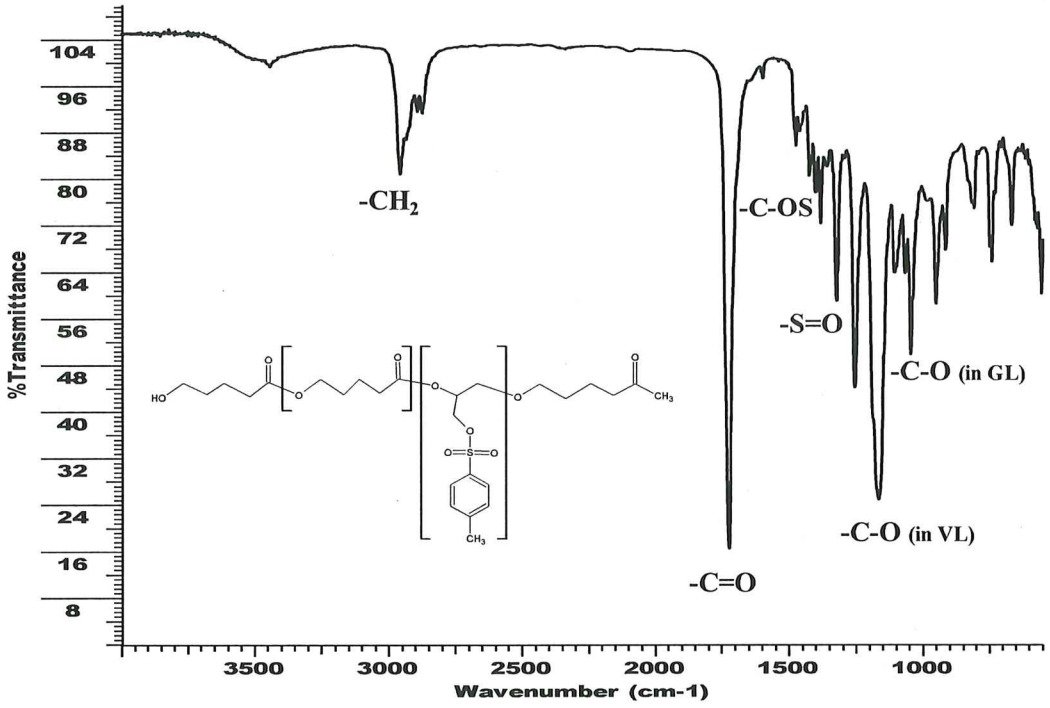

Figure 5.65 FTIR for poly(δVL-co-TsGL).

The ^{1}H-NMR spectrum of poly(δVL-co-TsGL) in $CHCl_3$ were shown in the Fig.5.66. It was evident in this spectrum that the tosyl group did not remove during the copolymerization. Because the Ar-$H^{2,6}$ and Ar-$H^{3,5}$ doublet peaks were obtained at 7.75 ppm and 7.40 ppm, respectively. The peaks at 4.14 ppm and 3.99 ppm were assigned to Ts-OCH_2. The singlet peak at 2.33 ppm was designated to Ar-CH_3. The signals on 4.31 ppm, and 3.63 ppm were assigned to -<u>CH</u>-CH_2-OTs, and -<u>CH_2</u>-CHOTs. Hence it was shown that glycidol monomer was present in the chain. The peak at 4.05 ppm, 2.31 ppm and 1.65 ppm was assigned to -CH_2O, -CH_2CO and –$COCH_2CH_2CH_2CH_2O$ peaks in the PVL.

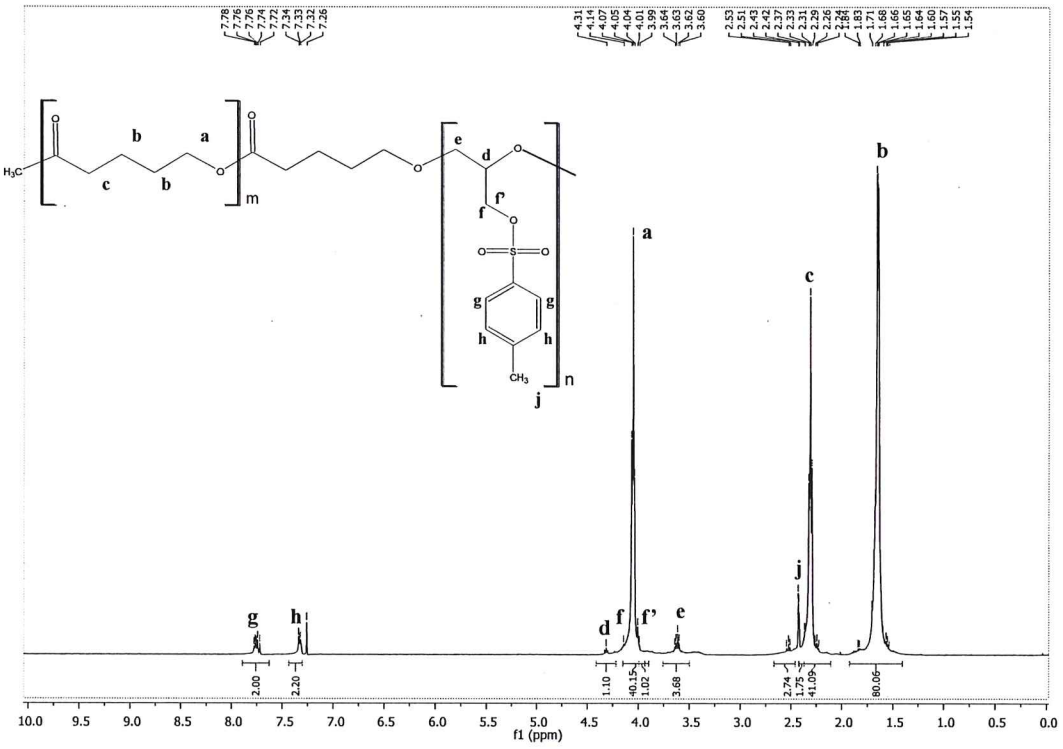

Figure 5.66 ^{1}H-NMR for poly(δVL-co-TsGL).

5.3.3.2 Removing Tosyl Group

After the copolymerization of δVL and Ts-GL, the protecting group (Ts) was removed. The product (~ 0,32 gr) and magnesium (~ 0,22 gr) was added into the two-neck balloon with calcium chloride guard tube (Sridhar et al., 1998). Then the mixture was stirred in dry methanol at 60 °C for overnight. When the reaction finished, the mixture was neutralized with %5 HCl and solved in dichloromethane. Subsequently the organic phase was washed with water and brine, solvent was evaporated and the product was dried under vacuum. FTIR, ^{1}H-NMR and TG analysis was done for characterization.

FTIR spectrum of poly (glycidol-co-valerolactone) was performed at the end of removing the tosyl group and it was given in Fig.5.67. When the spectra of copolymer with and without Tosyl were compared, it was determined that the characteristic Tosyl group absorbance peaks at 1358 cm^{-1} and 1597 cm^{-1} were disappeared. Besides, weak –OH band was appeared at 3500 cm^{-1}. This means that the glycidol monomer was not participate in the polymer chain too much with the ring opening reaction because of the steric effect of protecting group.

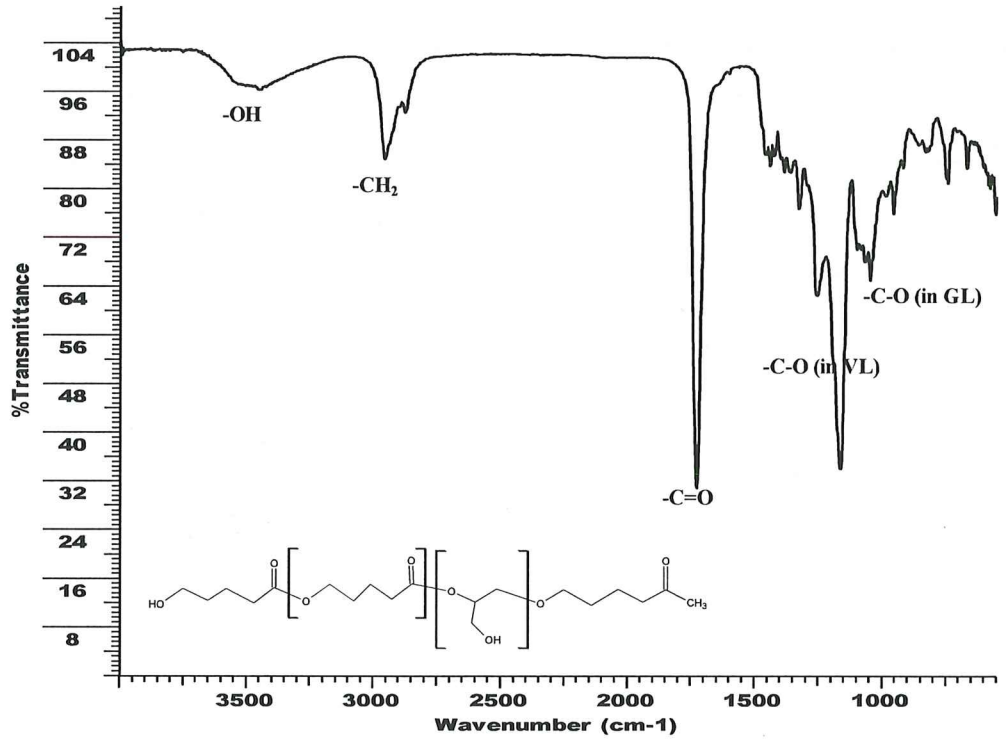

Figure 5.67 FTIR for poly(δVL-co-GL) after detosyl.

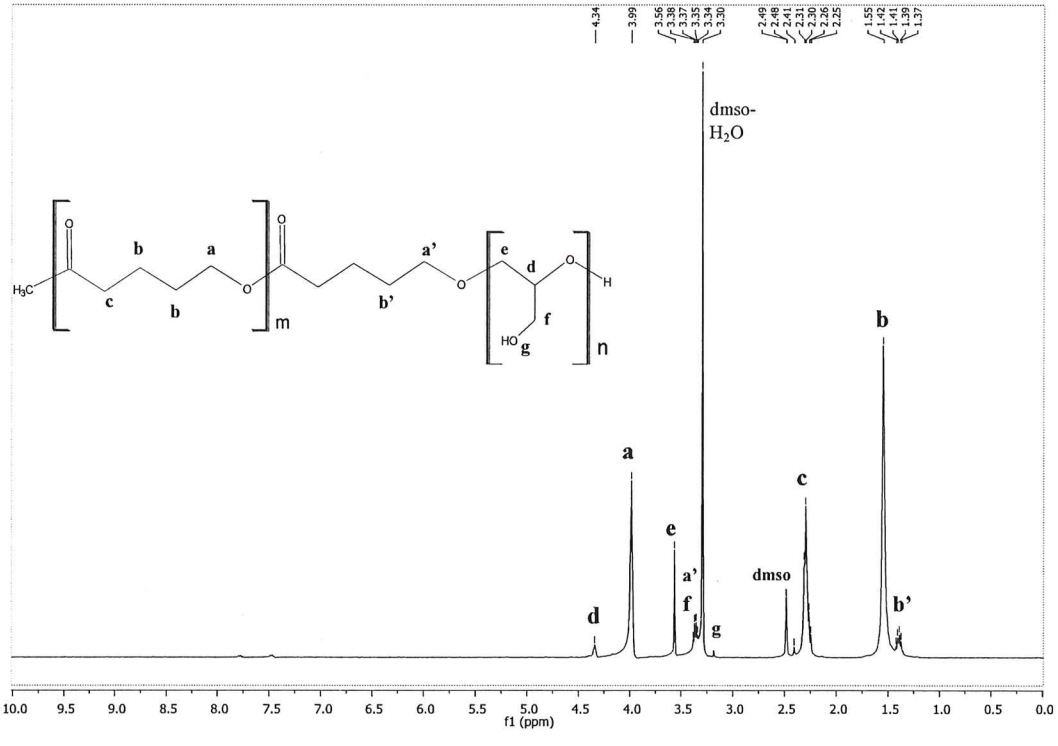

Figure 5.68 ^{1}H-NMR for poly(δVL-co-GL) after detosyl.

The ^{1}H-NMR spectrum of the obtained copolymer (Fig.5.68) supported the FTIR spectrum results. The signals of the tosyl group at 7.75 ppm, 7.40 ppm (Ar-H) and 2.33 (Ts-CH_3) were not observed in the spectrum. The peaks on 3-4 ppm were assigned to -CH_2 groups and small intensity signal on 4.34 was designated to –CH group of polyglycidol structure. Also the -CH_2O, -CH_2CO and –$COCH_2CH_2CH_2CH_2O$ groups of poly (δ-valerolactone) were obtained at 3.99 ppm, 2.30 ppm and 1.55 ppm, respectively.

The molecular weight analysis of the product was performed by GPC and found as ~1500 g/mol. It is thought that the reason for not obtaining high molecular weight copolymer may be due to the steric factor of the protecting group.

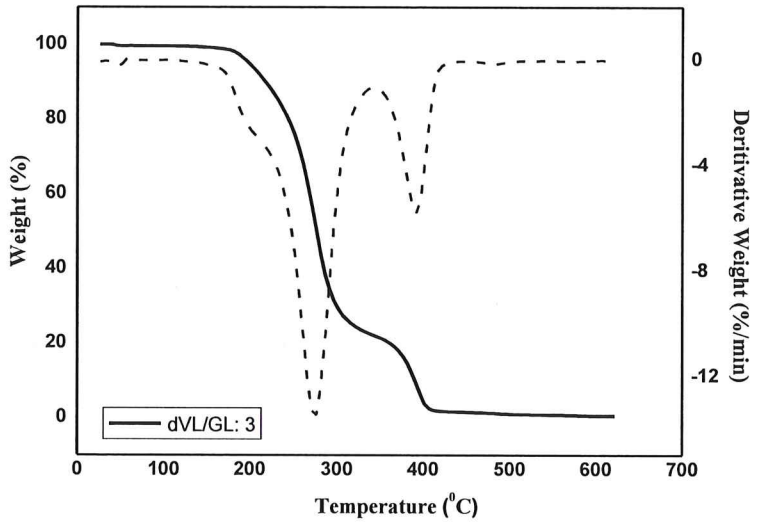

Figure 5.69 TG thermogram of poly(δVL-co-GL) after detosyl.

According to TG-DTG thermogram of copolymer (Fig.5.69), it was determined that degradation became in two stages between 200-400 °C. At this temperature range, the total weight loss was get as %99.5. The fact that the remaining mass is almost nonexistent indicates that the initiator separated from the chain while the protecting group was removing. The first degradation stage was occurred at 200-320 °C and maximum peak temperature was found about 280 °C. The weight loss was designated %75 at this stage. This degradation data reflected the thermal character of PVL. The second decomposition stage was started at 320 °C and continued up to 400 °C. The maximum degradation temperature was determined as 420 °C and the percent of this degradation stage is about %25. It was assigned to

the PGL. The obtained data demonstrated that the copolymerization of OH group protected glycidol and valerolactone was a more controlled reaction. Also it was found that the copolymerization reaction tends to form block copolymers.

5.3.4 Theoretical study of Glycidol

5.3.4.1 Coordination Insertion Mechanism for ROP of Glycidol

In the literature, there is no mechanistic study on the ring opening polymerization of glycidol using tin alkoxylates. Hence, we theoretically investigated the coordination-insertion ROP mechanism of glycidol initiated by $SnAcet_2$ in gas phase to both illuminate the reaction pathway and to interpret the copolymerization process.

The calculations were performed at ωB97X-D/LanL2DZdp level. The optimum geometry, electrostatic potentials and atomic charges of the glycidol was given in Fig.5.70. The schematic representation reaction mechanism and reaction energy profile were presented in Fig.5.71 and 5.72, respectively. In reaction path, two activation barriers as **TS0** and **TS1** were determined. The reaction begins with the interaction between the etheric oxygen atom (O18) in the ring and the tin atom (Sn5) of initiator, as in the coordination insertion mechanism of lactones. The first barrier (4.4 kcal/mol) was originated from variation in the attraction force between the tin atom (Sn5) and the acetate oxygen (O3) due to the interaction between the glycidol and the $SnAcet_2$. This process lengthens the Sn5-O3 distance (from 2.14 to 2.71 Å). The reaction barrier (**TS1**) occurs by cleavage step of the carbon oxygen bond in the ether ring and the enthalpy of this step was found to be 40.1 kcal/mol. The **product** structure obtained is a stable complex and its energy was found as -11.45 kcal/mol. Thus, the ring opening polymerization of glycidol is an exothermic reaction with a single step mechanism.

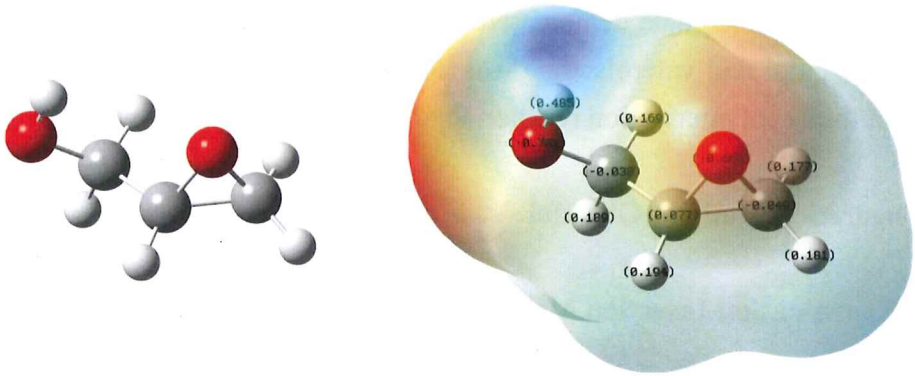

Figure 5.70 The geometries, electrostatic potentials and atomic charges of the glycidol obtained at ωB97X-D/LanL2DZdp level calculations.

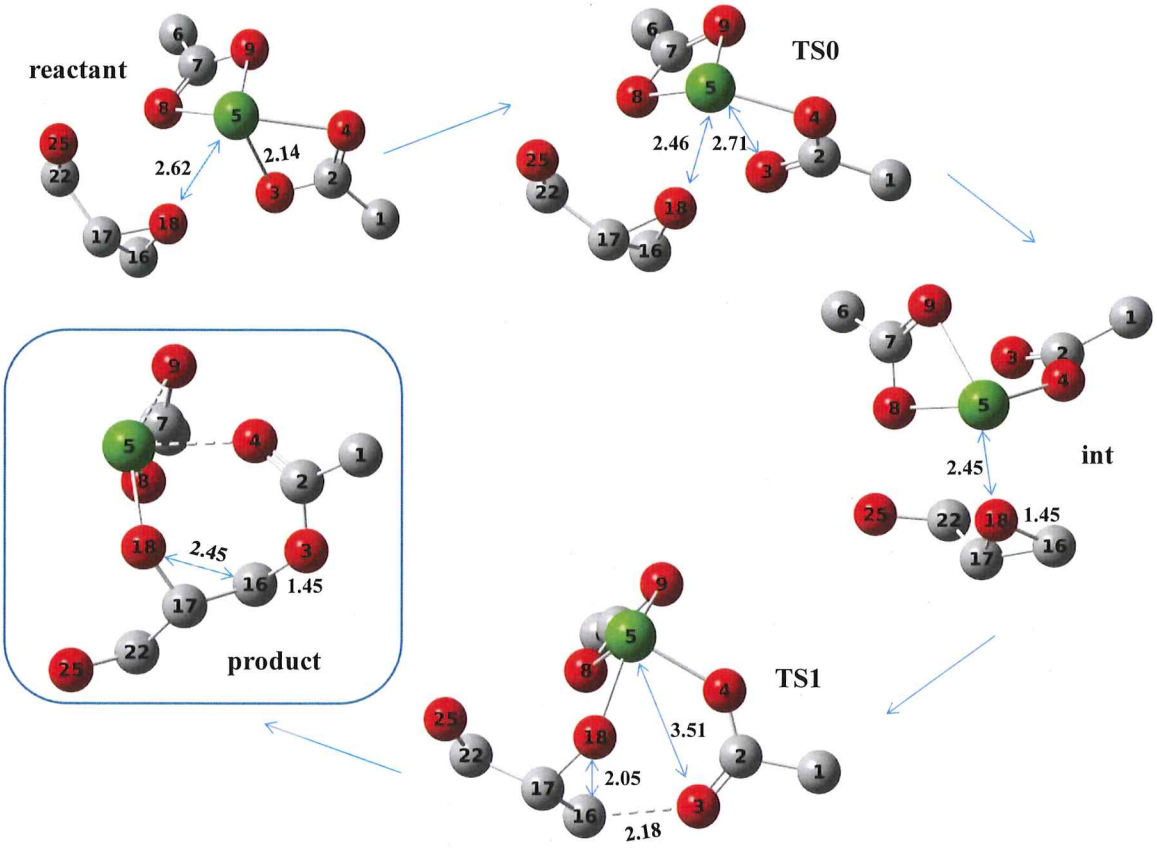

Figure 5.71 Initiation stage for the ROP of glycidol. Hydrogens are excluded. Distances are given in Å units. Oxygen, carbon and tin atoms are illustrated in red, gray and green, respectively.

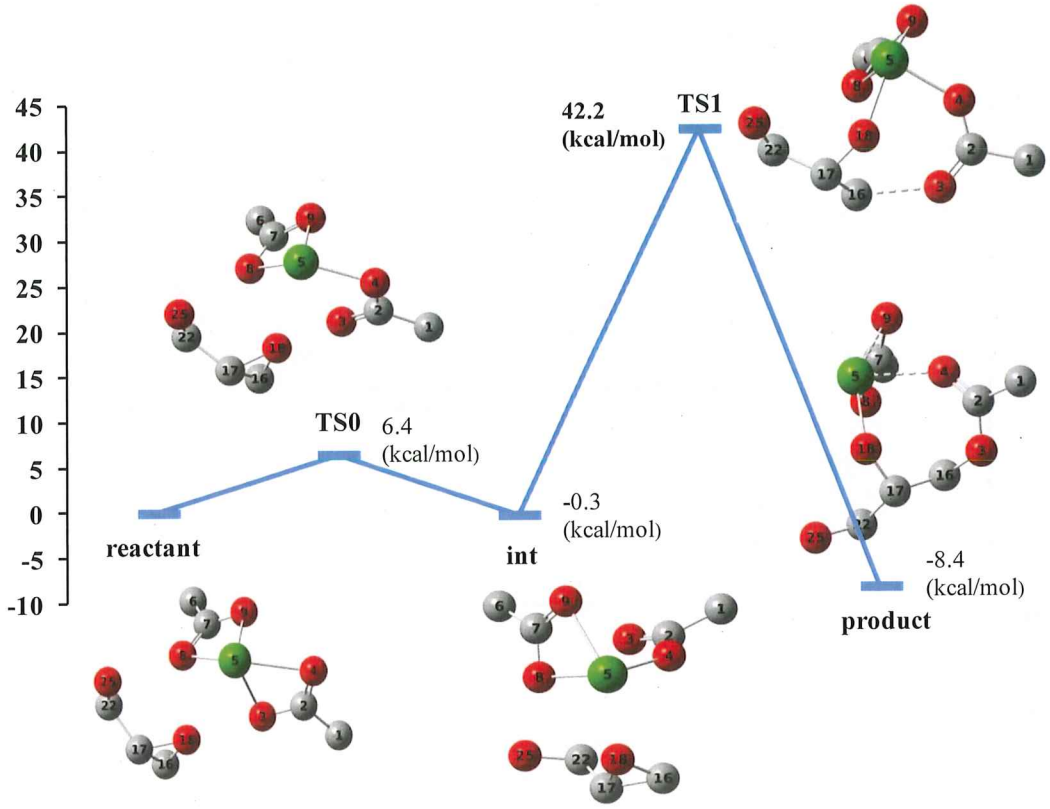

Figure 5.72 Gibbs free energy profile (in kcal/mol) for the initiation stage obtained by ωB97X-D/LanL2DZdp. All energies are relative to the complex.

The calculations revealed that the activation barrier for ROP of dVL is about 10 kcal/mol lower than that for ROP of glycidol (Fig.5.73). From this information, we would expect that the valerolactone character is dominant in the copolymer structure. Conversely, it has been experimentally found that the copolymer structure has more glycidol character in the random copolymerization study of δ-valerolactone and glycidol. As an explanation for this contradiction, it can be stated that although ROP of PVL is kinetically more favorable, the ROP of glycidol is a thermodynamically spontaneous reaction with only one activation barrier. So, the calculated values suggested that glycidol should polymerize much faster than δ-valerolactone.

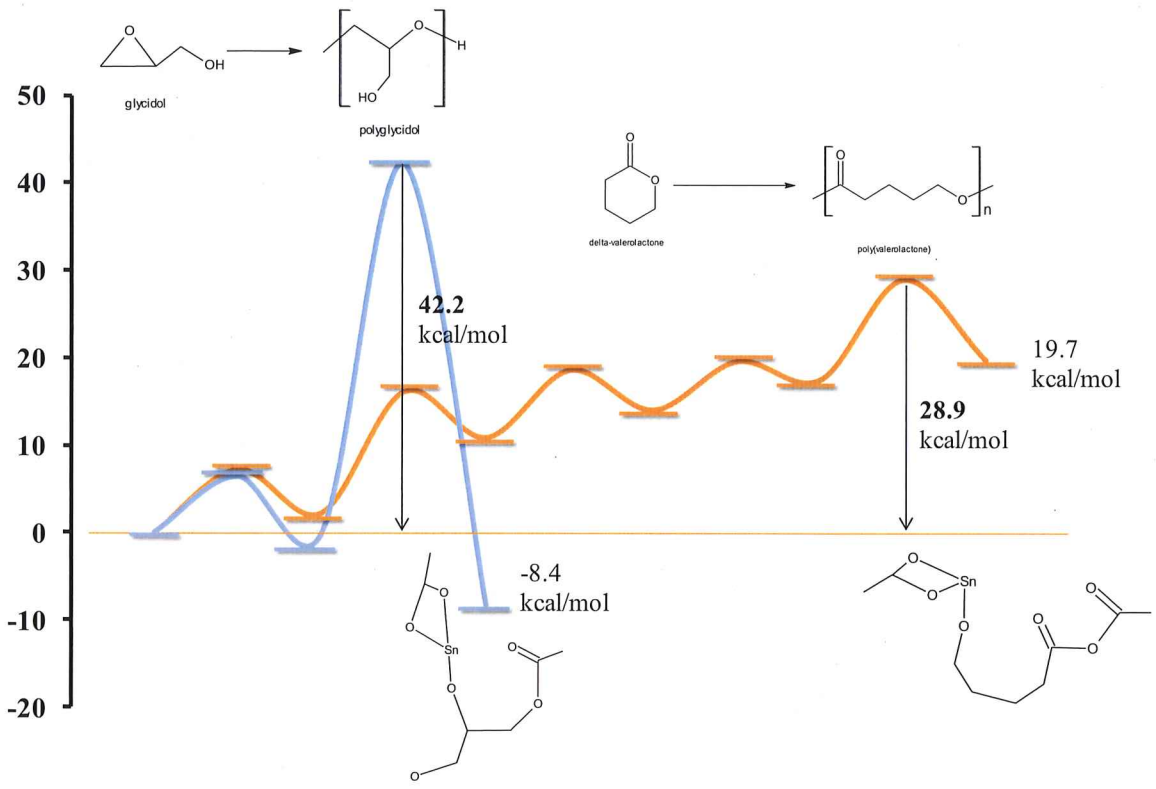

Figure 5.73 Gibbs free energy profile for ROP of δVL and GL (in kcal/mol).

6. CONCLUSION

Poly(α-angelica lactone), (PAL), was synthesized with tin acetate ($SnAcet_2$) and zinc acetate ($ZnAcet_2$) by ring opening polymerization (ROP). The initiation and propagation stages of coordination-insertion mechanism was computationally studied for the first time and the calculations revealed that the reason of high molecular weight polymer could not be obtained is entropic penalty originated from structural rigidity. Higher molecular weight PAL cannot be obtained since the tin acetate forms a stable complex with the monomer in the presence of water or alcohol (co-initiator). In the synthesis of poly(α-angelica lactone) by ROP, the efficiency of different initiators was investigated. It was computationally determined that zinc acetate could be a more effective initiator. However, experimentally, no significant difference was found in both of initiator activities.

Poly (δ-valerolactone), PVL was first synthesized by the use of $SnAcet_2$, $PbAcet_2.3H_2O$, $CdAcet_2.2H_2O$, $NiAcet_2.4H_2O$ and $CuAcet_2.H_2O$ complexes as initiators. Toxicity tests for different dilution ratios of PVL synthesized with Sn, Cd and Pb acetate complexes were performed. It was determined that PVL synthesized with lead acetate showed cytotoxic effect at all dilution ratios. For the first time, the coordination insertion mechanism of PVL was illuminated with ωB97X-D method. The highest molecular weight and polymerization yield was obtained with $CdAcet_2.2H_2O$ complex which also theoretically found as the most effective initiator. The results of NBO and LUMO analyses were confirmed with the experiment results.

Copolymer of δ-valerolactone and glycidol was first time synthesized with $SnAcet_2$. It was concluded that the copolymer preferred block copolymer structure. The copolymer synthesis of OH-protected-glycidol (protected by tosyl chloride) was performed for the first time. DFT calculations performed on the ROP mechanism of glycidol revealed spontaneity of the reaction.

The joint evaluation of NBO and LUMO analysis reveals that initiator activity can be determined without conducting any experiment. The computational determination of ROP mechanisms of lactones increases our level of knowledge on polymerization reactions and the ability to direct the reaction process. These functional polymers, which are biodegradable and biocompatible, are thought to be materials that have potentials to be used in many application fields, biomedical and pharmaceutical industries, since they allow for modification.

REFERENCES

Adamo, C. and Barone, V., 1998, Exchange functionals with improved long-range behavior and adiabatic connection methods without adjustable parameters: The mPW and mPW1PW models, *J. Chem. Phys.*, **108**:664-75 pp.

Albertsson, A.C. and Varma, I.K., 2003, Recent developments in ring opening polymerization of lactones for biomedical applications, *Biomacromolecules*, 4(6):1466-1486 pp.

Balcan, S., Balcan, M. and Çetinkaya, B., 2013, Poly(l-lactide) initiated by silver N-heterocyclic carbene complexes: synthesis, characterization and properties, *Polymer Bulletin,* 70:3475–3485 pp.

Becke, A.D., 1993, Density-functional thermochemistry.III. The role of exact exchange, *J. Chem. Phys.*, 98:5648 p.

Billmeyer, F.W., 1984, Textbook of polymer science, third edition, John Wiley&Sons, New York, 578 p.

Born, M. and Oppenheimer, R., 1927, Zur quantentheorie der molekeln., *Annalen der Physik*, 389(20):457-484 pp.

Braun, D., Cherdron, H., Rehahn, M., Ritter, H. and Voit, B., 2005, Polymer Synthesis: Theory and Practice, fourth edition, Springer-Verlag Berlin Heidelberg.

Chai, J.Da and Head-Gordon, M., 2008, Systematic optimization of long-range corrected hybrid density functionals, *J. Chem. Phys.*, 128.

Chakraborty, D. and Chen, E.Y.-X., 2003, Chiral amido aluminum and zinc alkyls: A synthetic, structural, and polymerization study, *Organometallics,* 22(4):769–774 pp.

Chandra, R. and Rustgi, R., 1998, Biodegradable polymers, *Progress in Polymer Science,* 23:1273-1335 pp.

REFERENCES (Continued)

Chen, T., Qin, Z., Qi, Y., Deng, T., Ge, X., Wang, J. and Hou, X., 2011, Degradable polymers from ring-opening polymerization of α-angelica lactone, a five-membered unsaturated lactone, *Polym. Chem.,* 2:1190-1194 pp.

Cheshmedzhieva, D., Angelova, I., Ilieva, S., Georgiev, G.S., and Galabov, B., 2012, Initiation of ring-opening polymerization of lactide: The effect of metal alkoxide catalyst, *Computational Theoretical Chemistry,* 995:8–16 pp.

Cohen, A.J., Mori-Sánchez, P., Yang, W., 2011, Challenges for density functional theory, *Chemical Reviews,* 112(1):289-320 pp.

Cramer, C.J., 2002, Essentials of computational chemistry theories and models, Second Edition, John Wiley&Sons, Ltd., England, 179 p.

Danko, M. and Mosnázek, J., 2017, Ring-opening polymerization of γ-butyrolactone and its derivatives: A review, *Polimery/Polymers,* 62: 272–282 pp.

Delidovich, I., Hausoul, P.J.C., Deng, L., Pfützenreuter, R., Rose, M. and Palkovits, R., 2016, Alternative monomers based on lignocellulose and their use for polymer production, *Chem. Rev.,* 116 (3):1540–1599 pp.

Dimitrov, P., Hasan, E., Rangelov, St., Trzebicka, B., Dworak, A. and Tsvetanov Ch.B., 2002, High molecular weight functionalized poly(ethylene oxide), *Polymer*, 43:7171-7178 pp.

Dobrzyński, P., Kasperczyk, J. and Bero M., 1999, Application of calcium acetylacetonate to the polymerization of glycolide and copolymerization of glycolide with ε-caprolactone and L-lactide, *Macromolecules*, 32:4735–4737 pp.

Duda, A. and S. Penczek, 2001, Mechanisms of aliphatic polyester formation, Wiley-VCH, Weinheim.

REFERENCES (Continued)

Duda, A. and Kowalski, A., 2009, Handbook of Ring-Opening Polymerization, Wiley-VCH Verlag GmbH & Co. KGaA, Weinheim.

Fay, F., Linossier, I., Langlois, V., Renard, E. and Vallee-Rehel, K., 2006, Degradation and controlled release behavior of ε-caprolactone copolymers in biodegradable antifouling coatings, *Biomacrololecules,* 7(3):851-857 pp.

Fleming, J., 1976, Frontier orbitals and organic chemical reactions, John Wiley & Sons, New York, 258 p.

Frisch, M. J., Trucks, G. W., Schlegel, H. B., Scuseria, G. E., Robb, M. A., Cheeseman, J. R., Scalmani, G., Barone, V., Mennucci, B., Petersson, G. A., Nakatsuji, H., Caricato, M., Li, X., Hratchian, H. P., Izmaylov, A. F., Bloino, J., Zheng, G., Sonnenberg, J. L., Hada, M., Ehara, M., Toyota, K., Fukuda, R., Hasegawa, J., Ishida, M., Nakajima, T., Honda, Y., Kitao, O., Nakai, H., Vreven, T., Montgomery, J. A., Peralta, J. E., Ogliaro, F., Bearpark, M., Heyd, J. J., Brothers, E., Kudin, K. N., Staroverov, V. N., Keith, T., Kobayashi, R., Normand, J., Raghavachari, K., Rendell, A., Burant, J. C., Iyengar, S. S., Tomasi, J., Cossi, M., Rega, N., Millam, J. M., Klene, M., Knox, J. E., Cross, J. B.,Bakken, V., Adamo, C., Jaramillo, J., Gomperts, R., Stratmann, R. E., Yazyev, O., Austin, A. J., Cammi, R., Pomelli, C., Ochterski, J. W., Martin, R. L., Morokuma, K., Zakrzewski, V. G., Voth, G. A., Salvador, P., Dannenberg, J. J., Dapprich, S., Daniels, A. D., Farkas, O., Foresman, J. B., Ortiz, J. V., Cioslowski, J., and Fox, D. J., 2010, Gaussian 09, Revision B.01, Gaussian, Inc., Wallingford CT.

Fock, V., 1930, Näherungsmethode zur Lösung des quantenmechanischen Mehrkörperproblems, *Zeitschrift für Physik*, 61(1-2):126-148 pp.

Frazza, E.J. and Schmitt E.E., 1971, A new absorbable suture, *J. Biomed. Mater. Res.*, 5(2): 43-58 pp.

Gottschalk, C., Wolf, F. and Frey, H., 2007, Multi- arm star poly(L- lactide) with hyperbranched polyglycerol core, *Macromolecular Chemistry and Physics,* 208:1657-1665 pp.

REFERENCES (Continued)

Gowda, R. R. and Chakraborty, D., 2010, Zinc acetate as a catalyst for the bulk ring opening polymerization of cyclic esters and lactide, *Journal of Molecular Catalysis A: Chemical,* 333:167-172 pp.

Grimme, S., 2006, Semiempirical GGA-type density functional constructed with a long-range dispersion correction, *J. Comput. Chem.,* 27:1787–1799 pp.

Guillaume, C., Carpentier, J.F. and Guillaume, S.M., 2009, Immortal ring-opening polymerization of β-butyrolactone with zinc catalysts: Catalytic approach to poly(3-hydroxyalkanoate), *Polymer (Guildf),* 50:5909–5917 pp.

Gunatillake, P., Mayadunne, R. and Adhikari, R., 2006, Recent developments in biodegradable synthetic polymers, *Biotechnology Annual Review,* 12:301-347 pp.

Gupta, A.P. and Kumar, V., 2007, New emerging trends in synthetic biodegradable polymers – Polylactide: A critique, *European Polymer Journal,* 43:4053–4074 pp.

Hartree, D.R.,1928, The wave mechanics of an atom with a non-coulomb central field. Part I. Theory and methods, *Mathematical Proceedings of the Cambridge Philosophical Society,* 24(1):89-110 pp.

Hay, P.J. and Wadt, W.R., 1985, Ab initio effective core potentials for molecular calculations. Potentials for the transition metal atoms Sc to Hg, J. *Chem. Phys.,* 82:270 p.

Heyd, J. and Scuseria, G., 2004, Efficient hybrid density functional calculations in solids: The HS-Ernzerhof screened Coulomb hybrid functional, *J. Chem. Phys.*, 121:1187-92 pp.

Hohenberg, P. and Kohn, W., 1964, Inhomogeneous Electron Gas, *Physical Review,* 136(3B): B864-B871

REFERENCES (Continued)

Houk, K.N., Jabbari, A., Hall, H.K. and Alemán, C., 2008, Why δ-valerolactone polymerizes and γ-butyrolactone does not, *J. Org. Chem.* 73:2674–2678 pp.

Hratchian, H.P. and Schlegel, H.B., 2004, Accurate reaction paths using a Hessian based predictor-corrector integrator, *J. Chem. Phys.,* 120:9918–9924 pp.

Jakubowicz, I., 2003, Evaluation of degradability of biodegradable polyethylene (PE), *Polymer Degradation and Stability*, 80:39-43 pp.

Jedlinski, Z., Kurcok, P. and Kowalczuk, M., 1985, Polymerization of beta-lactones initiated by potassium solutions, *Macromolecules,* 18:2679-2683 pp.

Jedlinski, Z., 2002, Single- electron and two- electron transfer in the anionic polymerization of vinyl monomers and the ring- opening polymerization of lactones, *J. Polym. Sci, Part A. Polym. Chem.,* 40:2158-2165 pp.

Jensen, F., 2007, Introduction to computational chemistry, Second Edition, John Wiley & Sons, Ltd., England, 620 p.

Jerome, R. and Teyssie, P., 1989, Anionic ring-opening polymerization: Lactones, Pergamon Press, London.

Jones, G.O., Chang, Y.A., Horn, H.W., Acharya, A.K., Rice, J.E., Hedrick, J.L. and Waymouth, R.M., 2015, N-Heterocyclic carbene-catalyzed ring opening polymerization of ε-caprolactone with and without alcohol initiators: Insights from theory and experiment, *J. Phys. Chem. B.,* 119: 5728–5737 pp.

Kaoukabi, A., Guillen, F., Qayouh, H., Bouyahya, A., Balieu, S., Belachemi, L., Gouhier, G. and Lahcini, M., 2015, The use of ionic liquids as an organocatalyst for controlled ring-opening polymerization of ε-caprolactone, *Ind. Crops Prod.,* 72:16–23 pp.

REFERENCES (Continued)

Kohn, W. and Sham, L.J., 1965, Self-consistent equations including exchange and correlation effects, *Physical Review,* 140(4A): A1133-A1138.

Kohn, W., Becke, A.D., Parr, R.G., 1996, Density functional theory of electronic structure, *The Journal of Physical Chemistry,* 100(31):12974-12980 pp.

Kricheldorf, H.R. and Serra, A., 1985, Polylactones.6. Influence of various metal salts on the optical purity of poly(L-lactide), *Polymer Bulletin,* 14(6):497-502 pp.

Kricheldorf, H.R., Berl, M. and Scharnagl, N., 1988, Poly(1actones). 9. Polymerization mechanism of metal alkoxide initiated polymerizations of lactide and various lactones, *Macromolecules*, 12:286–293 pp.

Kricheldorf, H.R., Kreiser-Saunders, I., Boettcher, C., 1995, Polylactones: 31. Sn(II)octoate-initiated polymerization of L-lactide: a mechanistic study, *Polymer (Guildf),* 36: 1253–1259 pp.

Kricheldorf, H.R. and Damrau, D.- O., 1997, Polylactones, 38.* Polymerization of L- lactide with Fe(II) lactate and other resorbable Fe(II) salts, *Macromolecular Chemistry and Physics,* 198:1767-1774 pp.

Lawan, N., Muangpil, S., Kungwan, N., Meepowpan, P., Lee, V.S. and Punyodom, W., 2013, Tin (IV) alkoxide initiator design for poly (d-lactide) synthesis using DFT calculations, *Computational Theoretical Chemistry*, 1020: 121–126 pp.

Lee, C., Yang, W. and Parr, R.G., 1988, Development of the Colle-Salvetti correlation-energy formula into a functional of the electron density, *Phys. Rev. B.,* 37:785–789 pp.

Lee, T.D. and Yang, C.N., 1959, Many-Body Problem in Quantum Statistical Mechanics. I. General Formulation, *Physical Review*, 113(5):1165-1177 pp.

REFERENCES (Continued)

Ling, J., Shen, J. and Hogen-Esch, T.E., 2009, A density functional theory study of the mechanisms of scandium-alkoxide initiated coordination-insertion ring-opening polymerization of cyclic esters, *Polymer (Guildf),* 50:3575–3581 pp.

Liu, J., Ling, J., Li, X. and Shen, Z., 2009, Monomer insertion mechanism of ring-opening polymerization of ε-caprolactone with yttrium alkoxide intermediate: A DFT study, *J. Mol. Catal. A Chem.,* 300:59–64 pp.

Lowe, J. and Peterson, K., 2006, Quantum Chemistry, Elsevier, 728 p.

Lundberg R.D. and Cox E.F., 1969, Lactones, in "Ring-Opening Polymerization". Ed. Frish K. and Reegen S., Marcel Dekker, New York, 247 p.

Macke, W., 1955, Wave Mechanical Treatment of the Fermi Gas, *Physical Review,* 100(4):992-993 pp.

Marvanova, P., Padrtova, T., Odehnalova, K,. Hosik, O., Oravec, M. and Mokry, P., 2016, Synthesis and Determination of Physicochemical Properties of New 3-(4-Arylpiperazin-1-yl)-2- hydroxypropyl 4-Alkoxyethoxybenzoates, *Molecules*, 21(12):1682 p.

Marvel, C.S. and Levesque, C.L., 1939, The structure of vinyl polymers. III. The polymer from α-angelica lactone, *J. Am. Chem. Soc.,* 61 (7): 1682–1684 pp.

Meelua, W., Bua-Own, V., Molloy, R. and Punyodom, W., 2012, Comparison of metal alkoxide initiators in the Ring-opening polymerization of Caprolactone, *Adv. Mater. Res.,* 506:142–145 pp.

Nair, K.L.; Jagadeeshan, S.; Nair, S.A. and Kumar, G.S., 2011, Evaluation of triblock copolymeric micelles of δ-valerolactone and poly (ethylene glycol) as a competent vector for doxorubicin delivery against cancer, *Journal of Nanobiotechnology,* 9(1):42 p.

REFERENCES (Continued)

Nair, L.S. and Laurencin, C.T., 2007, Biodegradable polymers as biomaterials, *Progress in Polymer Science,* 32:762-798 pp.

Nakayama, A., Kawasaki, N., Maeda, Y., Arvanitoyannis, I., Aiba, S. and Yamamoto, N., 1997, Study of biodegradability of poly(δ- valerolactone- co- L- lactide)s, *Journal of Applied Polymer Science,* 66:741-748 pp.

Nijenhuis, A.J., Grijpma, D.W. and Pennings, A.J., 1992, Lewis acid catalyzed polymerization of l-lactide. Kinetics and mechanism of the bulk polymerization, *Macromolecules,* 25:6419-6424 pp.

Odian, G., 2004, Principles of polymerization, fourth edition, John Wiley Interscience, New York, 554 p.

Okada, M., 2002, Chemical synthesis of biodegradable polymers, *Progress in Polymer Science,* 27:87-133 pp.

Olsén, P., Odelius, K. and Albertsson, A.C., 2016, Thermodynamic presynthetic considerations for ring opening polymerization, *Biomacromolecules*, 17: 699−709 pp.

Penczek, S. and Duda, A., 1993, Kinetics and mechanisms in anionic ring- opening polymerization, *Makromol. Chem., Macromol. Symp.,* 67:15-42 pp.

Perdew, J. P., Burke, K. and Ernzerhof, M., 1996, Generalized gradient approximation made simple, *Phys. Rev. Lett.*, 77:3865-68 pp.

Petchsuk, A., Nakayama, A. and Aiba, S., 2009, Synthesis and biodegradability of l-lactide/glycidol copolymers, *Polymer Degradation and Stability*, 94: 1700-1706 pp.

Pitet, L.M., Hait, S.B., Lanyk, T.J. and Knauss, D.M., 2007, Linear and branched architectures from the polymerization of Lactide with glycidol, *Macromolecules,* 40:2327–2334 pp.

REFERENCES (Continued)

Ramachandran, K.I., Deepa G. and Namboori K., 2008, Computational chemistry and molecular modeling, Principles and applications, Springer, Verlag Berlin Heidelberg, 405 p.

Reed, A.E., Curtiss, L. and Weinhold, F., 1988, Intermolecular interactions from a natural bond orbital, donor-acceptor viewpoint., *Chem. Rev.,* 88: 899–926 pp.

Řezáč, J. and Hobza, P., 2012, Advanced corrections of hydrogen bonding and dispersion for semiempirical quantum mechanical methods, *J. Chem. Theory Comput.,* 8:141–151 pp.

Rodríguez, E.F., Manso, J.A., Prior, M.T.P., Santos, M.del P.G., Calle, E. and Casado, J., 2007, The unusual ability of α- angelicalactone to form adducts: A kinetic approach, *International Journal of Chemical Kinetics,* 39:591-594 pp.

Royappa, A.T., Vashi, M.R., Russo, C.L. and Blackwell, A.C., 2013, A comparison of the cationic ring-opening polymerizations of 3-oxetanol and glycidol, *Macromolecular Research,* 21:1069-1074 pp

Ryner, M., Stridsberg, K., Albertsson, A.C., Schenck, H. Von and Svensson, M., 2001, Mechanism of ring-opening polymerization of 1,5-dioxepan-2-one and L-lactide with stannous 2-ethylhexanoate. A theoretical study, *Macromolecules,* 34:3877–3881 pp.

Sarazin, Y., Schormann, M. and Bochmann, M., 2004, Novel zinc and magnesium alkyl and amido cations for ring-opening polymerization reactions, *Organometallics,* 23:3296–3302 pp

Sattayanon, C., Sontising, W., Jitonnom, J., Meepowpan, P., Punyodom, W. and Kungwan, N., 2014, Theoretical study on the mechanism and kinetics of ring-opening polymerization of cyclic esters initiated by tin(II) n-butoxide, *Computational Theoretical Chemistry*, 1044:29–35 pp.

REFERENCES (Continued)

Sattayanon, C., Sontising, W., Limwanich, W., Meepowpan, P., Punyodom, W., and Kungwan, N., 2015, Effects of alkoxide alteration on the ring-opening polymerization of ε-caprolactone initiated by n-Bu3SnOR: A DFT study, *Structural Chemistry*, 26(3):695-703 pp.

Schenck, H. Von, Ryner, M., Albertsson, A.C. and Svensson, M., 2002, Ring-opening polymerization of lactones and lactides with Sn(IV) and Al(III) initiators, *Macromolecules,* 35:1556–1562 pp.

Schwach, G., Coudane, J., Engel, R. and Vert, M., 1997, More about the polymerization of lactides in the presence of stannous octoate, *J. Polym. Sci. Part A Polym. Chem.,* 35:3431–3440 pp.

Slater, J.C., 1930, Atamic shielding constatns, *Physical Review*, 36: 57-64 pp.

Sridhar, M., Kumar, B.A. and Narender R., 1998, Expedient and simple method for regeneration of alcohols from toluenesulfonates using Mg-MeOH, *Tetrehedron Letters*, 39:2847-2850 pp.

Stewart, J.J.P., 2007, Optimization of parameters for semiempirical methods V: Modification of NDDO approximations and application to 70 elements, *J. Mol. Model.*, 13:1173–1213 pp.

Stewart, J.J.P., 2013, Optimization of parameters for semiempirical methods VI: More modifications to the NDDO approximations and re-optimization of parameters, *J. Mol. Model.,* 19:1–32 pp.

Stewart, J.J.P., 2016, MOPAC2016, *Stewart Comput. Chem.*

Stolt, M., Krasowska, K., Rutkowska, M., Janik, H., Rosling, A. and Södergard A., 2005, More on the poly(L-lactide) prepared using ferrous acetate as catalyst, *Polymer International*, 54:362–368 pp.

Tarabanko, V.E., Kaygorodov, K.L. and Chernyak, M.Y., 2008, Polyesterification of alpha-Angelicalactone, *J. Sib. Fed. Univ. Chem.,* 2: 118–123 pp.

REFERENCES (Continued)

Tarabanko, V.E. and Kaygorodov, K.L., 2010, New Biodegradable Polymers Based on α-Angelicalactone, *Chem. Sustainable Develop.*, 3:395–403 pp.

Tomasi, J., Mennucci, B. and Cammi, R., 2005, Quantum mechanical continuum solvation models, *Chem. Rev.,* 105:2999–3093 pp.

Vainionpää, S., Rokkanen, P., Törmälä, P., 1989, Surgical applications of biodegradable polymers in human tissues, *Progress in Polymer Science*, 14(5):679-716 pp.

Vivas, M. and Contreras, J., 2003, Ring-opening polymerization of ε-caprolactone initiated by diphenylzinc, *European Polymer Journal,* 39: 43-47 pp.

Wadt, W.R. and Hay, P.J., 1985, Ab initio effective core potentials for molecular calculations. Potentials for main group elements Na to Bi, *J. Chem. Phys.,* 82:284–298 pp.

Wang C., Li H., Zhao X., 2004, Ring opening polymerization of L-lactide initiated by creatinine, *Biomaterials,* 25:5797–5801 pp.

Weinhold, F. and Landis, C., 1964, Discovering chemistry with natural bond orbitals, John Wiley & Sons, 132-133 pp.

Williams, C.K., Breyfogle, L.E., Choi, S.K., Nam, W., Young, V.G., Hillmyer, M.A. and Tolman, W.B., 2003, A highly active zinc catalyst for the controlled polymerization of lactide, *J. Am. Chem. Soc.,*125(37):11350–11359 pp.

Xi, X., Jiang, G., Wang, X., Hu, R. and Wang, R., 2013, Synthesis, characterization and degradation properties of Poly(α-angelica lactone-co-ε-caprolactone) copolymers, *Polymers from Renewable Resources*, 4:49–60 pp.

REFERENCES (Continued)

Xu, C., Yu, I. and Mehrkhodavandi, P., 2012, Highly controlled immortal polymerization of β-butyrolactone by a dinuclear indium catalyst, *Chemical Communications,* 48:6806-6808 pp.

Yanai, T., Tew, D. and Handy, N., 2004, A new hybrid exchange-correlation functional using the Coulomb-attenuating method (CAM-B3LYP), *Chem. Phys. Lett.*, 393:51-57 pp.

Young, D.C., 2001, Computational chemistry: A practical guide for applying techniques to real-world problems, John Wiley & Sons, New York, 434 p.

Zhao, Y. and Truhlar, D.G., 2006, Comparative DFT study of van der Waals complexes: Rare-gas dimers, alkaline-earth dimers, zinc dimer, and zinc-rare-gas dimers, *J. Phys. Chem.*, 110:5121-29 pp.

Zhao, Y. and Truhlar, D.G., 2008, The M06 suite of density functionals for main group thermochemistry, thermochemical kinetics, noncovalent interactions, excited states, and transition elements: two new functionals and systematic testing of four M06-class functionals and 12 other functionals," *Theor. Chem. Acc.*, 120:215-41 pp.

CURRICULUM VITAE

Personal Information

Name : Sıla GÜMÜŞTAŞ

Date / Place of Birth : 31.03.1985- Bornova, İZMİR

Nationality : Turkish Republic

e-mail : sila.gumustas@ege.edu.tr

Education

2011–2018 E.U. Institute of Natural and Applied Science, Izmir, TURKEY Ph.D. **in Physical Chemistry**

2007–2011 E.U. Institute of Natural and Applied Science, Izmir, TURKEY **MSc. in Physical Chemistry**, The subject of MSc. Thesis 'Synthesis and characterization of polylactides (PLA) by means of ring opening polymerization using initiators containing silver'

2003–2007 E.U. Faculty of Science Chemistry Dept. Izmir, TURKEY **BSc. in Chemistry** The subject of BSc. Thesis 'Polymer synthesis of allyl derivative monomers by radical method'

Employment

2013– Ege University, Faculty of Science, Department of Chemistry, Division of Physical Chemistry, **Chemist**

2008–2011 Ege University, Faculty of Science, Department of Chemistry, Division of Physical Chemistry, **Research Assistant**

2007–2008 Bornova Municipality, Young Explorer Science House, **Chemistry teacher**

Publications

Gümüştaş, S., Balcan, M., Kınal, A., 2018, Computational determination of ring opening polymerization reaction mechanism of α-angelica lactone, *Computational and Theoretical Chemistry,* 1142:1-8 pp.

Unal, B., Yalcinkaya, E.E., **Gumustas, S.,** Sonmez, B., Ozkan, M., Balcan, M., Odaci Demirkol, D., and Timur, S., 2017, Polyglycolide–montmorillonite as a novel nanocomposite platform for biosensing applications, *New J. Chem.,* 41:9371-9379 pp.

Gümüştaş, S., Köseoğlu, K., Yalçınkaya, E.E. and Balcan, M., 2014, Characterization and dielectric properties of sodium fluoride doped talc, *Clay Minerals*, 49:551-558 pp.

Balcan, S., Balcan, M. and Çetinkaya, B., 2013, Poly(L-lactide) initiated by silver N-heterocyclic carbene complexes: synthesis, characterization and properties, Polym. Bull., 70:3475-3485 pp.

Congress

Gümüştaş, S., Kınal, A., 'Determination of the effects of electronic properties of several metal-containing initiator complexes on polymer molecular weights in the ring opening polymerization of δ-valerolactone: A computational and experimental study', CPC-XII:12th Chemical Physics Congress, Safranbolu, 12-13 October 2018

Gümüştaş, S., Balcan, M., Yalçınkaya, E.E., 'Dielectric Properties of the Sodium Fluoride doped Talc Minerals', KompEGE, 4th International Ege Composite Materials Symposium, Izmir, 6-8 September 2018 (Poster Presentation).

Gümüştaş, S., Yalçınkaya, E.E., 'Thermal degradation kinetics of the polyglycolide/clay nanocomposites', KompEGE, 4th International Ege Composite Materials Symposium, Izmir, 6-8 September 2018 (Poster Presentation).

Gümüştaş, S., Balcan, M., Kınal, A., 'The Ring Opening Polymerization of delta-Valerolactone: A Theoretical Study', POLYMER 2018, International

Participation 7th Polymer Science and Technology Congress, Eskişehir, 9-12 September 2018 (Poster Presentation).

Gümüştaş, S., Kınal, A., Balcan., M., 'Ring Opening Polymerization of delta-Valerolactone with Tin Acetate and Lead Acetate', POLYMER 2018, International Participation 7th Polymer Science and Technology Congress, Eskişehir, 9-12 September 2018 (Poster Presentation).

Unal, B., Yalçınkaya, E.E., **Gumustas, S.**, Sönmez, B., Ozkan, M., Balcan, M.,et al., 'Polyglycolide-Montmorillonite as a Novel Nanocomposite Platform for Biosensing Applications' XXIV. International Symposium on Bioelectrochemistry and Bioenergenites, Lyon, France, 3-7 July 2017 (Poster Presentation)

Gümüştaş, S., Kınal, A., Balcan, M., 'Experimental and Computatonal Studies of Ring Opening Polymerizaton of alpha angelica lactone with Zinc Acetate' MACRO, 2016 46th Iupac World Polymer Congress, Istanbul, 17-21 July 2016 (Poster Presentation).

Güreşci, M., **Gümüştaş, S.**, Balcan M., Kınal, A., 'Computational Investigation of the complete reaction path of poly l lactide initiated by Tin II 2 ethylhexanoate with DFT methods' MACRO 2016, 46th Iupac World Polymer Congress, Istanbul, 17-21 July 2016 (Poster Presentation)

Gümüştaş, S., Kınal, A., Balcan, M., 'The Reaction Mechanism of alpha Angelica Lactone Ring Opening Polymerization A Computational Study', Chemistry Conference for Young Scientists 2016, Blankenberge, Belgium, 16-18 March 2016 (Poster Presentation).

Yalçınkaya, E.E., **Gümüştaş, S.,** Köseoğlu, K., Balcan, M., 'Characterization of Sodium Fluoride doped Talc', Chemistry Conference for Young Scientists 2016, Blankenberge, Belgium, 16-18 March 2016 (Poster Presentation).

Yalçınkaya, E.E., **Gümüştaş, S.,**'Exfoliated biopolymer/clay nonocomposites synthesis via in-situ polymerization and its characterization', 4th International Conference on Biodegradable and Biobased Polymers (BIOPOL-2013), Roma, Italy, 2-4 October 2013 (Poster Presentation)

Ayan, U., Bostancıoğlu, İ., Deniz, O., **Gümüştaş, S.,** Balcan, M., 'Synthesis and characterization of poly (lactide-co-glycolide) using silver complexes', 4th National Chemistry Student Congress, Manisa, 18-20 May 2013 (Poster Presentation)

Balcan,S., Kunduracıoğlu, A., Balcan, M., Çetinkaya, B., 'Synthesis and characterization of polylactide by ring opening polymerization using silver containing initiators', 24th National Chemistry Congress, Zonguldak, 29 June-2 July 2010 (Poster Presentation)

Projects

2016-2018 Ege University, Research Funds, 2016 FEN 041

2009-2011 Ege University, Research Funds, 2009 FEN 035

Research Interest

Ring opening polymerization, biodegradable and biocompatible lactones, computational chemistry, polymer chemistry, reaction mechanisms